Transboundary particulate matter in Europe

Status Report 4/2010

PM10 in 2008 (ug/m3)
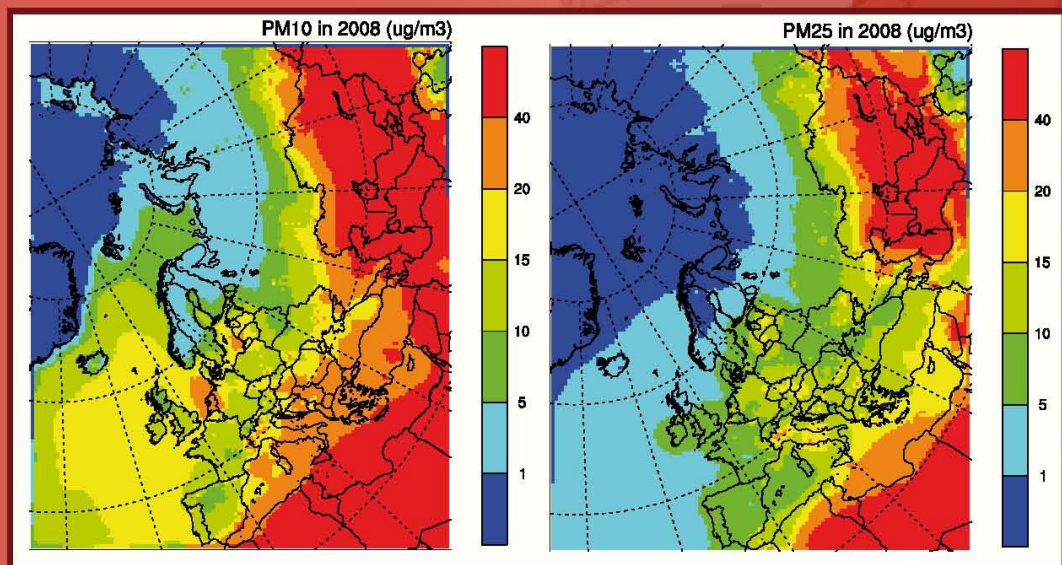
PM25 in 2008 (ug/m3)

ccc & msc-w & ceip & ciam

EMEP Co-operative Programme for Monitoring and Evaluation of the Long-Range Transmission of Air Pollutants in Europe

Transboundary particulate matter in Europe Status report 2010

Joint CCC, MSC-W, CEIP and CIAM Report 2010

Norwegian Institute for Air Research
P.O. Box 100, NO-2027 Kjeller, Norway

Norwegian Meteorological Institute
P.O. Box 43 Blindern, NO-0313 Oslo, Norway

Umweltbundesamt GmbH
Spittelauer Lände 5, AT-1090 Vienna, Austria

IIASA – International Institute for Applied Systems Analysis
Schlossplatz 1, AT-2361 Laxenburg, Austria

2

List of Contributors

Karl Espen Yttri[1], Wenche Aas[1], Kjetil Tørseth[1], Kerstin Stebel[1],
Aasmund Fahre Vik[1], Ann Mari Fjæraa[1], David Hirdman[1],
Svetlana Tsyro[2], David Simpson[2],
Katarína Marečková[3], Robert Wankmüller[3]
Zbigniew Klimont[4], Kaarle Kupiainen[4], Markus Amann[4], Robert Bergström[5],
Eiko Nemitz[6], Xavier Querol[7], Andres Alastuey[7], Jorge Pey[7],
Robert Gehrig[8]

1) Norwegian Institute for Air Research, Kjeller, Norway
2) Norwegian Meteorological Institute, Oslo, Norway
3) Umweltbundesamt, Vienna, Austria
4) International Institute for Applied Systems Analysis, Laxenburg, Austria
5) Swedish Meteorological and Hydrological Institute, Norrköping, Sweden
6) Centre for Ecology and Hydrology (CEH), Edinburgh, United Kingdom
7) Institute of Environmental Assessment and Water Research (IDÆA), Barcelona, Spain
8) Empa; Swiss Federal Laboratories for Materials Testing and Research, Duebendorf, Switzerland

[1] EMEP Chemical Coordinating Centre
[2] EMEP Meteorological Synthesizing Centre – West
[3] EMEP Centre on Emission Inventories and Projections
[4] EMEP Centre on Integrated Assessment Modelling

4

Contents

Executive Summary

The current report presents the status and progress of the emission reporting, observations and modelling activities undertaken under EMEP in relation to particulate matter in the European rural background environment. It also includes sections related to aerosol phenomenology in the Mediterranean region, elemental carbon concentrations across Europe, including the Arctic, and on the observations of aerosols from space.

Emission reporting

The number of Parties providing primary particulate matter emissions data increased by one from 2007 to 2008, and the total number of Parties was 34 (67%). Rather limited information is provided for the EECCA region, the Balkans, and Turkey. The reported PM emissions trends vary quite considerably among the Parties. For most countries which have reported data since 2000, PM emissions have decreased, although with a few exceptions. PM_{10} emissions have increased for 6 Parties, whereas $PM_{2.5}$ emissions have increased for 5 Parties. Improved (more complete) inventories reported for recent years could partly explain the increased PM emissions seen for the last two years in certain countries.

The distribution of key emission categories identified for Eastern and Western Europe is different and the total number of key categories is higher in Western Europe for both PM_{10} and $PM_{2.5}$. Residential Stationary Combustion is the most significant key source for PM_{10} and $PM_{2.5}$ in both regions. In Eastern Europe, Public Electricity and Heat Production and Stationary Combustion in Manufacturing Industries and Construction-Other follow in importance. Road Transport contributes also significantly to PM_{10} and $PM_{2.5}$ in both Eastern and Western Europe; in the latter, large population of diesel vehicles plays a major role. International maritime navigation is regarded a significant source of PM_{10} for Western Europe.

Historical gridded emissions for use in EMEP models have been updated, and the revised emissions show significant changes. For a few countries relative changes exceed 100% for selected years, whereas for the whole EMEP area, PM emissions decreased by almost 17% from 2000 and with 20% from 2005. The main reason for this decrease is the update of gridded emissions for the Russian Federation (European part) and Ukraine.

Measurement and model assessment of particulate matter

The number of sites undertaking PM_{10} measurements increased by 5 from 2007 to 2008. The total number of sites is thus 57. Similarly the number of sites measuring $PM_{2.5}$ increased from 26 to 32. 5 Parties reported PM observations for the first time (i.e. Estonia Finland, Hungary, Latvia and Moldova). This makes an important extension towards the eastern parts of the EMEP domain.

The lowest measured concentrations of PM_{10} were observed in the northern and north-western parts of Europe, i.e. the Nordic countries, Northern Ireland and Scotland, and for high altitude sites (> 800 m asl) on the European mainland.

Combined maps of EMEP model results and measurements show a pronounced north to south gradient, with the annual mean PM_{10} concentrations varying from 1-5 µg m^{-3} in Northern Europe to 10-25 µg m^{-3} in southern Europe. The lowest observed annual mean PM_{10} concentration was observed at the Hyytiälä (5.6 µg m^{-3}) site, situated in the boreal forest of Finland, whereas the highest was recorded at the Cypriote site Ayia Marina (31.5 µg m^{-3}). The concentrations seen for Southern, Eastern and Western Europe are notably higher and reflect both population density and major anthropogenic sources; e.g. the concentrations reported for Eastern Europe are > 70% higher than that seen for Scandinavia.

The spatial pattern of annual mean $PM_{2.5}$ concentrations largely reflects that of PM_{10}. However, the mean concentration of $PM_{2.5}$ in coastal areas is not found to be elevated as seen for PM_{10}, thus pointing towards the influence of coarse particles, and sea salts in particular, for $PM_{10.}$ As for PM_{10}, close to 60% of the urban background concentration is likely to be attributed to the mean rural background concentration of $PM_{2.5}$.

The annual mean concentration of PM_1 was reported for seven sites. The highest annual mean was observed at the Austrian site Illmitz (AT0002R) (11.4 µg m^{-3}), which was five times higher than that observed at the Birkenes site (2.2 µg m^{-3}) in Norway, reporting the lowest annual mean. No model calculated PM_1 concentrations are available.

The longest time series of PM mass data reported to EMEP goes back to the late 1990ies. Profound inter annual variations in the PM concentrations are observed of which those associated with the peak in 2003 is the most pronounced. PM levels for 2008 are typically lower than or equal to 2007, which was characterized by rather low concentrations in both size fractions at most sites.

The combined model and observation maps show that the annual mean regional background PM_{10} concentration in 2008 was below the EU limit value of 40 µg m^{-3} in most of Europe, with the exception of the most southern European parts and the EECCA countries. WHO recommended air quality guidelines (AQG) was however exceeded in the Netherlands, in the southern parts of the Mediterranean and in the EECCA region. The regional background annual mean $PM_{2.5}$ concentrations were above the WHO recommended AQG value of 10 µg m^{-3} in the same areas as seen for PM_{10}, but additionally also for several countries in Central and Eastern Europe.

Problems in using automated measurement systems for providing sufficiently homogeneous long-term datasets for reliable analysis of trends is discussed. Experience show that the use of inappropriate methods may significantly affect data quality, and that reference methods should be used to the extent possible.

Chemical composition data is essential to evaluate aerosol mass concentrations. Observations show that anthropogenic primary and secondary aerosols dominate the PM concentrations across most of Europe, whilst the influence of natural dust from Sahara and other semi-arid regions is significant in the southern parts. The contribution of sea salt is very dependent on distance to the sea and range from

0.6% at the continental site Illmitz in Austria to 18% at Birkenes in southern Norway. Significantly higher contributions may occur in coastal areas.

Eight countries reported measurements of EC and OC for 2008, which is twice the number for 2007. Seven of the sites apply the EUSAAR2 analytical protocol which is an important step towards harmonized and comparable data. A brief overview of the data reported for these sites are presented and show that there are large regional differences in the carbonaceous aerosol concentration. The results further show large inter-annual variations in the levels of the carbonaceous aerosol. This calls for a continued increase in the number of sites performing such measurement on a continuous basis.

The EMEP model for particulate carbonaceous matter (PCM) is an extension of the standard EMEP MSC-W photochemistry model, and includes the formation of secondary organic aerosol (SOA). Further developments and testing is presented in the present report. The volatility basis set (VBS) approach are computationally efficient and, with suitably chosen reaction parameters for aging reactions for semi-volatile organic aerosols components, it seems possible to reproduce total OC measurements rather well, at least for parts of Europe. However, large uncertainties still exists for SOA modelling and it is not yet clear if the models reproduce the measurements for the right reasons.

A full mass closure is still lacking at most EMEP sites, and Parties are strongly encouraged to implement the EMEP monitoring strategy. Results from the EMEP Intensive Measurement Periods (EIMP) are presented in Chapter 3. The measurements were performed in close cooperation with ongoing activities in the EU funded projects EUSAAR and EUCAARI and include a wide range of variables defined in the EMEP monitoring strategy. A total of eighteen sites participated in the second EIMP, but not all sites had a full suite of measurements. Efforts included carbonaceous aerosols, source apportionment using isotopic and organic tracers and aerosol mass spectrometers.

Aerosols in the Mediterranean area

The Mediterranean Basin (MB) has a complex aerosol phenomenology caused by factors such as high particle emissions from anthropogenic and natural sources, enhanced formation of secondary aerosols due to the high concentrations of gaseous precursors, elevated relative humidity and solar radiation, a characteristic meteorology that favours the stagnation of pollutants on a regional scale, and low precipitation rates, which increase the atmospheric life time of the aerosol. Chapter 5 presents an overview of the aerosol phenomenology in this region, comparing western and eastern patterns, the mass concentration and composition characteristics of the regional background, as well as for the urban environments. Results show a profound increase in the regional background annual mean PM_{10} and $PM_{2.5}$ levels along a West to East and North to South transect across the MB. Seasonal evolution of regional background PM levels in the West MB is characterized by a summer maximum. The Mediterranean regional background aerosol is characterized by relatively high levels of crustal material and sulphate, and lower levels of carbonaceous matter and nitrate than that of Central Europe.

PM levels in urban Mediterranean areas are generally higher than for Northern, Western and Central Europe. This has been attributed to certain particular features of the Mediterranean cities: i.e. a high population and car density, numerous construction and demolition activities, a vehicle fleet mainly running on diesel, substantial emissions from the harbors surrounding the cities, large emissions of ammonia from road traffic and sewage. The urban increment of PM appears to be particularly high compared to Central Europe.

Elemental (black) carbon

EC accounts for only a minor fraction (i.e. $3.4\pm1.1\%$) of the annual mean PM_{10} concentration in the European rural background environment. Compared to the World Health Organization Air Quality Guidelines for PM_{10} of 20 μg m^{-3} pr. year, EC contribute less than 4% on average, whereas it constitutes less than 2% of the EU PM_{10} annual limit value of 40 μg m^{-3}. However, recent epidemiological studies have demonstrated that EC, and associated compounds, have the highest risk factors concerning cardiovascular and respiratory hospitalization. Further, it is fair to argue that the carbonaceous aerosol is currently the most important with respect to aerosol effect on climate and that this mainly is attributed to its black carbon (BC) fraction. BC is regarded to be the second most important contributor to global warming after CO_2, although the magnitude of the BC climate effect has been somewhat debated (e.g. Forster et al., 2007). Chapter 5 presents available information on emissions, observations and modelling results of elemental carbon in EMEP and in the Arctic.

Observations of aerosols from space

Observations at EMEP sites offer unique possibilities to validate satellite data and satellite based products. Previous reports have discussed the SYNAER product in relation to EMEP model estimates and ambient mass concentration measurements. In this report, a presentation is given on new satellites and sensors under development, which may offer new products and services in the years to come. These include Saharan dust and volcanic ash products.

1   Status of emissions, 2008

By Katarína Marečková, Robert Wankmüller

1.1   PM emission reporting under LRTAP Convention

Parties to the LRTAP Convention submit air pollution emissions[1] and projections annually to the EMEP Centre on Emission Inventories and Projections (CEIP) and notify the LRTAP Convention secretariat thereof. Parties are requested to report emission inventory data using standard formats in accordance with the EMEP Reporting guidelines (UNECE, 2009). Particulate matter (PM_{10} and $PM_{2.5}$) emissions should be reported for years 2000 - 2008 as a minimum. Gridded emissions and LPS data should be provided in 5-year interval.

1.1.1   Status of reporting

In 2010 fortythree Parties (out of 51) to the LRTAP Convention submitted inventories for the year 2008 before 30 June. Of these, only 34 Parties provided PM emissions, but comparing to the year 2002 this is a slight improvement from 53% to 67% of the Parties. Rather limited information is provided for the EECCA region, the Balkans and Turkey. Data submitted by the Parties can be accessed via the CEIP homepage at http://www.ceip.at/submissions-under-clrtap/2010-submissions/. Completeness, consistency, comparability and transparency of reported emissions are analyzed in an annual review process[2]. Feedback is provided to the Parties in form of individual country reports and summary findings are published in the EEA & CEIP technical report *Inventory Review 2010*.

1.1.2   PM emission trends[3]

The PM emissions trends (as reported) vary quite considerably among the Parties to the CLRTAP. Emission trends for the countries with the highest emissions in 2008 are shown in Figure 1.1. It is not possible to assess an overall trend for the whole EMEP area, as complete time series are missing for 20 Parties. For most countries which have reported data since 2000, PM emissions have decreased, although with a few exceptions; i.e. PM_{10} emissions have increased for 6 Parties, whereas $PM_{2.5}$ emissions have increased for 5 Parties. The biggest increase in $PM_{2.5}$ emissions is reported for Moldova (196%) and Malta (40%). From 2007 to 2008, $PM_{2.5}$ emissions rose for 11 Parties, with the most substantial increase seen for Romania (16%) and Bulgaria (13%) (Table 1.1, Table 1.2). Improved (more complete) inventories reported for recent years could partly be responsible for the increased PM emissions seen for the last two years in certain countries.

---

[1] SO_x, NO_x, NMVOCs, NH_3, CO, HMs, POPs and PM
[2] Methods and Procedures for the Technical Review of Air Pollutant Emission Inventories Reported under the Convention and its Protocols (EB.AIR/GE.1/2007/16)
[3] The trend tables contain only data as reported by Parties, no expert estimates are included.
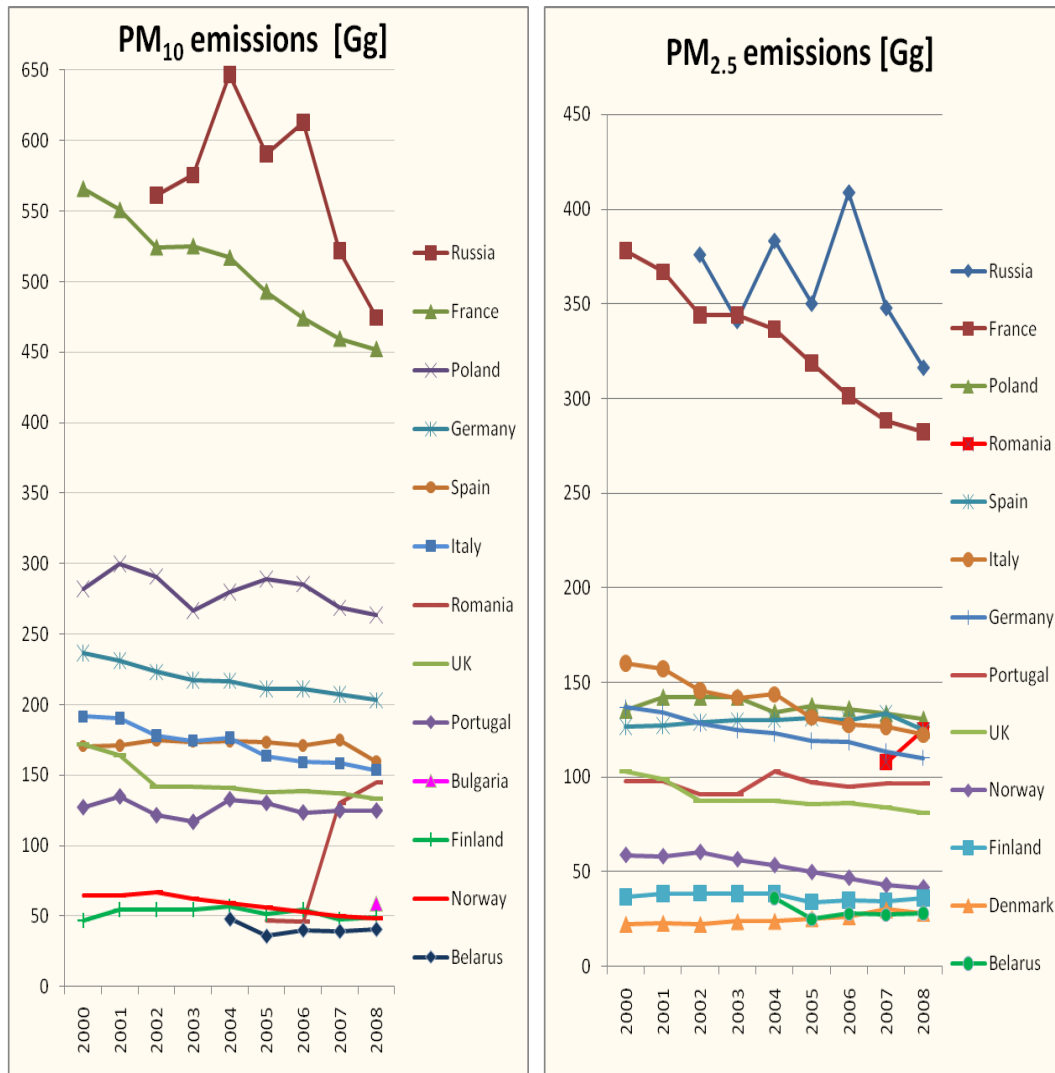
Figure 1.1:   PM$_{10}$ (left) and PM$_{2.5}$ (right) emission trends (2000 - 2008) for the 13 Parties with the highest emissions in 2008.

Note: Emissions presented for the Russian Federation correspond only to "Russian Federation in the former official EMEP domain"

Major countries such as Kazakhstan, Ukraine and Turkey do not report PM emission data, therefore Figure 1.1 does not provide the full picture of emission trends in the EMEP domain.

Table 1.1:   PM₁₀ emission trends (2000-2008) as reported by Parties.

Country / PM₁₀ [Gg]	2000	2001	2002	2003	2004	2005	2006	2007	2008	Change 2007 - 08	Change 2000 - 08
Albania											
Armenia								0.64			
Austria	37	37	36	36	36	37	35	35	36	2%	-3%
Azerbaijan											
Belarus			NE	NE	48	36	40	39	41	4%	
Belgium	48	45	44	44	42	38	37	33	30	-8%	-37%
Bosnia and Herzegovina											
Bulgaria		NE	NO	NE	NE	NE	NE	44	59	33%	
Canada	NR	NR	NR	NR	NR	NR	NR	NR	NR		
Croatia	11	7	7	9	9	15	14	14	13	-7%	19%
Cyprus	5	4	4	4	4	4	4	4	4	-3%	-13%
Czech Republic		43	0.05	51	47	34	35	35	35	1%	
Denmark	30	30	29	31	31	33	34	37	35	-6%	18%
Estonia	37	37	33	30	30	26	20	28	25	-12%	-32%
European Community	2 299	2 297	2 387	2 202	2 186	2 137	2 088	2 122	2 126	0%	-8%
Finland	47	54	55	55	57	51	55	48	49	2%	5%
France	566	551	524	525	517	493	474	459	452	-2%	-20%
Georgia											
Germany	237	231	223	217	217	211	211	207	203	-2%	-14%
Greece											
Hungary	47	43	44	48	47	52	48	36	38	6%	-20%
Iceland	NR	NR	NR	NR	NR	NR	NR	NR	NR		
Ireland	18	18	17	16	16	17	16	15	15	-3%	-16%
Italy	192	190	178	174	176	163	159	158	154	-3%	-20%
Kazakhstan											
Kyrgyzstan											
Latvia	24	27	26	28	28	28	27	27	27	-2%	10%
Liechtenstein	0.04	0.04	0.04	0.04	0.04	0.04	0.04	0.04	0.04	0%	-6%
Lithuania		1	NE	NE	11	11	11	12	12	6%	
Luxembourg	NR	NR	NR	NR	NR	NR	NR	NR			
FYR of Macedonia				NE	NE	NE	NE	NE	NE		
Malta	1	2	2	2	2	2	2	2	2	1%	54%
Republic of Moldova	5	3	5	6	11	8	8		10		120%
Monaco		NE	NE	NE	NE	NE	NE	NE	NE		
Montenegro							10				
Netherlands	44	42	41	39	38	38	37	37	37	-1%	-16%
Norway	65	64	67	63	59	56	53	50	48	-4%	-26%
Poland	282	300	291	267	280	289	285	269	263	-2%	-7%
Portugal	127	135	122	117	133	130	123	125	125	0%	-2%
Romania	NE	NE	NE	NE	NE	47	46	130	144	11%	
Russian Federation			561	576	647	591	613	522	475	-9%	
Serbia						NE	NE	NE			
Slovakia	39	40	35	34	36	45	39	34	32	-7%	-18%
Slovenia	18	18	17	17	17	17	16	16	14	-12%	-20%
Spain	170	171	174	174	174	173	171	175	160	-9%	-6%
Sweden	40	40	40	41	41	42	41	41	39	-5%	-3%
Switzerland	23	23	22	22	22	22	21	21	21	1%	-7%
Turkey											
Ukraine		NO	3		119	131	NE		NA		
United Kingdom	172	164	142	141	141	138	139	137	133	-3%	-23%
USA	20 901	21 266	19 346	19 335	19 322	19 275	17 533	15 762	13 028	-17%	-38%

Notes: Blank cell indicates that no data have been reported to EMEP

Shaded cells (red) indicate increased emissions for the given period

Emissions in the row "Russian Federation" corresponds only to "Russian Federation in the former official EMEP domain"

Table 1.2:   PM$_{2.5}$ emission trends (2000 - 2008) as reported by Parties.

Country / PM$_{2.5}$ [Gg]	2000	2001	2002	2003	2004	2005	2006	2007	2008	Change 2007 - 08	Change 2000 - 08
Albania											
Armenia								0.28			
Austria	22	23	22	22	22	23	21	21	21	1%	-6%
Azerbaijan											
Belarus			NE	NE	36	25	28	27	28	3%	
Belgium	33	30	30	29	28	25	25	22	20	-9%	-41%
Bosnia and Herzegovina											
Bulgaria		NE	NO	NE	NE	NE	NE	21	24	13%	
Canada	NR	NR	NR	NR	NR	NR	NR	NR	NR		
Croatia	9	6	6	7	7	11	11	11	10	-10%	10%
Cyprus	3	3	3	3	3	3	3	3	3	-2%	-4%
Czech Republic			NE	38	35	21	22	21	21	-1%	
Denmark	22	23	22	24	24	25	26	30	28	-6%	26%
Estonia	21	22	23	21	22	20	15	20	20	-2%	-5%
European Community	1 612	1 593	1 526	1 514	1 510	1 466	1 428	1 400	1 403	0%	-13%
Finland	37	38	39	38	38	34	35	34	36	5%	-1%
France	378	367	344	344	337	319	301	288	282	-2%	-25%
Georgia											
Germany	137	134	128	125	123	119	119	113	110	-3%	-19%
Greece											
Hungary	26	24	25	27	27	31	29	21	23	6%	-12%
Iceland	NR	NR	NR	NR	NR	NR	NR	NR	NR		
Ireland	12	12	11	11	11	11	11	10	10	-3%	-16%
Italy	160	157	146	142	144	131	128	127	122	-3%	-24%
Kazakhstan											
Kyrgyzstan											
Latvia	23	25	25	26	27	27	26	26	25	-1%	11%
Liechtenstein	0.03	0.03	0.03	0.03	0.03	0.03	0.03	0.03	0.03	0%	-3%
Lithuania			NE	NE	9	9	9	10	10	8%	
Luxembourg	NR	NR	NR	NR	NR	NR	NR	NR			
FYR of Macedonia				NE	NE	NE	NE	NE	NE		
Malta	1	1	1	1	1	1	1	1	1	0%	40%
Republic of Moldova	2	2	1	3	6	6	7		6		196%
Monaco		NE	NE	NE	NE	NE	NE	NE	NE		
Montenegro							7				
Netherlands	25	24	23	23	21	21	20	20	19	-3%	-23%
Norway	59	58	60	56	53	50	47	43	42	-3%	-29%
Poland	135	142	142	142	134	138	136	134	131	-2%	-3%
Portugal	98	98	91	91	103	97	95	96	97	0%	-1%
Romania	NE	NE	NE	NE	NE	NE	NE	108	125	16%	
Russian Federation			376	341	383	350	409	348	316	-9%	
Serbia						NE	NE	NE			
Slovakia	32	32	29	27	31	40	35	28	27	-6%	-16%
Slovenia	14	14	14	14	14	14	13	14	13	-6%	-10%
Spain	127	127	129	130	130	131	130	134	125	-7%	-1%
Sweden	28	28	28	29	29	29	29	29	27	-6%	-4%
Switzerland	12	11	11	11	11	10	10	10	10	2%	-15%
Turkey											
Ukraine		NO	0.01		15	125	NE		NA		
United Kingdom	103	99	88	87	87	86	86	84	81	-4%	-21%
United States of	6 061	6 154	5 059	5 048	5 036	5 029	4 981	4 944	4 091	-17%	-33%

Notes: Blank cell indicates that no data have been reported to EMEP

Shaded cells (red) indicate increased emissions for the given period

Emissions in the row "Russian Federation" corresponds only to "Russian Federation in the former official EMEP domain"

1.1.3   PM key categories[4]

The distribution of key categories identified for Eastern[5] and Western[6] Europe is different and the total number of identified key categories is higher in Western Europe for both PM_{10} and $PM_{2.5}$. Most of the emission categories identified as being the *key* for both - Western and Eastern Europe - occur in combustion processes. The results of the Key Category Analysis (KCA) in Figure A.2 and A.3 show that:

- The most significant key source for PM_{10} and $PM_{2.5}$ is *1A4bi Residential: Stationary combustion* accounts for approximately 29% of the PM_{10} emissions in Eastern Europe, whereas the corresponding number for Western Europe is 19 %. For $PM_{2.5}$ emissions from stationary combustion accounted for almost 34% in Eastern Europe and 27 % in Western Europe.

- In Eastern Europe the second and third most important categories are *1A1a Public Electricity and Heat Production* (13% to PM_{10}, 12 % to $PM_{2.5}$) and *1A2a Stationary Combustion in Manufacturing Industries and Construction-Iron and Steel* (5% to PM_{10}, 6 % to $PM_{2.5}$). For Western Europe the share of *1A1a* does not account for more than 3% of the PM_{10} and $PM_{2.5}$ emissions, whereas *1A2a* is not even among key categories.

- The various subcategories within the road transport category (*1A3bi Road Transport - Passenger cars, 1A3bii Road Transport – Light duty vehicles, 1A3biii Road Transport – Heavy duty vehicles and 1A3bvi Road Transport – Automobile tyre and brake wear*) contributes significantly to the PM_{10} and $PM_{2.5}$ emissions. For Eastern Europe[7] this category amounts to about 7%, for both size fractions, whereas for Western Europe it constitutes approximately 13% of PM_{10} and 15% of $PM_{2.5}$.

- The high share (12%) of PM emissions attributed to category *7A Other* for Eastern Europe is one of the reasons for the differences seen for the KCA when comparing Eastern and Western Europe.

If all emission categories, including international transport, would be considered and subsequently aggregated, the top 5 categories of PM_{10} for Eastern Europe would comprise *1A4 (35%), 1A2 (15%), 1A1* (15%), *7A* (12%), and *1A3b* (9%), whereas for Western Europe the following categories *1A4* (23%), *1A3b* (13%), *1A3d* (12%), *1A2* (8%), and *4D* (8%) would be included. This analyses shows that

---

[4] The threshold for identifying the key categories is 80%, following the revised EMEP/EEA Air Pollutant Emission Inventory Guidebook (EEA/EMEP, 2009). Categories refer to the NFR09 nomenclature.

[5] **Eastern European countries as referred to in the EMEP database** = Albania, Armenia, Azerbaijan, Bosnia & Herzegovina, Bulgaria, Belarus, Cyprus, Czech Republic, Estonia, Georgia, Croatia, Hungary, Kyrgyzstan, Kazakhstan, Lithuania, Latvia, Republic of Moldova, Montenegro, Macedonia, Poland, Romania, Serbia, Russian Federation, Slovenia, Slovakia, Turkey, Ukraine.

[6] **Western European countries as referred to in the EMEP database** = Austria, Belgium, Switzerland, Germany, Denmark, Spain, Finland, France, United Kingdom, Greece, Ireland, Iceland, Italy, Liechtenstein, Luxemburg, Malta, Monaco, the Netherlands, Norway, Portugal, Sweden.

[7] 1A3bii and 1A3bvi does not appear among key categories in Eastern Europe

1A3di(i) International maritime navigation is a significant source of PM_{10} for Western Europe (9.4%). For Eastern Europe countries hardly any emissions are reported for this category.

It should be noted that the share of PM key categories in individual countries differs from that agglomerated for Eastern and Western Europe. Sectoral distribution of emissions in big countries (e.g. Russian Federation and France) can significantly influence the share of individual categories for the entire region. For detailed key category analysis results for individual Parties, please have a look at the EEA & CEIP technical report Inventory Review 2008, Appendix 7 (Mareckova et al., 2008).

In order to further improve the atmospheric monitoring and modelling under the Convention, it is important to identify key categories that have a significant influence on a country's total inventory in terms of absolute level of emissions. Further, more KCA analyses can help by setting up priorities for improvement of national inventories.
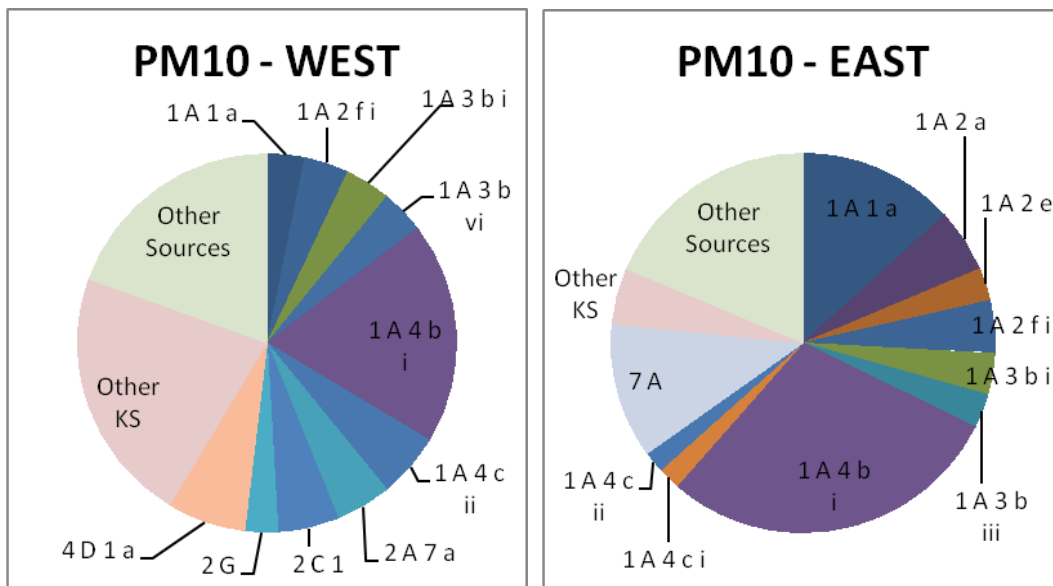

Figure 1.2: *Comparison of Eastern and Western European PM_{10} Key Category Analysis based on 2008 emissions.* **Numbering of categories corresponds to NFR09.**
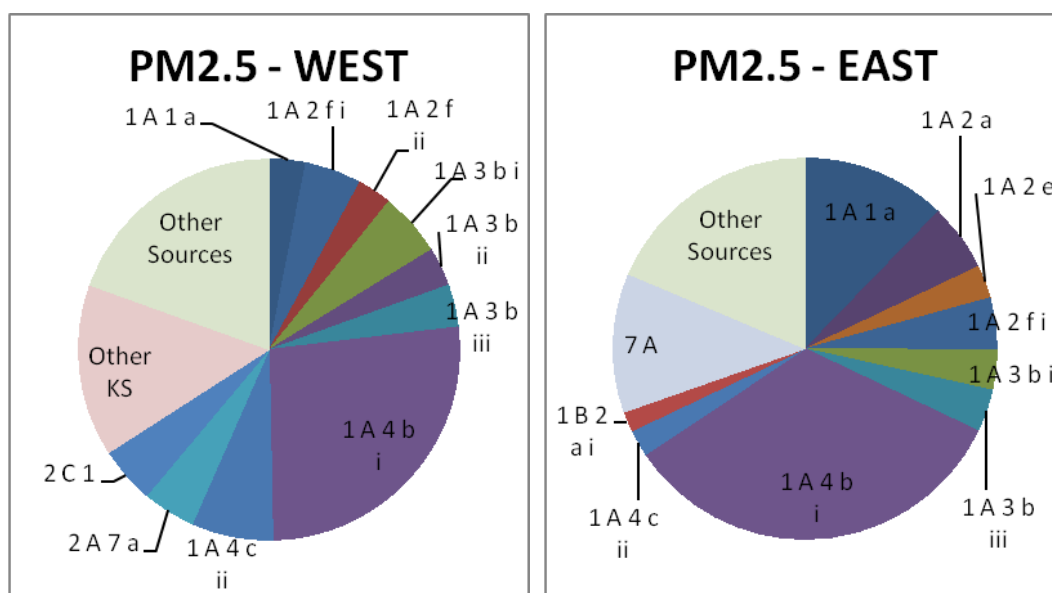
*Figure 1.3: Comparison of Eastern and Western European PM$_{2.5}$ Key Category Analysis based on 2008 emissions. **Numbering of categories corresponds to NFR09.***

Note: Numbering of categories corresponds to EMEP nomenclature for reporting NFR09 (UNECE, 2009). If the total number of key categories for a particular pollutant was more than 10, emissions were summed up in 'Other key sources'. 'Other sources' contain the remaining (non-key) categories

1 A 1 a	*Public Electricity and Heat Production*
1 A 2 a	*Stationary Combustion in Manufacturing Industries and Construction - Iron and Steel*
1 A 2 e	*Stationary Combustion in Manufacturing Industries and Construction - Food Processing, Beverages and Tobacco*
1 A 2 f i	*Stationary Combustion in Manufacturing Industries and Construction - Other*
1 A 2 f ii	*Mobile Combustion in Manufacturing Industries and Construction*
1 A 3 b i	*Road Transport - Passenger Cars*
1 A 3 b ii	*Road Transport - Light duty vehicles*
1 A 3 b iii	*Road Transport - Heavy duty vehicles*
1 A 3 b vi	*Road Transport - Automobile tyre and brake wear*
1 A 4 b i	*Residential - Stationary plants*
1 A 4 c i	*Agriculture/Forestry/Fishing - Stationary*
1 A 4 c ii	*Agriculture/Forestry/Fishing - Off-road Vehicles and Other Machinery*
1 B 2 a i	*Exploration, Production, Transport*
2 A 7 a	*Quarrying and mining of minerals other than coal*
2 C 1	*Iron and Steel Production*
2 G	*Other production, consumption, storage, transportation or handling of bulk products*
4 D 1 a	*Synthetic N-fertilizers*
7 A	*Other*

1.1.4 Emission data prepared for modelers

Modellers use PM$_{2.5}$ and PMcoarse[8] (PM$_{10-2.5}$) emissions distributed in the 50 x 50 km EMEP grid[9]. The extended EMEP domain comprises approximately

---

[8] PMcoarse emissions are not reported but estimated as the difference between PM$_{10}$ and PM$_{2.5}$
[9] Information regarding the gridding procedure can be downloaded at
http://www.ceip.at/fileadmin/inhalte/emep/pdf/gridding_process.pdf

20 000 grid cells, but PM sectoral data is reported for less than 50% of this area. More or less complete emissions are available for Europe, except for some Balkan countries. No PM emissions were reported by a number of EECCA countries, Turkey and for the "Russian Federation extended EMEP domain". To make submitted emission data usable for modellers, emissions reported in NFR09 categories are converted to 10 SNAP sectors, whereas missing information (not reported by Parties) has to be filled in[10]. The calculated differences between reported 2008 emissions and expert estimates used in models are presented in maps (Figure 1.4). Light blue areas mean that the expert estimates emission values in particular grids are slightly above zero (e.g. PMcoarse emissions over North Atlantic). It should be noted that the biggest differences between reported and gapfilled data is observed for the Eastern part of the EMEP grid, and that this region contributes by approximately 50% to total PM emissions entering the EMEP model (Figure 1.5). An additional challenge is the limited reporting of emissions occurring in international maritime shipping and hence the high uncertainty of estimates used for this category.

Gap-filled and gridded data can be accessed via the CEIP homepage at http://www.ceip.at/emission-data-webdab/emissions-used-in-emep-models/ and gridded data can also be visualized in Google Maps/Earth at http://www.ceip.at/emission-data-webdab/gridded-emissions-in-google-maps/.
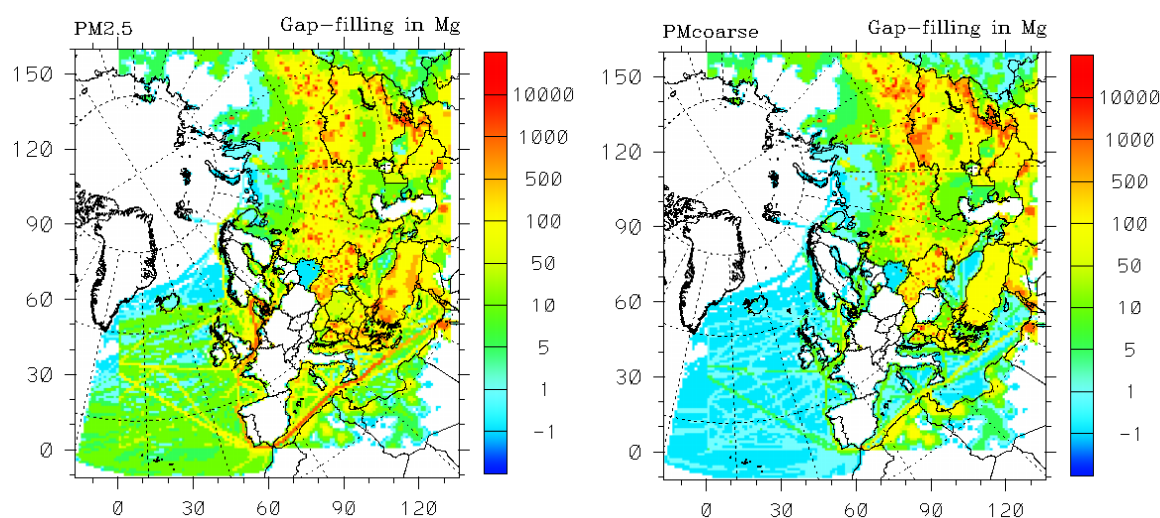
Figure 1.4: *Differences between reported PM emissions and emissions used in models for the extended EMEP grid for the 2008 inventory (Mg PM/grid).*

Notes: **White colour indicates no difference between reported data and data used in models.**
Because of late submissions from Iceland and the Russian Federation it was not possible to take the updated data into account for the model runs by MSC-W.
For the extended EMEP domain the same emissions were considered in the gap-filling and gridding process as considered last year for 2007. Because of not reported PM emissions from a number of countries in this area, MSC-W estimates for year 2006 were extrapolated and gridded with current population data of this area, as provided by IIASA.

---

[10] Basic principles are described in the EEA, 2009*b Proposed gap-filling procedure for the European Community LRTAP Convention emission inventory.*

Figure 1.5:   Contribution from different EMEP regions to the total 2008 emissions. Gap filled data for the extended EMEP domain
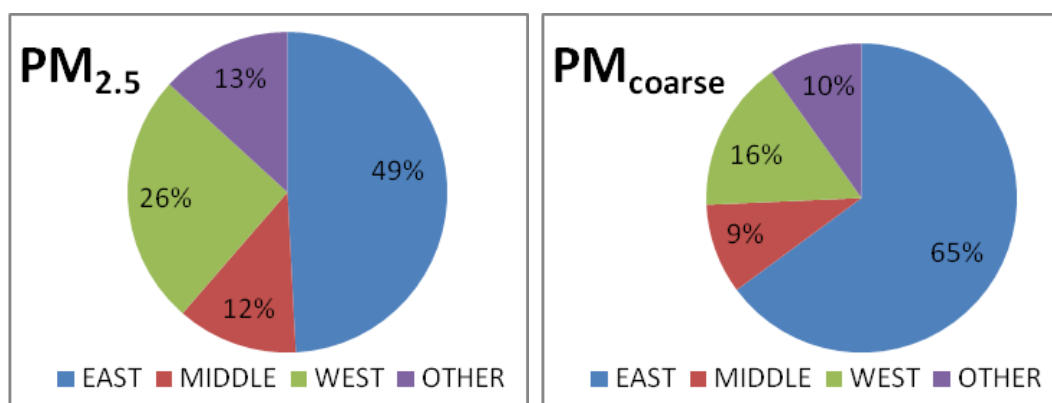
East: Albania, Armenia, Azerbaijan, Belarus, Georgia, Kyrgyzstan, Kazakhstan, Republic of Moldova, Russian Federation, Russian Federation extended, Turkey, Ukraine, Uzbekistan, Turkmenistan, Tajikistan

Middle: Bosnia & Herzegovina Bulgaria, Cyprus, Czech Republic, Estonia, Croatia, Hungary, Lithuania, Latvia, Montenegro, Malta, Macedonia, Poland, Romania, Slovenia, Slovakia, Serbia

West: Austria, Belgium, Switzerland, Germany, Denmark, Spain, Finland, France, United Kingdom, Greece, Ireland, Iceland, Italy, Liechtenstein, Luxemburg, Monaco, the Netherlands, Norway, Portugal, Sweden

Other: Arctic Ocean, Aral Lake, Remaining Asian Areas, Atlantic Ocean, Baltic Sea, Black Sea, Caspian Sea, Mediterranean Sea, North Africa, North Sea

The share of individual SNAP sectors on total emission significantly differs among the regions (Figure 1.6 and Figure 1.7). The observed differences can only partly be explained by country specific/regional circumstances. Limited resources do not allow performing detailed analyses of the countries data and comparisons with other data sources (Worldbank, Eurostat, FAO, IEA, etc.). Such analyses could help justify and/or improve sectoral data entering the EMEP model.
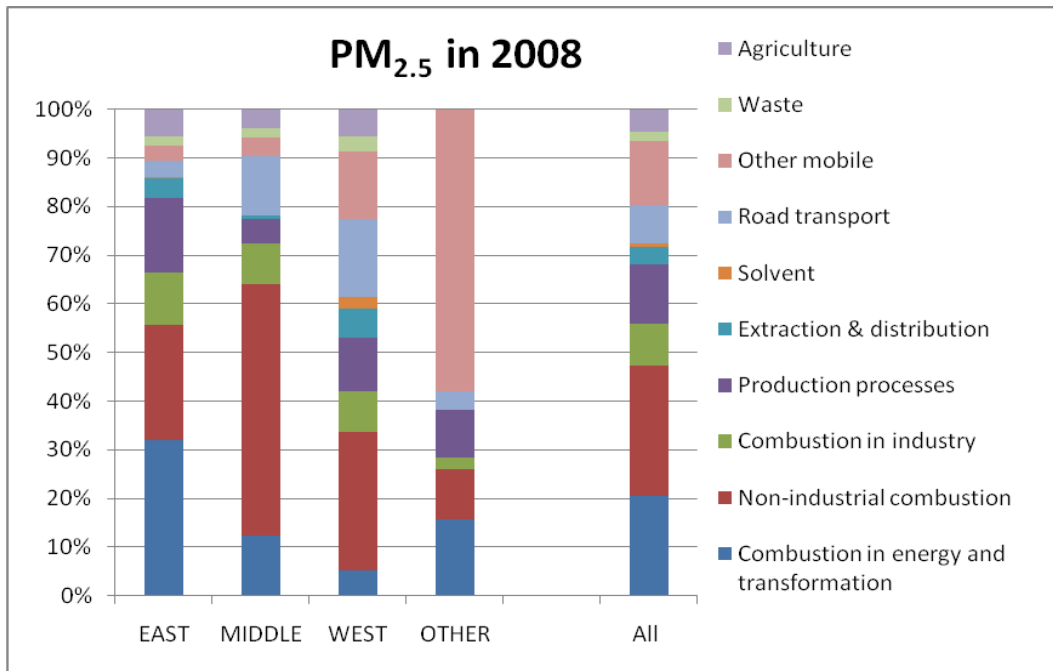
Figure 1.6: Sectoral (SNAP 10) contribution to PM$_{2.5}$ emissions for the year 2008 for different EMEP regions.
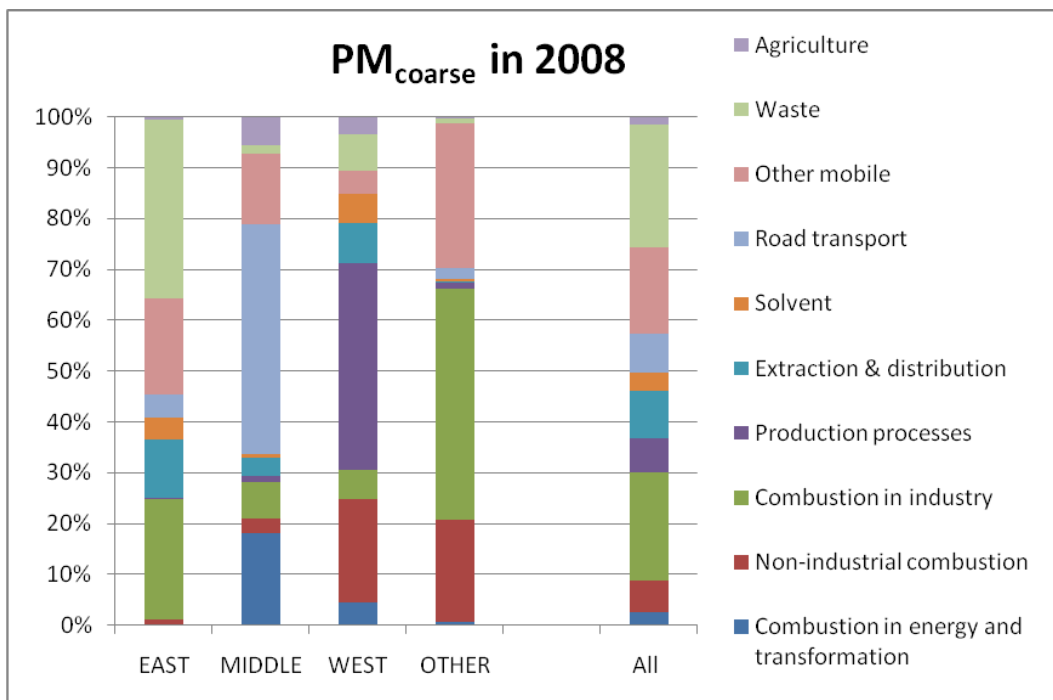

Figure 1.7: Sectoral (SNAP 10) contribution to PMcoarse emissions for the year 2008 for different EMEP regions.

1.1.5 Update of historical gridded emissions used in EMEP models (2000 – 2007)

To provide modellers with historical data that is consistent with the latest (recalculated) data reported by Parties, CEIP[11] has re-gridded data from previous years (from 2000 to 2007). These updated emissions should be used in the source–receptor models in the year 2010.

Revised emissions show significant changes. For a few countries (Cyprus, Latvia, Malta and Slovenia), updated $PM_{2.5}$ emissions increased by more than 100% for selected years, whereas for the whole EMEP area PM emissions decreased by almost 17% for 2000 and 20% for 2005 (Table 1.3)**.** The main reason for this decrease is the update of gridded emissions for the Russian Federation (European part) and Ukraine. The decrease (around -50%) seen for the 2005 PM emissions in the Russian Federation was caused by the replacement of expert estimates with data reported by the country in the year 2007. An example of the magnitude of these recalculations for individual EMEP 50x50 km grids is provided in maps with calculated emission differences of $PM_{2.5}$ and PM_{coarse} (Figure 1.8) for the years 2000 and 2005.

Table 1.3:   Total differences between gridded PM emissions in 2000 and 2005 used in the models until 2009 and re-gridded in 2010.

	Previous expert data	Updated expert data	Difference [Gg]	Difference [%]
$PM_{2.5}$ Total 2000	3 629	3 636	7	0.20%
$PM_{2.5}$ Total 2005	3 563	2 966	-597	-16.76%
PM_{coars} Total 2000	2 006	1 967	-40	-1.98%
PM_{coars} Total 2005	1 992	1 602	-390	-19.56%

A table listing the differences between gridded emissions from 2000 to 2007 used in the models until 2009 and emissions re-gridded in 2010 (per country/pollutant/ year and expressed both as a percentage and in Gg) can be downloaded at http://www.ceip.at/fileadmin/inhalte/emep/xls/2010/Diff_gridded_regridded.xls.

---

[11] CEIP has developed a software "RG tool" for distributing resubmitted emissions, which uses the given spatial distribution of a particular year. It was developed in 2010 to re-grid air pollutants reported to UNECE on SNAP 10 sector level.
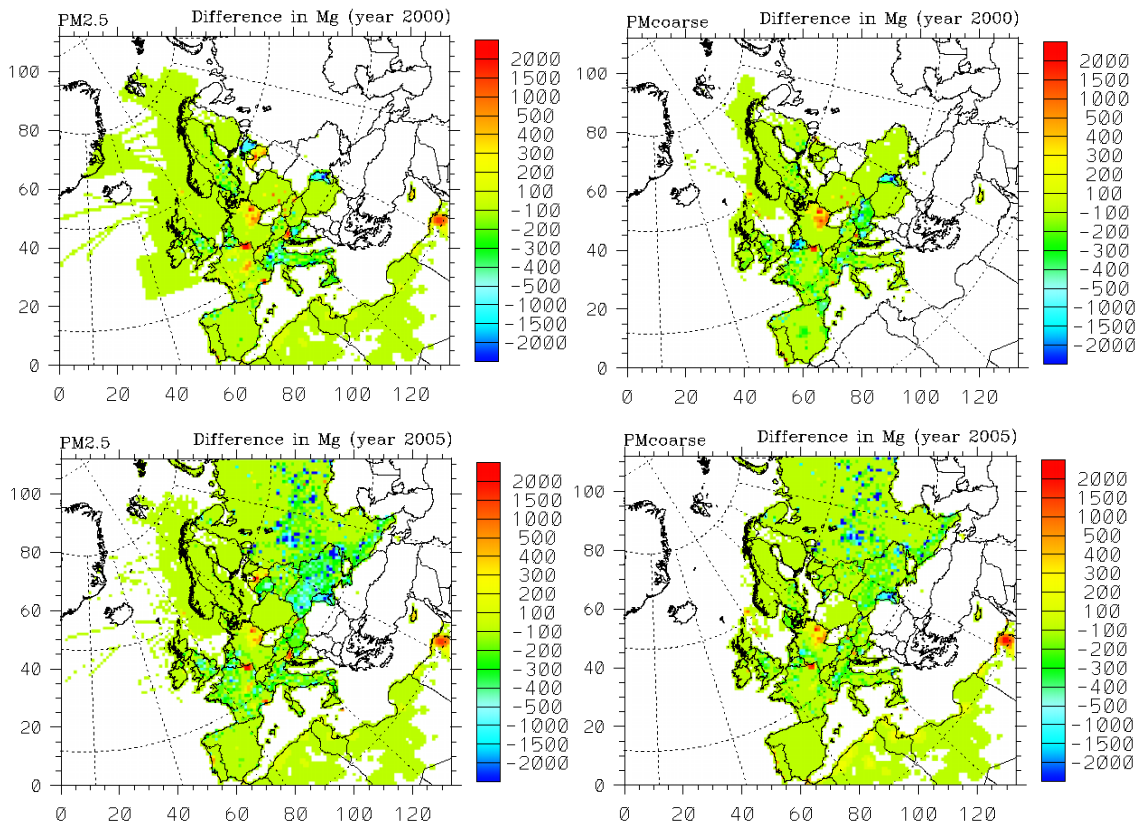
*Figure 1.8:   Example of differences between gridded emissions used until 2009
and re-gridded emissions for the years 2000 and 2005 (Mg
PM/grid).*

2 Measurement and model assessment of particulate matter in Europe, 2008

2.1 PM mass concentrations

By Svetlana Tsyro, Karl Espen Yttri and Wenche Aas

2.1.1 Introduction

The current assessment of the concentration levels of regional background particulate matter, PM_{10} and $PM_{2.5,}$ in 2008 has been made based on EMEP model calculations and data from the EMEP monitoring network. In the present chapter, the PM_{10} and $PM_{2.5}$ concentrations are presented for the extended EMEP area, covering also the EECCA countries.

2.1.2 The measurement network

The observed annual mean concentrations of PM_{10}, $PM_{2.5}$ and PM_1 for 2008 at European rural background sites can be found in Hjellbrekke and Fjæraa (2010). For 2008, mass concentrations of PM are reported for 57 regional background sites (57 for PM_{10} and 32 for $PM_{2.5}$). For the sites EE0009R (Laheema; Estonia), FI0050R (Hyytiälä, Finland), FR0015R (La Tardiére, France), HU0002R (K-Puszta, Hungary), LV0010 (Rucava) and LV001 (Zoseni), both in Latvia, MD0013R (Leova, Moldova), NL0009R (De Zilk, The Netherlands), and SE0014R (Råö, Sweden), 2008 was the first time mass concentrations of PM have been reported to EMEP. 5 of these sites are situated in countries which have previously not reported PM to EMEP, i.e. Estonia, Finland, Hungary, Latvia, and Moldova, thus raising the number of countries to 23, compared to 18 for 2007. The new sites reported in 2008 extend the EMEP monitoring network in Western, Northern and in particular Eastern Europe. An eastward extension of the monitoring network has since long been anticipated, and is thus particularly welcomed. PM_1 was reported for seven sites in 2008, compared to five for 2007. The new sites reporting PM_1 were Montseny (ES1778R) and Hyytiälä (FI0050R).

2.1.3 The EMEP model and runs setup

Model A complete description of the Unified EMEP model can be found in Simpson et al. (2003), Fagerli et al. (2004) and (Tsyro, 2008), while the most recent model development is documented in EMEP Status Report 1/2010 and Simpson et al. (2010). The model version rv3.6 has been used to perform calculations presented in the current report.

Meteorology The meteorological data for 2008 used in the model simulations was produced using the ECMWF-IFS meteorological model (Integrated Forecast System). The original fields from the ECMWF-IFS model was generated on a Gaussian grid using spectral representation of T799 (approximately 0.225°) and at 60 vertical layers in η-coordinates. The extracted data contained meteorological fields for the lowest 36 layers (up to about 90 hPa) converted to a geographical grid with a 0.2° x 0.2° resolution. These fields were interpolated to the EMEP 50 x 50 km^2 grid and to 20 model vertical σ-layers.

In 2008, the PARLAM-PS model, which had been used since 1998, was run for the last time to generate meteorological input for the EMEP model calculations for the year of 2006. In addition to PARLAM-PS for the 2008 reporting, model runs for 2006 were also performed using meteorology calculated with the most recent version of the HIRLAM model and with the ECMWF-IFS model. The first comparison and evaluation of model results obtained using different meteorological inputs was presented in EMEP (2008). Differences in the Unified model results due to using the three different meteorological drivers have been further analysed and are discussed in EMEP Status Report 1/2010, while the main conclusions relevant to PM calculations are outlined in this chapter.

Emissions The national emissions of SO_x, NO_x, NH_3, NMVOC, PM_{10} and $PM_{2.5}$ for the year 2008 were prepared by EMEP/CEIP. For a number of countries, rather large differences (in excess of 50 - 100%) were found when comparing emissions of the pollutants for 2007 with that of 2008, (see EMEP Status Report 1/2010). The largest differences (> 50%) in national total emissions of PM precursors are reported for Kyrgyzstan, Iceland, Malta, Montenegro, Georgia, Moldova, Spain and Turkey, whereas the largest difference (>50%) for total PM emissions were observed for. Kyrgyzstan, Malta, Slovenia, Romania and Latvia. In some countries, e.g. Ukraine for SO_x and NO_x and Austria for SO_x, changes in the emissions from different activity sectors brought about considerable changes in the spatial distribution of emissions for 2008 compared to 2007, although the annual totals for these years do not differ much. In such cases, changes in the emissions affected the spatial distribution of calculated concentrations only for primary pollutants, but not for secondary components.

2.1.4 Annual PM_{10}, $PM_{2.5}$ and PM_1 concentrations in 2008

The lowest measured concentrations of PM_{10} were observed in the northern and north-western parts of Europe, i.e. the Nordic countries, Northern Ireland and Scotland, and for high altitude sites (> 800 m asl) on the European mainland (Figure 2.1). These measurements have been combined with the EMEP model to create annual mean concentration fields of regional background PM_{10} and $PM_{2.5}$ (Figure 2.2).

The following procedure has been used to generate the combined maps: For each measurement site with PM data in 2008, the difference between the measured value and the modelled value in the corresponding grid cell has been calculated. The differences for all sites have been interpolated spatially using radial base functions, which provide a continuous 2-dimentional function describing the difference in any cell within the modelled grid. The maps of interpolated differences and normalized differences between model calculated and measured PM_{10} and $PM_{2.5}$ are included in Appendix (Figure A.1). The combined maps have been constructed by adjusting the model results with the interpolated differences, giving larger weight to the observed values close to the measurement site, and using the model values in areas with no observations. The range of influence of the measured values has been set to 500 km.
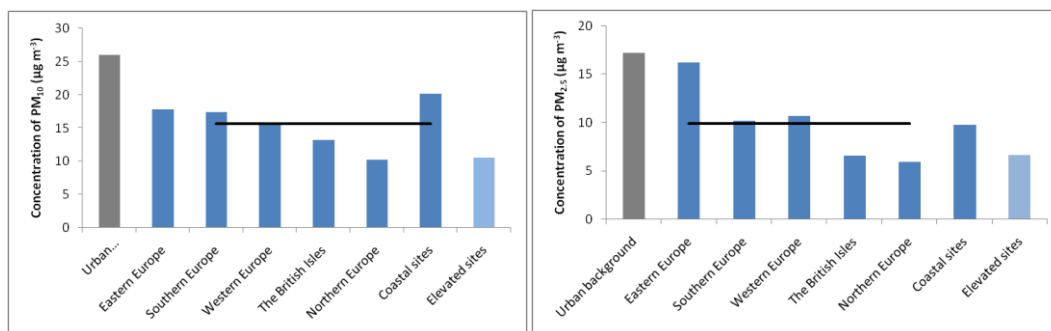
Figure 2.1: *Annual mean concentrations of PM$_{10}$ and PM$_{2.5}$ for various regions of the EMEP domain in 2008 (µg m^{-3}). Annual mean concentrations of PM$_{10}$ and PM$_{2.5}$ for European urban background sites (from AirBase) are included for comparison.*
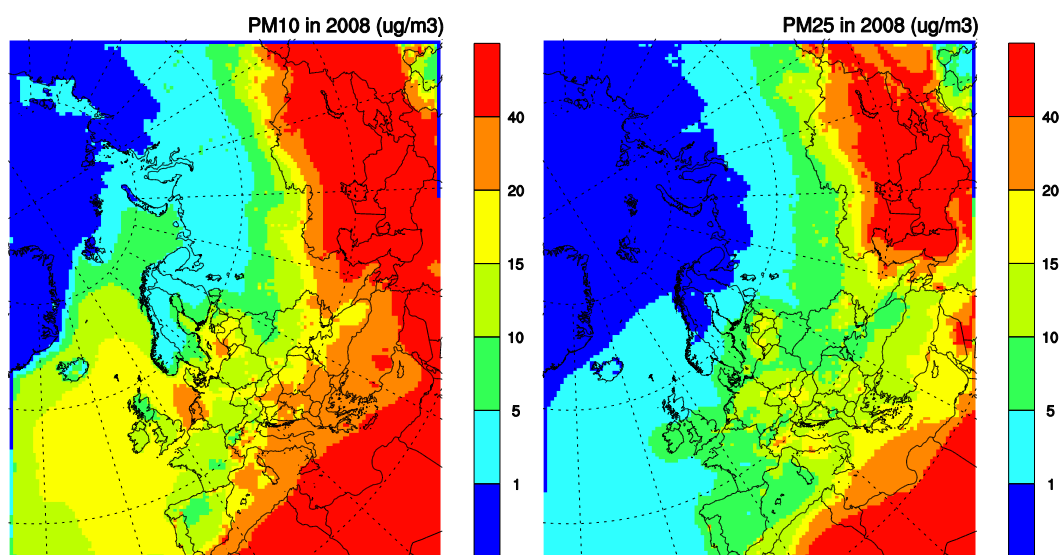
Figure 2.2: *Annual mean concentrations of PM$_{10}$ (left) and PM$_{2.5}$ (right) in 2008 based on EMEP model calculations and EMEP observation data.*

In these combined maps of EMEP model and measurements (Figure 2.1), a pronounced north to south gradient can be observed, with the annual mean PM$_{10}$ concentrations varying from 1-5 µg m^{-3} in Northern Europe to 10-25 µg m^{-3} in southern Europe. The lowest observed annual mean PM$_{10}$ concentration was observed at the Hyytiälä (FI0050R) (5.6 µg m^{-3}) site, situated in the boreal forest of Finland, whereas the highest was recorded at the Cypriote site Ayia Marina (CY0002R) (31.5 µg m^{-3}).

The concentrations seen for Southern, Eastern and Western Europe are notably higher and reflect both population density and major anthropogenic sources; e.g. the concentrations reported for Eastern Europe are > 70% higher than that seen for Scandinavia. Anthropogenic primary and secondary aerosols dominate the PM concentrations across most of Europe, whilst the influence of natural dust from Sahara and other semi-arid regions is significant in the southern parts.

Concentrations in coastal areas are found to be particularly high for PM_{10} and appear to be characterized by a high share of coarse particles, likely reflecting the influence of sea salts (see Figure 2.1).

The mean European urban background concentration of PM_{10} has been included in Figure 2.1 to give an idea of the rural background influence. 60% of the urban background concentration is likely to be attributed to the mean rural background concentration.

The annual mean concentration of $PM_{2.5}$ range from 0.5-3 µg m^{-3} in Northern Europe to 5-20 µg m^{-3} in southern Europe (Figure 2.1). Measured annual mean $PM_{2.5}$ concentrations exceeding 20 µg m^{-3} were only observed for Italy, with the highest annual mean observed at Montelibretti (IT0001R) (22.1 µg m^{-3}). Annual mean concentrations in the range $10 - 20$ µg m^{-3} were observed for all regions of the EMEP domain, except Northern Europe. The lowest levels (here: 25 percentile) were exclusively associated with sites in Northern Europe, as well as for selected high altitude sites in continental Europe. The lowest annual mean $PM_{2.5}$ concentration was observed at the Norwegian site Birkenes (3.0 µg m^{-3}). The spatial pattern of annual mean $PM_{2.5}$ concentrations largely reflects that of PM_{10} (see Figure 2.1). However, the mean concentration of $PM_{2.5}$ in coastal areas is not found to be elevated as seen for PM_{10}, thus pointing towards the influence of coarse particles, and sea salts in particular, for PM_{10}. As for PM_{10}, close to 60% of the urban background concentration is likely to be attributed to the mean rural background concentration of $PM_{2.5}$ (Figure 2.1).

The annual mean concentration of PM_1 was reported for seven sites. The highest annual mean was observed at the Austrian site Illmitz (AT0002R) (11.4 µg m^{-3}), which was five times higher than that observed at the Birkenes site (2.2 µg m^{-3}) in Norway, reporting the lowest annual mean. Only minor changes ($\pm$ 6%) were observed when comparing the annual mean concentration of PM_1 observed for 2008 with the previous year. This finding reflects the minor inter annual changes of PM_{10} and $PM_{2.5}$ at these sites as well. No model calculated PM_1 concentrations are available.

2.1.5 *PM₁₀ and PM₂.₅ in 2008 compared to 2007*

85% of the sites which reported levels of PM_{10} both for 2007 and 2008 experienced lower annual mean concentrations in 2008 compared to the previous year. The average decrease for these sites was 9%, hence, there have been two consecutive years (2007 and 2008) with a European wide decrease in the ambient PM_{10} level. Less than 10% of the sites experienced a decrease of 20% or more. The decrease in PM_{10} experienced by the majority of the sites going from 2007 to 2008 appears to be attributed to $PM_{2.5}$. Of the 15% with higher levels in 2008, the average increase was 7%. Only two of the 10 sites observed an increase exceeding 10%. The most substantial increase was observed for the Spanish site ES0012; i.e. 13% compared to 2007.

77% of the sites which reported levels of $PM_{2.5}$ both for 2007 and 2008 experienced lower annual mean concentrations in 2008 compared to 2007. For these sites the decrease was on average 17%. The most substantial decrease was observed for sites in Southern Europe. Eight out of nine sites in Spain experienced

a decrease in the annual mean > 20%, of which two observed a more than 30% decrease. Only 23% of the sites which reported levels of $PM_{2.5}$ both for 2007 and 2008 experienced higher annual mean concentrations in 2008 compared to 2007. For these sites the increase was less than 5%.

Positive and negative differences in the range of 5-15%, exceeding 25 % in some areas, are found when comparing model calculated PM_{10} and $PM_{2.5}$ concentrations for 2008 with that of 2007, reported in Report 4/2009 (EMEP, 2009b). The main causes for the changes in calculated PM concentrations for 2008 are due to changes in emissions and meteorological conditions and the applied model version, which are briefly discussed below.

Changes due to emissions There are considerable changes in emissions in 2008 compared to 2007. Both increases and decreases are reported in emissions of gaseous PM precursors and primary PM emissions going from 2007 to 2008, and for some countries the changes are quite significant (for details see Chapter 2 in EMEP Report 1/1010 (EMEP, 2010)). The changes in $PM_{2.5}$ concentrations are within 5% in most of the EMEP area. However, there are also more significant changes, e.g. a 25-35% decrease for Kyrgyzstan and Spain, 10-20% decrease for Bulgaria and Macedonia, a 70% increase for Iceland, and 10-20% increase for Romania, Slovenia, Latvia, and Georgia. The increase in $PM_{2.5}$ concentrations for Iceland and Georgia and the decrease in Kyrgyzstan and Spain are due to changes of SIA emissions, while the increase in Romania, Latvia and Slovenia and the decrease in Bulgaria are mainly due to primary $PM_{2.5}$. Regarding PM_{10} concentrations, the differences are in general somewhat smaller compared to those of $PM_{2.5}$. In some countries (e.g. Romania, Bulgaria) this is due to the opposite changes in emissions of $PM_{2.5}$ and coarse PM from 2007 to 2008. For some countries (e.g. Sweden, Lithuania, Hungary), the decrease of SIA concentrations due to SO_x, NO_x and NH_3 emission reductions was accompanied by the increase of PPM due to coarse PM emissions. This caused minor changes for the PM_{10} concentrations, whilst modifying their chemical composition.

Changes in meteorological data. Meteorological fields, which are inputs to the Unified model, also affected the calculated PM concentrations for 2008. The differences in meteorological data for 2008 compared to 2007 are due to both meteorological inter-annual variability and different meteorological models used to prepare the data. The meteorology for 2008 has been generated using the ECMWF-IFS model. This is different from the last year, when HIRLAM meteorology was used in model calculations presented in EMEP Report 4/2009 (EMEP, 2009b). The effect of inter-annual meteorological variability alone on pollutant concentrations using the same meteorological driver (notably HIRLAM) is discussed in detail in the EMEP Status Report 1/2010 (EMEP, 2010).

According to HIRLAM data, 2008 was warmer than 2007 in the northern parts of the EMEP area, with a warmer belt stretching zonally north of approximately 55°N, while to the south of 55°N 2008 was on average colder than 2007. Compared to HIRLAM, the ECMWF-IFS model predicted higher surface temperatures in northern Scandinavia and in Russia, while lower temperatures in central and southern parts of Europe in 2008. Thus, the variation in surface temperature between 2007 and 2008 is probably somewhat exaggerated in the

meteorological input to the EMEP model calculations (Figure 2.3, left). The higher surface temperature predicted by ECMWF-IFS over the Arctic part of the North Atlantic is associated with a region of relatively higher pressure. This suggests somewhat less northward transport in the ECMWF-IFS data compared to HIRLAM. Less transport to the Nordic areas in ECMWF compared to PARLAM-PS was already pointed out in EMEP (2008).
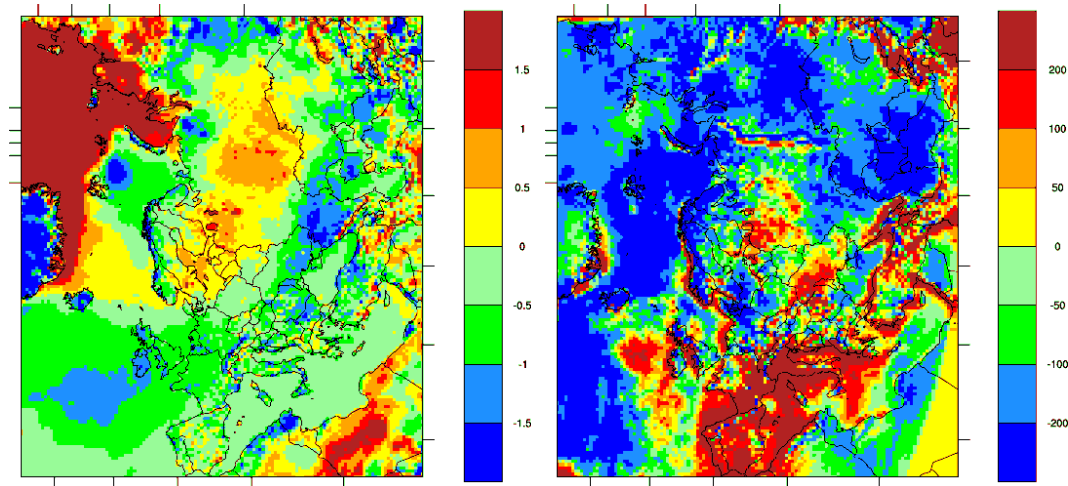

Figure 2.3: Differences between 2008 meteorology from ECMWF-IFS and 2007 meteorology from HIRLAM for 2 m temperature in °C (left) and annual accumulated precipitation in mm (right)

According to calculations with the HIRLAM model the accumulated precipitation was on average larger in 2008 than in 2007 in Europe (with exception of some central and south-eastern European countries, and eastern parts of Russia). There are two areas which received particularly much precipitation in 2008; i.e. the area covering the south of Scandinavia, the Baltic countries and north-western Russia, and one covering Portugal, Spain, France, the UK, Italy, southern parts of the Northern Atlantic and Western Mediterranean). Compared to HIRLAM, the ECMWF-IFS model calculates less precipitation for 2008 for a vast part of the EMEP area, except from southern Europe and the Mediterranean region. Figure X.3 (right map) shows the differences between precipitation calculated for 2008 and 2007 due to the combined effect of inter-annual variability and using different meteorological models. It can be seen that compared to meteorological data for 2007, considerably more precipitation and consequently wet scavenging occurs over the Mediterranean region, the European western coasts and mountain areas in 2008. At the same time, considerably less precipitation and less wet scavenging takes place over most of Central and northern Europe, Russia and Kazakhstan in 2008 than 2007. It should also be noted that ECMWF-IFS calculates more precipitation in mountain areas (e.g. the Alps, the Ural mountains) and over seas along the western and southern coasts (e.g. of Norway, the UK, Ireland, Turkey).

Overall, the annual mean surface stress in 2008 data is less than for 2007. This is mostly due to the use of ECMWF-IFS instead of HIRLAM for calculation. Surface stress affects the efficiency of dry deposition of gaseous and particulate pollutants. Furthermore, using ECMWF-IFS data yields on average less efficient

turbulent exchange compared to HIRLAM (see EMEP 1/2010 for further details). Thus, using ECMWF-ISF meteorology, the Unified model can be expected to calculate higher levels of pollutants for the lower levels, as pollutants are mixed up and dry deposited less efficiently compared to HIRLAM data.

Changes in PM due to meteorology. The effect of <u>inter-annual meteorological variability</u> on calculated PM concentrations has been studied with HIRLAM data, which are available for both 2007 and 2008. The changes in PM_{10} and $PM_{2.5}$ concentrations due to meteorological conditions in 2007 and 2008 alone are mostly between -20% and 10%, showing a general tendency of lower concentration levels in 2008 compared to 2007.

Changing <u>meteorological driver</u> from HIRLAM to ECMWF-IFS, caused an increase of PM levels by 5-30% for 2008 over much of the EMEP area. The concentrations resulting from ECMWF-IFS data show a general tendency to be higher north of 47°N and lower south of this latitude, as compared to concentrations based on HIRLAM data. Thus, the typical north-south concentration gradients are somewhat reduced when calculated with ECMWF-IFS meteorology. This is particularly true for the SIA compounds, which are more hygroscopic and thus wet scavenged more efficiently than primary PM.

On the other hand, coarse PM concentrations experience just the opposite changes from 2007 to 2008. That is, they decrease in the north and increase in the south due to meteorological variability, while they increase in the north and decrease in the south due to the use of ECMWF data compared to HIRLAM data. A closer look reveals that this is to a large degree due to the impact of coarse sea salt. Overall, the changes in PM concentrations due to changing the meteorological driver have been found to be comparable to that of the inter-annual meteorological variability from 2007 to 2008.

Changes due to both emissions and meteorology. The model calculated concentrations of PM_{10} and $PM_{2.5}$ are between 5 and 20% lower in 2008 than in 2007 for large parts of the EMEP area. In particular, PM_{10} and $PM_{2.5}$ concentrations were found to be 20-35% lower in Spain, northern Scandinavia and France, which were attributed both to lower emissions and more precipitation in those regions in 2008 compared to 2007. Areas which experienced a 5-20% increase of anthropogenic PM_{10} and $PM_{2.5}$ levels in 2008 included the UK, the North Sea and the southern part of Norway, the Adriatic region, Romania, Bulgaria, eastern Ukraine and the Caucasus area. This increase is mostly attributed to emission changes, whereas there was an additional effect of decreased precipitation in Kazakhstan, Uzbekistan, and for the southern and north-eastern parts of Russia. The 20-30% increased concentrations calculated for PM_{10} and $PM_{2.5}$ for the eastern Mediterranean, parts of south-eastern and central Europe, and for areas in the south of Russia and Kazakhstan, is attributed to an increased contribution of natural dust.

2.1.6   Trends in PM_{10} and $PM_{2.5}$

The longest time series of PM data reported to EMEP goes back to 1997; i.e. for four Swiss sites and one British. Profound inter annual variations in the PM concentrations are observed of which those associated with the peak in 2003 is the

most pronounced (Figure 2.4). PM levels for 2008 are typically lower than or equal to 2007, which was characterized by rather low concentrations in both size fractions at most sites. Trend analysis, using the Mann Kendall test, of data from sites with more than eight years of measurements and sufficient data coverage show a significant decrease for six sites (AT05, CH02, CH05, DE01, SE12, ES13) and an increase for one site (GB36) of the eighteen sites with long term PM_{10} measurements. For $PM_{2.5}$, there is a significant decrease at three (ES13, IT04, DE03) of the seven sites where trend analysis can be applied. The downward tendency in the observed annual mean concentration of PM, corresponds to a rather broad reduction in the emissions of primary PM and secondary PM precursors in Europe in the actual period.
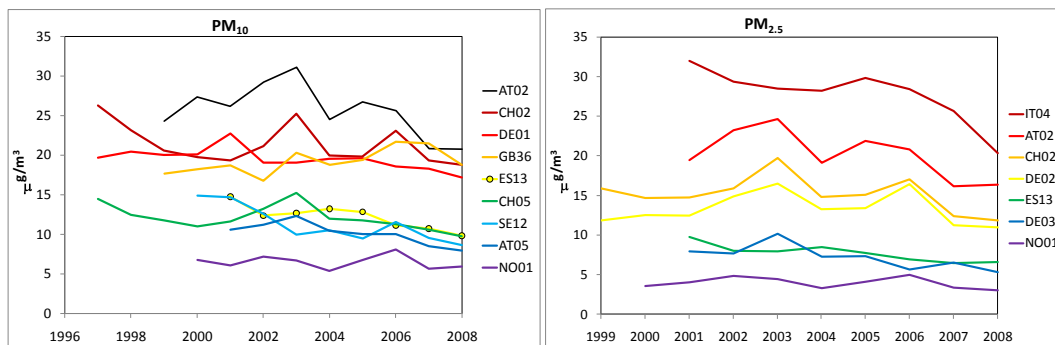

Figure 2.4: Time series of PM_{10} and $PM_{2.5}$ at selected EMEP sites.

2.1.7 PM size fractions

Table 2.1 shows the annual mean $PM_{2.5}$ to PM_{10} ratio at EMEP sites based on observational data and model calculations for 2008. The ratios have been calculated for common days, i.e. when both observational and modelled concentrations of $PM_{2.5}$ and PM_{10} were available.

There is a good agreement between modelled (0.59) and observational (0.62) data with respect to the $PM_{2.5}$ to PM_{10} ratio, when averaged over all sites. The model calculated $PM_{2.5}$ to PM_{10} ratio for 2008 is somewhat lower than for 2007. The fine fraction of PM has not changed much, but the concentrations of coarse PM are higher compared to 2007. This increase is mainly due to a higher concentration of coarse NO_3^- due to modifications in the dry deposition scheme of the model, as documented in EMEP (2010), but also coarse sea salt and mineral dust, which were calculated with the current model version rv3.6 compared to rv3.1 last year, made a contribution to the observed shift in the $PM_{2.5}$ to PM_{10} ratio.

From the observations, the fraction of fine PM (i.e. $PM_{2.5}$ to PM_{10} ratio) is on average smaller for the southern sites compared to the northern and central European ones. This is a confirmation of the dominating role of anthropogenic sources in northern and central Europe, in contrast to the substantial influence of windblown dust in southern Europe. The model calculates lower $PM_{2.5}$ to PM_{10} ratios for both southern and northern sites compared to the sites in central Europe. It should be noted that there may be non-negligible uncertainties in the calculated coarse PM, which can be associated with uncertainties in emissions of coarse PM, especially from fugitive industrial and agricultural sources. Re-suspended road

dust, which is considered an important sources of coarse particles, has not been included in the calculations. With respect to natural sources, there are considerable uncertainties in modelling of wind blown dust from semi-arid areas, arable lands and other erosive surfaces. Also, primary biogenic aerosols, which may contribute significantly to the coarse aerosol mass in certain regions, were not accounted for in the model calculations.

Table 2.1:   Observed and model calculated annual mean PM ratios at EMEP sites in 2008.

		Site	$PM_{2.5}/PM_{10}$ Obs	$PM_{2.5}/PM_{10}$ Mod	PM_1/PM_{10} Obs	$PM_1/PM_{2.5}$ Obs
Northern Europe	Norway[1]	NO01	0.51	0.51	0.41	0.75
	Sweden	SE11[2]	0.72	0.51		
		SE12	0.71	0.43		
		SE14	0.43	0.46		
	Finland	FI50	0.83	0.56	0.65	0.77
Central / Western Europe	Austria	AT02	0.79	0.75	0.58	0.73
	Switzerland	CH02	0.60	0.74	0.50	0.84
		CH05	0.69	0.73	0.63	0.87
	Czech Rep.	CZ03[2]	0.84	0.72		
	Germany	DE02	0.69	0.65	0.41	0.60
		DE03	0.73	0.73		
		DE44	0.76	0.71		
	Great Britain	GB36	0.53	0.52		
		GB48	0.44	0.46		
	France	FR09[2]	0.62	0.70		
		FR13[3]	0.76	0.62		
Eastern Europe	Latvia	LV10	0.65	0.49		
		LV16	0.68	0.57		
Southern Europe	Spain	ES07	0.58	0.42		
		ES08	0.51	0.46		
		ES09[2]	0.66	0.58		
		ES10	0.44	0.47		
		ES11	0.49	0.53		
		ES12	0.39	0.61		
		ES13	0.65	0.56		
		ES14	0.60	0.61		
		ES16	0.58	0.55		
		ES1778	0.63	0.73	0.51	0.79
	Italy	IT01	0.70	0.59		
South-Eastern Europe	Slovenia	SI08	0.65	0.73		
	Cyprus	CY02	0.47	0.54		
Average			0.62	0.59	0.53	0.76

1) Estimated based on weekly data;   2) Up to 50% data coverage;   3) 37 days with data

2.1.8   *Exceedances of EU limit values and WHO Air Quality Guidelines in the regional background environment in 2008*

The EMEP model calculates regional background PM concentrations. EU limit values for PM for protection of human health and WHO Air Quality Guidelines (AQGs) for PM apply to PM concentrations for so-called zones, or agglomerations, in rural and urban areas, which are representative of the exposure of the general population. Clearly, the rural and urban PM levels are higher than then that of the background values calculated with the regional model due to the influence of local sources. However, comparison of model calculated PM_{10} and

$PM_{2.5}$ with EU limit values and WHO AQGs can provide an initial assessment of air quality with respect to PM pollution, flagging the regions where already the regional background PM is in excess of the critical values.

The EU limit values for PM_{10} (Council Directive 1999/30/EC) are 40 μg m^{-3} for the annual mean and 50 μg m^{-3} for the daily mean. The daily mean should not be exceeded more than 35 times per calendar year.

The WHO AQGs (WHO, 2005) are:
for PM_{10}: < 20 μg m^{-3} annually, 50 μg m^{-3} 24-hour (99th percentile or 3 days/year)
for $PM_{2.5}$: < 10 μg m^{-3} annually, 25 μg m^{-3} 24-hour (99th percentile or 3 days/ year).

The combined model and observation maps show that the annual mean regional background PM_{10} concentration in 2008 was below the EU limit value of 40 μg m^{-3} in most of Europe, with the exception of the most southern European parts and the EECCA countries (Figure 2.2). However, the annual mean PM_{10} concentrations calculated by the model exceeded the WHO recommended AQG of 20 μg m^{-3} in the Netherlands. Calculated PM_{10} concentrations were also found to be in excess of 20 μg m^{-3} in the southern parts of the Mediterranean basin and in the EECCA countries due to the influence of windblown dust from deserts and semi-arid soils. The regional background annual mean $PM_{2.5}$ concentrations were above the WHO recommended AQG value of 10 μg m^{-3} in the same areas as seen for PM_{10}, but additionally also for several countries in Central and Eastern Europe.

Figure 2.5 and Figure 2.6 show the model calculated number of days exceeding 50 μg m^{-3} for PM_{10} and 25 μg m^{-3} for $PM_{2.5}$ in 2008, respectively. To illustrate the relative importance of man-made and natural particulates in the deterioration of air quality, Figure 2.5 and Figure 2.6 show separately the exceedance maps for total PM (left panel) and for PM from anthropogenic sources only (right panel). For most of Europe, except from southern parts of Spain, Italy, Greece, and Turkey, and for certain areas in northern Italy and the EECCA countries, PM_{10} did not exceed 50 μg m^{-3} more than 35 days in the rural background (i.e. the EU limit value). However, in a rather extensive area, except from Northern Europe and the north of Russia, PM_{10} exceeded 50 μg m^{-3} more than for the 3 days recommended by the WHO. Furthermore, the WHO AQG for $PM_{2.5}$ is exceeded by regional background concentrations for more than 3 days in most EMEP countries, except from Scandinavia and northern Russia. Figure 2.5 and Figure 2.6 illustrate the significant contribution from natural dust to the calculated exceedances of the EU limit values and the AQGs for PM_{10} and $PM_{2.5}$.
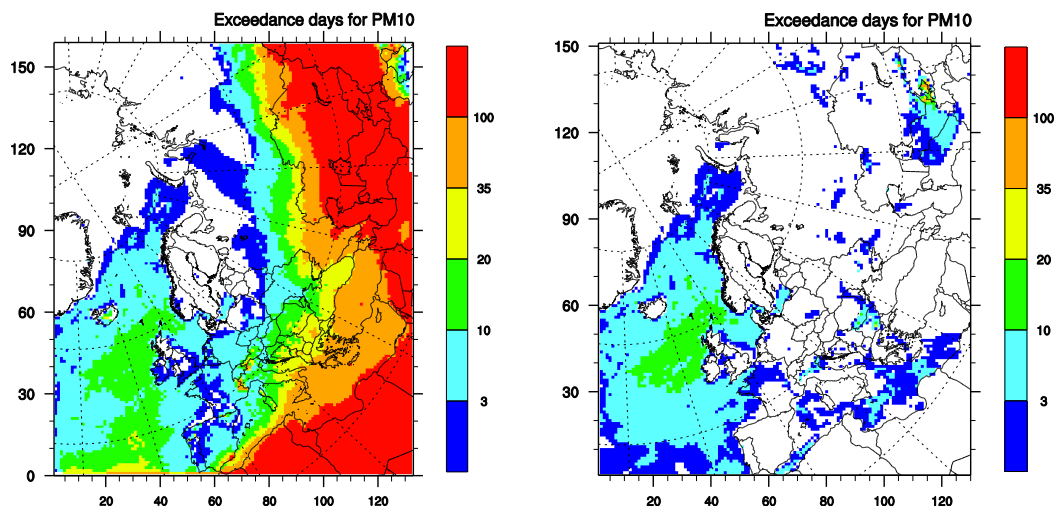
Figure 2.5: *Calculated number of days with PM$_{10}$ exceeding the WHO AQG of 50 μg m^{-3} in 2008: for total PM$_{10}$ (left) and for anthropogenic PM$_{10}$ (right). Note: EU Directive requires that no more than 35 days exceed the limit value, while the WHO AQG recommendation is not to be exceeded more than 3 days.*
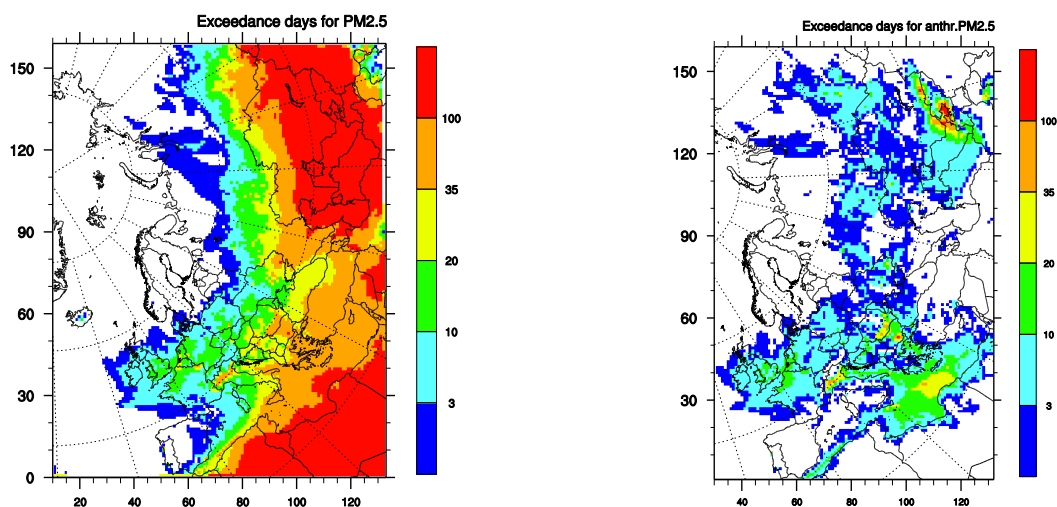
Figure 2.6: *Calculated number of days with PM$_{2.5}$ exceeding the WHO AQG of 25 μg m^{-3} in 2008: for total PM$_{2.5}$ (left) and for anthropogenic PM$_{2.5}$ (right). Note: the WHO AQG recommendation is not to be exceeded more than 3 days.*

Based on model and measurements data, we have calculated the number of days which exceeded the WHO AQGs in 2008 at EMEP sites. The observed and calculated numbers of exceedance days, as well as the number of common exceedance days, i.e. the days for which observed PM exceedances were also predicted by the model, are presented in Table 2.2.

Table 2.2: Number calculated and observed days exceeding the WHO AQGs (50 $\mu g\ m^{-3}$ for PM_{10} and 25 $\mu g\ m^{-3}$ for $PM_{2.5}$) at EMEP sites.

	PM_{10}				$PM_{2.5}$			
	Obs	Model	Common	Hit ratio	Obs	Model	Common	Hit ratio
AT02	19	9		0	54	11	8	15
AT05	0	9		0				
AT48	2	10	2	100				
CH01	1	7		0				
CH02	14	6	1	7	27	10	5	19
CH03	9	11	1	11				
CH04	2	6		0				
CH05	2	8	1	50	5	9	1	20
CY02	41	67	28	68	24	62	19	79
CZ01	2	4		0				
CZ03	2	6		0	11	8	1	9
DE01	5	0		0				
DE02	5	2		0	24	5	2	8
DE03	0	4		0	0	7		0
DE07	1	1		0				
DE08	0	4		0				
DE09	1	0		0				
DE44	8	4		0	47	11	9	19
ES07	13	28	5	38	5	2		0
ES08	3	18	1	33	8	1	1	13
ES09	2	3		0	2	0		0
ES10	3	1		0	1	1		0
ES11	5	4	2	40	0	0		0
ES12	7	4	2	29	0	0		0
ES13	0	1		0	1	0		0
ES14	5	4		0	7	1		0
ES16	3	2		0	1	0		0
ES1778	4	2	1	25	7	7	1	14
FI50	0	0			0	0		
FR09	0	2		0	2	11	1	50
FR13	0	2		0	0	8		0
FR15	0	3		0				
GB06	0	1		0	3	13	2	67
GB36	2	0		0	0	4		0
GB43	1	0		0				
GB48	0	0		0				
GR02	0	84		0				
HU02	33	11	2	6				
IE31					4	4	1	25
IT04					86	32	18	21
LV10	16	0		0	55	0		0
LV16	18	0		0	42	0		0
MD13	29	13	1	3				
NL07	10	2		0				
NL09	4	3		0				
NL10	10	2		0				
NL91	10	2		0				
PL05	4	1		0				
SE11	0	0		0	2	0		0
SE12	0	0		0	7	0		0
SE14	2	1		0	2	2	1	50
SE35	0	0		0				
SI08	0	6		0	9	7	2	22

Hit ratio (%) shows the percentage of observed exceedance days correctly predicted by the model (common_days/obs_days x100%).

For about half of the sites, the model under-predicts the number of exceedance days for PM_{10} and $PM_{2.5}$. In particular, the model under predicts the exceedance days for PM_{10} for Dutch, Polish, Danish, Italian, and some of the German and Swiss sites, but also for AT02, ES07, GB36, and FR09. The under-prediction of the number of exceedance days for $PM_{2.5}$ occurs mostly at the same sites as for PM_{10}. While the model overestimates the number of exceedance days for about 40% of the sites for PM_{10}, this is only observed for a limited number of sites for $PM_{2.5}$.

The "Hit ratio" in the table shows the percentage of observed exceedance days correctly predicted by the model. The hit ratios is found to vary a substantially (from 0 to 100%) between the sites. The average hit ratio of exceedance days is slightly better for PM_{10} (35%) than for $PM_{2.5}$ (30%). On the other hand, non-zero hit ratio is achieved for 50% of the sites for $PM_{2.5}$, but only for 25% of the sites for PM_{10}.

2.1.9 *Evaluation of the model performance for PM in 2008*

Compared to the model version used for last year's reporting (2007), several modules in the Unified EMEP model have been updated. The main updates concern the chemical scheme, the schemes for dry deposition of gases and particles, and calculations of the turbulent diffusion coefficient and mixing height. A more detailed documentation of the model changes can be found in the EMEP Status Report 1/2010 (EMEP, 2010). Furthermore, the changes in the model performance for 2008 compared to that of 2007 are also due to changing the meteorological driver (see chapter 2.1.5). In addition, the observational data set for 2008 is different from that of 2007, as the number of monitoring stations has changed. The ability of the EMEP model to reproduce observed PM concentrations for 2008 has been evaluated. The calculated concentrations of PM_{10}, $PM_{2.5}$ and the main aerosol components have been compared to observed concentrations at EMEP sites in 2008.

Overall statistic analysis Table 2.3 provides a summary of annual and seasonal statistical analysis of model results versus EMEP monitoring data for 2008. In addition to the traditionally used statistical parameters, i.e. Mean values, Relative Bias, Root Mean Square Error and correlation, also the Index of Agreement (IOA) has been included. IOA can be interpreted as a difference measure of the degree to which the observed value is accurately estimated by the calculated value. The IOA says something about the degree to which the model predictions are error free and varies from 0.0 (theoretical minimum) to 1.0 (perfect agreement).

There are changes in the model performance for some of the aerosol components compared to model evaluation for 2007 (EMEP, 2009b). The largest changes are for NO_3^-, SIA and PM_{10}, for which the model underestimation is decreased. This is mostly related to higher concentrations of coarse NO_3^- calculated by the model, and to some extent sea salt. It should be noted that though the changes in dry deposition parameterisation for gaseous components had an appreciable effect on HNO_3 and consequently NO_3^- concentrations, the concentrations of SO_2 were much less affected because its lifetime is much shorter compared to that of HNO_3.

Table 2.3: *Annual and seasonal comparison statistics between EMEP model calculated and EMEP observed concentrations of PM_{10}, $PM_{2.5}$, SIA, SO_4^{2-}, NO_3^- and NH_4^+ for 2008. Note that for "Annual mean", only sites with a data coverage larger than 50% are included.*

Period	N sites	Obs (ug/m³)	Mod (ug/m³)	Rel.Bias,%	RMSE	R	IOA
PM_{10}							
Annual mean	49	15.6	10.7	-31	7.39	0.57	0.68
Daily mean	49	15.5	10.5	-33	15.52	0.46	0.64
Jan-Feb	46	17.7	14.9	-16	7.69	0.60	0.67
Spring	47	15.1	10.5	-30	9.46	0.57	0.71
Summer	49	15.2	7.6	-50	9.39	0.51	0.56
Autumn	48	15.4	10.9	-29	6.38	0.69	0.72
PM_{25}							
Annual mean	29	10.1	5.8	-43	5.60	0.56	0.60
Daily mean	29	10.1	5.7	-44	8.96	0.57	0.69
Jan-Feb	27	13.1	8.2	-38	7.56	0.85	0.75
Spring	27	9.7	4.9	-50	6.79	0.39	0.57
Summer	28	9.2	4.0	-56	6.06	0.24	0.44
Autumn	29	9.5	5.9	-39	4.91	0.73	0.69
SO_4^{2-}							
Annual mean	58	1.7	1.0	-42	0.97	0.64	0.65
Daily mean	58	1.7	1.0	-42	1.60	0.54	0.69
Jan-Feb	57	1.8	1.2	-34	1.16	0.60	0.71
Spring	58	1.8	0.8	-54	1.17	0.54	0.53
Summer	58	1.6	0.9	-45	0.92	0.72	0.65
Autumn	53	1.5	0.9	-40	0.98	0.66	0.71
NO_3^-							
Annual mean	31	1.5	1.6	11	0.79	0.67	0.80
Annual mean	31	1.4	1.5	14	2.23	0.55	0.72
Daily mean	30	2.2	2.9	32	1.58	0.65	0.77
Jan-Feb	31	1.6	1.3	-19	0.87	0.69	0.77
Spring	31	1.0	0.7	-29	0.62	0.71	0.72
Summer	26	1.3	1.9	46	1.21	0.63	0.74
NH_4^+							
Annual mean	38	0.8	0.6	-25	0.35	0.80	0.83
Daily mean	38	0.8	0.6	-25	0.82	0.64	0.78
Jan-Feb	37	1.1	1.0	-10	0.46	0.78	0.87
Spring	38	0.9	0.6	-38	0.48	0.76	0.71
Summer	38	0.6	0.4	-41	0.35	0.76	0.74
Autumn	33	0.7	0.6	-13	0.38	0.74	0.85
SIA							
Annual mean	26	4.0	3.2	-20	1.64	0.78	0.84
Daily mean	29	4.0	3.2	-20	3.91	0.61	0.77
Jan-Feb	28	5.3	5.2	-3	5.53	0.63	0.79
Spring	29	4.2	2.6	-37	3.60	0.59	0.71
Summer	29	3.2	2.0	-39	2.71	0.56	0.69
Autumn	24	3.6	3.5	-3	3.94	0.63	0.78

Here, Ns – the number of stations, Obs – the measured mean, Mod – the calculated mean, Bias is calculated as $\Sigma(Mod-Obs)/Obs \times 100\%$, RMSE – the Root mean Square Error= $[1/Ns\Sigma(Mod-Obs)^2]^{1/2}$, R – the tempo-spatial correlation coefficient between modelled and measured daily concentrations and spatial correlation for seasonal mean concentrations. IOA=$1-(\Sigma(Mod-Obs)^2 / \Sigma(|Mod-<Obs>|+\Sigma|Obs-<Obs>|)^2)$

Averaged over the entire year, the model has a small positive bias of 11% for NO_3^- compared to the negative bias of -28% for 2007. As a result, the negative bias for SIA has decreased from -34% for 2007 to -20% for 2008. The model underestimates for 2008 SO_4^{2-} by 42 % and NH_4^+ by 25 %, which is a small improvement compared to 2007.

The annual mean spatial correlation between calculated and observed concentrations of all secondary inorganic components for 2008 appears somewhat

lower (or about the same) compared to 2007. However, the changes from 2007 to 2008 in correlations for different seasons are rather variable.

The average underestimation of PM_{10} for 2008 is 31%, which is less than the 43% underestimation reported for 2007, while $PM_{2.5}$ is underestimated by 43%. The annual mean spatial correlation between calculations and measurements is 0.57 for $PM_{10,}$ while it is 0.56 for $PM_{2.5}$. These results are somewhat poorer than those for 2007. Among the outliers are the new stations LV0010R and LV0016R, for which the model under-prediction is about a factor of 3 for PM_{10} and about a factor of 5 for $PM_{2.5}$. Also, PM concentrations for SE0035R and IE0035R ($PM_{2.5}$) are underestimated by nearly 50%.

On a seasonal basis, the systematic underestimation of PM_{10} and $PM_{2.5}$ is largest for summer, and also for spring for $PM_{2.5}$. For both PM_{10} and $PM_{2.5}$, the correlation is better for winter and autumn than for spring and summer.

The IOA parameter shows that the model reproduces the observed PM_{10} and $PM_{2.5}$ concentrations with an accuracy of 68% and 60% respectively. For SIA compounds, the IOA is 65% for SO_4^{2-}, 80% for NO_3^- and above 80% for NH_4^+ and SIA. These results are considered fairly good.

Individual stations The statistical analysis of model calculated PM_{10} and $PM_{2.5}$ versus daily observations at individual sites are summarised in Tables A.1 and A.2 in the Appendix. Note that for several sites (shaded grey), only weekly measurements were available, while for Swedish and British sites hourly concentrations of PM_{10} and $PM_{2.5}$ measured with TEOM were averaged to 24-hour concentrations.

There is a great deal of spreading in the statistical parameters of the model performance for the individual sites. The model tends to overestimate PM_{10} and $PM_{2.5}$ for mountain sites, e.g. CH0001R, AT0005R, and AT0048R, due to a relatively coarse grid resolution. The normalised RSM Errors are also relatively large for these sites. A substantial overestimation is also seen for the Greek site GR0002R, but only data for May through July was available for this site. The greatest model underestimation is found for two Latvian sites (LV0010R and LV0016R), where also the correlation is rather poor, especially for PM_{10}. Otherwise, the correlation between calculated and measured concentrations is mostly between 0.5 and 0.7 for $PM_{2.5}$ and between 0.35 and 0.65 for PM_{10}. Averaged over all sites, the model bias is -26% for PM_{10} and -38% for $PM_{2.5}$, whereas the temporal correlation between model results and observations is 0.5 and 0.6 respectively.

2.2 Problems and considerations concerning measurements of PM with automated measurement systems (AMS)

By Robert Gehrig

Exposure to ambient air fine particles (PM_{10}, $PM_{2.5}$) is a matter of concern in almost all regions of Europe and even worldwide due to their adverse effects to human health. The respective limit values given by the European directives are often exceeded and a substantial part of the population is thus exposed to excessive concentrations of PM. Therefore, reliable measurements of fine particles (PM_{10}, $PM_{2.5}$) in ambient air are of prime importance. In order to ensure reliability and comparability of PM measurements all over Europe, strict requirements for QA/QC are of crucial importance. According to a new requirement of the recent European air quality directive 2008/50/EC, all EU member states are obliged to monitor $PM_{2.5}$ at urban background sites. Based on these data the trend of the so-called national Average Exposure Indicator (AEI) has to be determined over the next 10 years. Because these trends may be quite small the measurements have to be as accurate as possible and have to satisfy very high requirements concerning long-term consistency of the measurements.

To obtain these requirements is a substantial challenge. To give an example, severe difficulties have recently been reported by several countries using TEOM-FDMS monitors during long-term comparability of data with the gravimetric reference method, as defined by EN 12341 (for PM_{10}) and EN 14907 (for $PM_{2.5}$). TEOM-FDMS monitors are widely used in European networks in order to obtain high time resolution measurements and to reduce the work load and personal cost of the manual gravimetric reference method. After extended periods of good comparability with the reference method increasing deviations were observed for initially unknown reasons. These deviations were only detected at sites with collocated gravimetric measurements. Figure 2.7 gives a typical example of the situation from two sites of the Swiss National Monitoring Network (NABEL). After comprehensive tests performed by the producer, it turned out that the difficulties were probably caused by a new dryer system.

The example shows that PM data series based alone on measurements with the automated monitoring system (AMS) not always provide sufficiently homogenous long-term data series for a reliable analysis of trends.

The EU commission, as well as AQUILA - the European union of national reference laboratories and monitoring network operators - expressed their deep concern about this situation and urgently recommended:

- For measurements of the AEI exposure measurements of $PM_{2.5}$, the standard reference method shall be used where possible.

- Not to use new instruments for PM until the demonstration of equivalence is available.

- Current instrumentation may be used on the decision of the National Reference Laboratories and more rigorous QA/QC procedures shall be introduced as soon as possible.
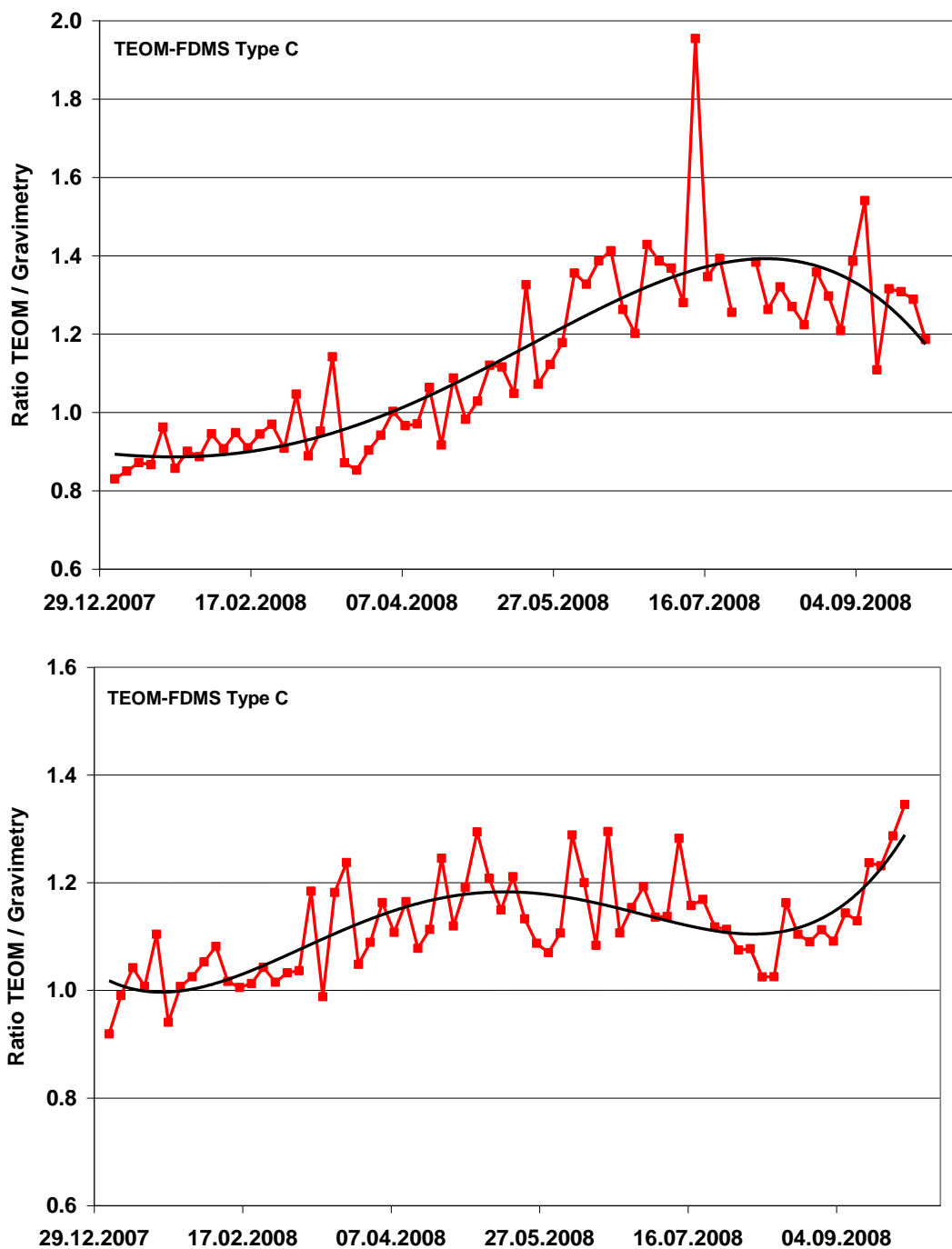
Figure 2.7:   Ratio of TEOM FDMS vs. gravimetry for PM$_{10}$ measurements at two Swiss urban NABEL sites (Lausanne above, Lugano Bottom).

The difficulties reported above for the TEOM-FDMS monitoring system are just an example. Generally, AMS for PM cannot yet be considered to provide sufficiently stable data over long time periods without periodic comparison with the reference method. Therefore, an Ad-hoc group of CEN TC 264 WG15 is currently preparing a Technical Specification giving guidance how to operate AMS for PM. This will include requirements for periodic comparison of the AMS with the gravimetric reference method.

40

Also in EMEP PM has received increasing attention during the past years and international comparability as well as homogeneity of long term data series is essential. Therefore, the following conclusions can be drawn for EMEP:

- Also within EMEP, the gravimetric reference method should be used where possible for measurements of PM. When using AMS periodic comparison campaigns with the reference method should be performed.

- In the existing data base, correct documentation of metadata for PM (e.g. used methods) is crucial.

- When comparing PM data from different sites or analyzing long term trends, considerations concerning data homogeneity are very important.

2.3   Contribution of primary particles, secondary inorganic aerosols (SIA), sea salt and base cations to PM mass

By Wenche Aas and Svetlana Tsyro

The modelled PM_{10} and $PM_{2.5}$ concentrations include primary PM and secondary inorganic aerosols (SIA) from anthropogenic precursor emissions, sea-salt and windblown dust from natural sources and particulate water. Note that the model calculated PM does not include secondary organic aerosols (SOA), causing a bias in the calculated relative contribution of SIA and the other inorganic species to PM mass.

In the EMEP measurement programme, speciation of PM has historically been focused on the secondary inorganic constituent (SIA), which are known to have a long range transport potential; i.e. sulphate, ammonium and nitrate. Thus, the majority of the EMEP Parties have measured these ions for decades. In 2008, concurrent measurement of sulphate and PM_{10} is performed at a total of 34 sites. At the majority of these sites, SO_4^{2-} is collected using a sampler with an undefined cut-off, whereas at a few sites a sampler with a PM_{10} inlet is applied. The sampling conditions are similar for nitrate and ammonium, but these variables are collected at somewhat fewer sites; i.e. 27 for NO_3^- and 20 for NH_4^+. However, this doesn't reflect the total picture of the number of sites performing reactive nitrogen measurements, as there are almost 50 sites measuring nitrate as the sum of NO_3^- and HNO_3 and more than 40 measuring ammonium as the sum of NH_4^+ and NH_3; though not all of these sites do have concurrent PM measurements. For details see the EMEP/CCC data report (Hjellbrekke and Fjæraa, 2010). It should be noted that only IT01 and Netherlands measure NO_3^- and NH_4^+ using the recommended denuder method. The method used at the other sites may give a positive artefact due to absorption of NH_3 or HNO_3 or a negative artefact due to evaporation of NH_4NO_3. Also base cations, sea salt ions and mineral dust are part of the monitoring programme, but only a few countries are currently reporting data. 12 sites measure the three major sea salt ions (Na^+, Cl^- and Mg^{2+}). Mineral dust is mainly measured during intensive measurement periods and typically at sites in southern Europe. For a few selected sites, these various chemical species, along with EC and OC, has been used to attempt a mass closure of the PM mass loading (see chapter 2.6).

Anthropogenic primary and secondary aerosols dominate the PM concentrations across most of Europe, whilst the influence of natural dust from Sahara and other semi-arid regions is significant in the southern parts of the model domain (see Figure 2.8). The maps show that SIA typically prevail over primary emissions for PM_{10}. However, the relative importance of primary PM increases significantly for PM_{10} in the vicinity of major urban agglomerates due to substantial emissions from traffic and residential heating. Maps of the individual SIA concentrations are found in EMEP status report 1/2010 (EMEP, 2010). The average relative contribution of SO_4^{2-} to PM_{10} and NO_3^- to PM_{10} based on the data reported for 2008 are quite comparable; i.e. 12±4% for SO_4^{2-} and 11±5% for NO_3^-, though the spatial distribution of sulphate and nitrate is somewhat different. For NH_4^+ the relative contribution to PM_{10} based on observations was 6±2%. The contribution

of sea salt is very dependent on distance to the sea, i.e. 0.6% at the continental site Illmitz (AT02) in Austria and 18% at Birkenes (NO01) in southern Norway.

The modelled data show in general somewhat higher relative contribution of SIA to PM_{10} than that based on observations, and also greater variation. This is partly due to the model underestimating the PM mass concentration, although also SIA is underestimated by the model by 20% (see Table 2.3). Furthermore, the measurement sites are not uniformly distributed within the EMEP domain, and the relative contribution in some of the most polluted areas may differ from what stated above, i.e. there are no sites in the southeast of Europe where the model shows the highest sulphur concentrations. For nitrate and ammonium the spatial pattern is similar for both model and observations with the highest contribution seen for central Europe.

There are only six sites with a full year of chemical speciation in the fine fraction. For sites with concurrent chemical speciation measurements in both size fractions, the relative contribution of SIA which is somewhat lower for PM_{10} than for $PM_{2.5}$. This is to be expected as most of these ions reside in the fine fraction of PM_{10}. To be able reflect on the European spatial resolution of SIA contribution to $PM_{2.5}$, it necessary to look at the model results. SIA accounts for more than 30 % of $PM_{2.5}$ in most of Europe, and a substantial 40-45% for parts of Central and Eastern Europe. This is consistent with the EMEP sites in central Germany (DE0044R) and Northern Italy (IT0004R), reporting a ~ 40% contribution of SIA to $PM_{2.5}$. For the easternmost part of the EECCA region, the SIA contribution to $PM_{2.5}$ is substantial less (10-20%) (Figure 2.8).
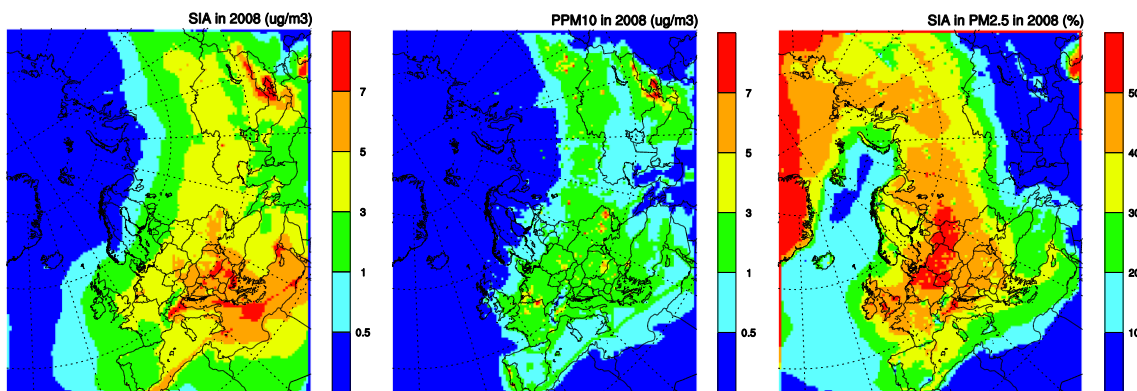

Figure 2.8:   Annual mean concentrations of SIA (left), primary PM_{10} (middle), and relative contribution (in %) of SIA to $PM_{2.5}$ (right) for 2008, calculated using the EMEP model.

Time series of the relative contribution of the individual SIA constituents to PM_{10} were examined for those sites reporting such data for a period of seven years or more (Figure 2.9). The relative contribution of SO_4^{2-} was found to be rather consistent until the last two-three years where several sites show a clear reduction in the relative contribution of sulphate. For nitrate and ammonium there is no clear tendency and there is a relatively large inter-annual variability. Note that Germany has several sites with long time series of concurrent SIA and PM mass

concentrations, but that these are not included due to lack of reported filter pack data for several months in 2008.
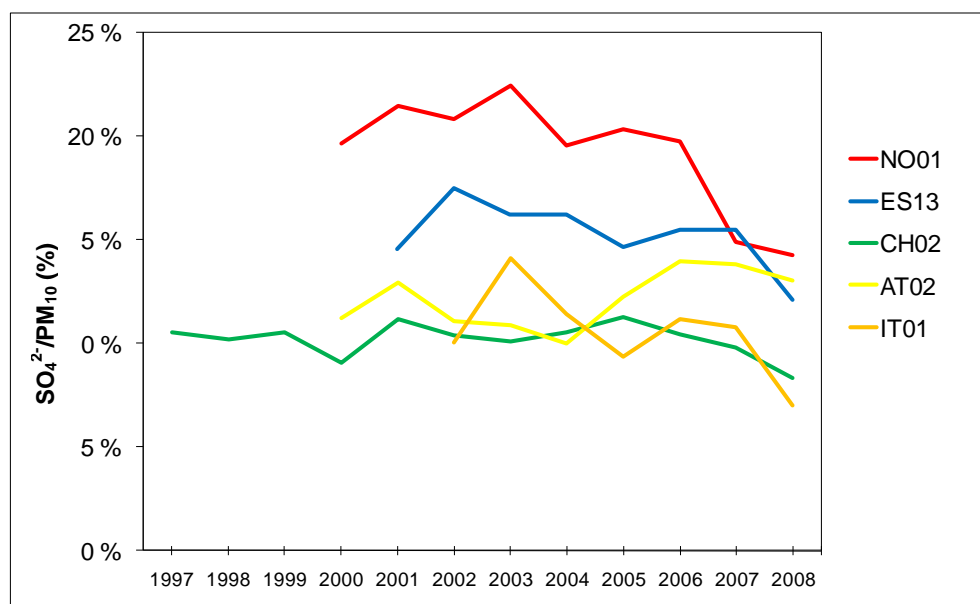

Figure 2.9: Time series showing the observed relative contribution of SO_4^{2-} to PM_{10}. Unit: %.

2.4 Elemental and Organic Carbon

2.4.1 *Status of sampling and measurement, and quality of observation data*

By Karl Espen Yttri

There is a lack of comparable EC/OC data in Europe, which makes it difficult to address the spatial and temporal variation of these variables on the regional scale. At present, only the EMEP EC/OC campaign (Yttri et al., 2007), and the CARBOSOL project (Pio et al., 2007), with data for the period 2002 – 2004, can be used for such a purpose. More recent measurements are needed to get an overview of the current situation, and to validate the progress made with respect to model development.

Table 2.4: Sites reporting EC and OC, including size fractions and sampling period.

Site (Country)	EC	OC	PM$_{2.5}$	PM$_{10}$	Period
Birkenes (Norway)	x	x	x	x	2001, 2002, 2003, 2004, 2005, 2006, 2007, 2008
Ispra (Italy)	x	x	x		2002[1], 2003[2], 2004[2], 2005[2], 2006, 2007, 2008
Melpitz (Germany)	x	x	x	x	2006, 2007, 2008
Montseny (Spain)	x	x	x	x	2007, 2008
Pay de Dome (France)	x	x	x		2008
Cambisabalos (Spain)	x	x	x	x	2008
Aspvreten (Sweden)	x	x		x	2008
Vavihill (Sweden)	x	x		x	2008

1. EMEP EC/OC campaign
2. Both PM$_{2.5}$ and PM$_{10}$.

An increased number of countries and sites have been expected to start reporting levels of EC and OC with the development of the unified EUSAAR protocol. Eight countries reported measurements of EC and OC for 2008, which is twice the number for 2007, i.e. measurements performed at the sites Pay de Dome (France), Cambisabalos (Spain), Aspvreten and Vavihill (both Sweden) are reported for the first time for 2008. See Table 2.4 for all sites reporting levels of EC and OC for 2008. In addition, total carbon (TC) was reported for the Hungarian site K-Puszta. Seven of the eight sites listed in Table 2.4 used the EUSAAR2 thermal protocol (Cavalli et al., 2010) for EC/OC analyses, being an important step towards harmonized and comparable data for EC and OC within EMEP. Within the two latest EMEP intensive measurement periods, all EC/OC data were analyzed using the EUSAAR2 analytical protocol. A detailed description of the EUSAAR2 thermal protocol and its performance was published in the journal Atmospheric Chemistry and Physics previously this year (Cavalli et al., 2010) and is thereby made available to the scientific community. The EUSAAR2 thermal protocol has already been used for other site categories than that of the rural background, and it is one of the candidate methods to be tested for a standardized method for EC/OC measurements within CEN. Particular concern should be made regarding EC/OC

data obtained by other than thermal-optical analysis methodology, which do not account for charring of OC during analysis. For 2008, this concerns the German site Melpitz, only, for which the EC concentration is grossly overestimated.

Only the analytical part of the EUSAAR protocol is finalized at present, as some challenges still remain concerning the design of the "artefact-free" sampling train. Comparable data, in particular for OC, require that both the analytical and the sampling protocol are harmonized, which currently is not the case. The variability amongst the various sampling approaches used is apparent from the variables listed in Table 2.5. Most sites sample for 24 hours, whereas the sampling time range from 48 hours to one week for low loading sites such as Birkenes and Pay De Dome. From the datasets it is apparent that the combination of low ambient levels and 24 hour sampling time cause poor data capture for certain sites, particularly with respect to EC. Only one site (Aspvreten) attempted to account for both positive and negative sampling artefacts, whereas three used a denuder to account for positive artefacts. 50% of the sites did not address sampling artefacts on a regular basis.

Table 2.5:   *Sampling equipment and analytical approach used at the sites reporting EC and OC to EMEP for 2008.*

Site (Country)	Sampling time/frequency	Filter face velocity	Sampling equipment	Analytical approach
Birkenes (Norway)	7 days, weekly	54 cm s^{-1}	Single filter (no correction)	Sunset TOT (EUSAAR-2)
Ispra (Italy)	24 hr, daily	20 cm s^{-1}	Denuder (pos. artifact)	Sunset TOT (EUSAAR-2)
Melpitz (Germany)	24 hr, daily	54 cm s^{-1}	Single filter (no correction)	VDI 2465 Part 2
Montseny (Spain)	24 hours, irregular	54 cm s^{-1}	Single filter (no correction)	Sunset TOT (EUSAAR-2)
Pay de Dome (France)	48 hours, weekly	69 cm s^{-1}	Denuder (pos. artifact)	Sunset TOT (EUSAAR-2)
Cambisabalos (Spain)	24 hours, weekly	54 cm s^{-1}	Single filter (no correction)	Sunset TOT (EUSAAR-2)
Aspvreten (Sweden)	24 hr, daily	54 cm s^{-1}	Denuder/Backup filter pos/neg artifact	Sunset TOT (EUSAAR-2)
Vavihill (Sweden)	Irregular, irregular	54 cm s^{-1}	Denuder (pos. artifact)	Sunset TOT (EUSAAR-2)

50% of the sites performed concurrent measurements of EC and OC in PM_{10} and $PM_{2.5}$. Such data do not only provide valuable information on the size distribution of these variables, but could also add to the understanding of sources and atmospheric processes. An overview of the annual mean EC/OC/TC concentration reported for 2008 are shown in Table 2.6.

Since 2009, i.e. data from 2007, EC/OC data are reported to EBAS according to the EUSAAR format. We have experienced that this is somewhat more challenging than the previous format, as it is more complex and requires the addition of quite a few meta-data. This complexity is needed in order evaluate upon the comparability of various dataset. We are continuously working to improve this but we assume that reporting of EC and OC will not be substantially much easier until a unified protocol for EC and OC is ready.

An effort to establish a large and harmonized dataset which goes beyond the ordinary EC/OC/TC measurements when addressing the carbonaceous content of the rural background aerosol has been made in the two most recent EMEP intensive measurement periods. A brief introduction and some preliminary results from this effort are presented in chapter 3.1.2 of the current report.

Table 2.6: *Annual mean concentrations of EC, OC and TC for 2008. Only sites which reported for more than 6 months have been included.*

	EC PM$_{10}$ (µg C m^{-3})	OC PM$_{10}$ (µg C m^{-3})	TC PM$_{10}$ (µg C m^{-3})	EC/TC (%)	EC PM$_{2.5}$ (µg C m^{-3})	OC PM$_{2.5}$ (µg C m^{-3})	TC PM$_{2.5}$ (µg C m^{-3})	EC/TC (%)
Aspvreten (Sweden)	0.22	1.6	1.8	14				
Birkenes (Norway)	0.14	0.84	0.98	14	0.12	0.63	0.75	16
Vavihill (Sweden)	0.18	1.3	1.5	12				
Melpitz (Germany)	1.3	2.7	4.0	34	1.3	1.8	3.1	42
Ispra (Italy)					1.7	7.0	8.7	22
Pay de Dome (France)					0.18	0.93	1.1	17
Montseny (Spain)	0.29	1.6	1.9	17	0.23	1.3	1.5	17
Campisábalos (Spain)	0.17	2.4	2.6	7	0.14	2.1	2.2	6

2.4.2   Northern Europe

2.4.2.1   EC and OC levels at the Swedish sites Aspvreten (SE0012R) and Vavihill (SE0011R)

Measurements of EC and OC in PM$_{10}$ were performed at the two Swedish sites Aspvreten (SE0012R) and Vavihill (SE0011R). Vavihill is situated in an area dominated by grass and farm land and within 25 – 45 km distance from densely populated areas such as Greater Malmö (630 000 inhabitants), and Greater Copenhagen (1.9 mill inhabitants). Aspvreten is located approximately 80 km south of Greater Stockholm (2 mill inhabitants) at the Baltic Sea coast. By the inclusion of these two sites the sites measuring EC/OC in Scandinavia has been extended along an Eastern transect. Due to rather poor data coverage (in particular for SE0011R), e.g. there are no samples for the period January – April, the annual mean concentration will be biased, and any seasonal variability will be indicative only.

As expected, the EC and OC levels are amongst the lowest reported for Europe, thus confirming the findings by Yttri et al. (2007). The EC levels are higher in winter compared to summer, i.e. 40% higher in winter at the Aspvreten site, whereas OC are found to be 20% higher in summer (here: Aspvreten). An increased influence of biogenic sources in summer is a likely explanation for the observed summertime increase of OC. The different seasonal variation for EC and

OC cause a substantial difference in the EC/TC ratio, which is nearlyly a factor of 2 higher in winter (18%) compared to summer (10%) (here: Aspvreten).

2.4.2.2   EC and OC levels at the Norwegian site Birkenes (NO0001R)

The Birkenes site is situated approximately 20 km from the Skagerrak coast in the Southern Norway and is commonly influenced by episodes of transboundary air pollution from continental Europe and thus frequently used to study long-range air pollution. Nevertheless, annual mean concentrations of EC and OC at Birkenes are considered amongst the lowest in Europe (Yttri et al., 2007), a finding which is confirmed for 2008 as well (See Table 2.6).

The concentration of OC is always higher during summer compared to winter at Birkenes. This seasonal variation is seen both for PM_{10} and $PM_{2.5}$, but it is more pronounced for PM_{10} than for $PM_{2.5}$. This is at least partly attributed to the increased levels of $OC_{PM10-2.5}$ in summer, which likely stems from primary Biological Aerosol Particles (PBAP). For EC, the concentration tends to be higher in winter both for PM_{10} and $PM_{2.5}$, but this is not a consistent pattern. Rather, a peak of EC is observed in spring, which likely is associated with an increased influence of long range transport from continental Europe. The opposite seasonal variation for EC and OC leads to a substantial change in the EC/TC ratio, being close to and more than two times higher in winter compared to summer for $PM_{2.5}$ and PM_{10}, respectively.

The majority of OC (approximately 75%) in PM_{10} can be attributed to the fine fraction on an annual basis. Fine OC makes a less contribution to OC in PM_{10} in summer and fall, which is attributed to PBAP (Yttri et al., 2007), mainly residing in the coarse fraction of PM_{10}. During summer, coarse OC may actually be the major fraction, accounting for more than 50% of OC in PM_{10} on a monthly basis. EC is almost exclusively associated with $PM_{2.5}$ throughout the year.

Birkenes is somewhat unique in a European context as it has a continuous time series of EC, OC, and TC for PM_{10} and $PM_{2.5}$ using thermal optical analysis going back to 2001 (See Figure 2.10). Given its strategic position it is well suited to monitor the outflow of air pollutants from the European continent, and the time series of the carbonaceous content of PM_{10} and $PM_{2.5}$ closely resemble that of the secondary inorganic constituents. This resemblance appears to be greater for $PM_{2.5}$ than for PM_{10}. This is likely attributed coarse mode PBAP contributing to PM_{10}, which typically have a more local than regional origin. From 2007 to 2008 there was less than 10% reduction in OC for PM_{10} and $PM_{2.5}$; previously inter annual variation in the OC concentration ranging between 30-40% has been reported. There was a 50% reduction in the annual mean EC concentration going from 2007 to 2008. Such a substantial reduction in EC has not previously been reported.
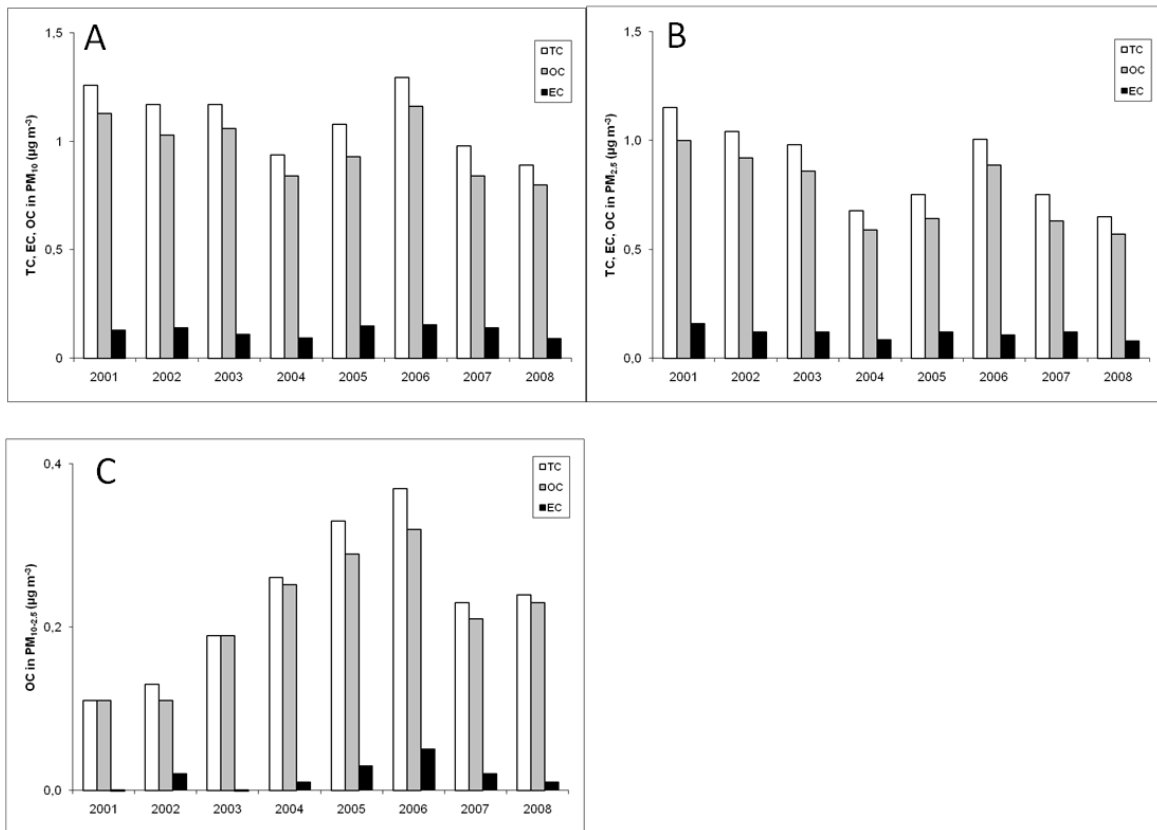
Figure 2.10: Annual mean concentrations of EC, OC and TC in PM$_{10}$ (A), PM$_{2.5}$ (B) and PM$_{10-2.5}$ (C) at the Norwegian site Birkenes for the period 2001 – 2008.

Figure 2.11 shows the relative contribution of TCM [(TCM = Total carbonaceous matter (TCM = OC x 1.7 + EC x 1.1)] to PM$_{10}$, PM$_{2.5}$ and PM$_{10-2.5}$ at Birkenes for the time-period 2001 – 2008. The relative contribution of TCM to PM$_{10}$ and PM$_{2.5}$ typically shows a modest annual variation, with the exception of 2001 - 2002, ranging between 25 – 29% for PM$_{10}$ and 30 – 36% for PM$_{2.5}$. The relative contribution of TCM-to-PM$_{2.5}$ has the same temporal pattern as for TCM-to-PM$_{10}$, A slight decrease in TCM to both PM$_{10}$ and PM$_{2.5}$ was observed for 2008 compared to 2007. The relative contribution of TCM to PM$_{10-2.5}$ ranged from 9-21% for the actual period. While TCM-to-PM$_{10-2.5}$ increased substantially from 2001–2004, corresponding to the major increase in the OC$_{PM10-2.5}$ concentration shown in Figure 2.10C, the relative contribution have declined slightly again from 2004 and onwards.
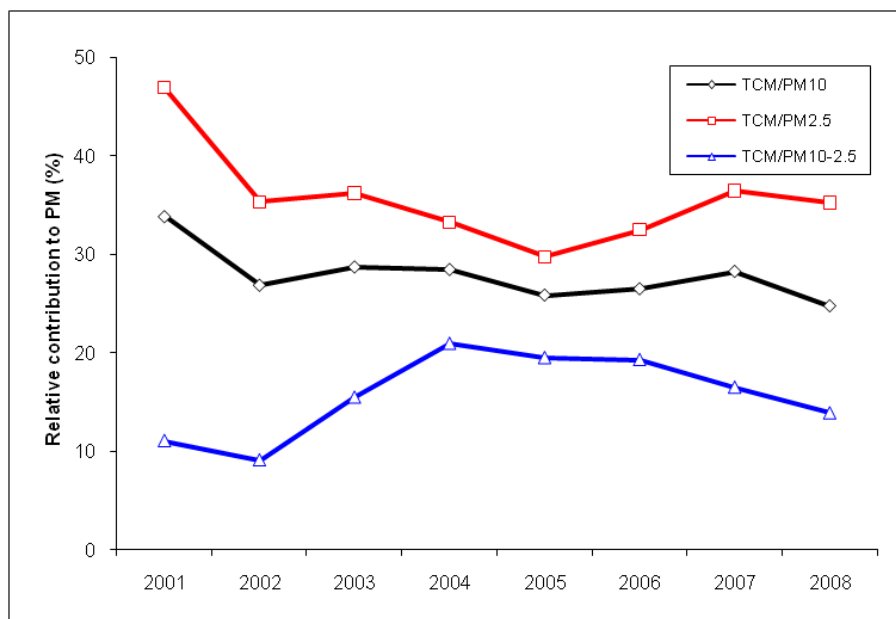
Figure 2.11: Relative contribution of TCM (Total Carbonaceous Matter) to PM$_{10}$, PM$_{2.5}$ and PM$_{10-2.5}$.

2.4.3 Central Europe

2.4.3.1 EC and OC levels at the German site Melpitz (DE0044R)

The German site Melpitz, situated in an agricultural area and surrounded by meadows and farm land, has reported annual mean concentrations of EC, OC and TC for three consecutive years (2006 - 2008). Using the VDI protocol for analysis, levels of EC and OC reported for Melpitz cannot be compared to those obtained by thermal-optical analysis (here: EUSAAR2); i.e. 7/8 sites listed in Table 2.5. VDI does not correct for charring of OC during analysis, thus artificial EC generated during the analysis grossly overestimates the true EC concentration in the sample. This is apparent from the fact that the EC/TC ratio for Melpitz is 2-7 times higher than that reported for the other sites listed in Table 2.6. It should be noted that the discrepancy might not be entirely attributed to the different analytical protocols but partly also reflect the various influence of EC at the different sites. Despite the erroneous feature of the VDI protocol, the results could still provide useful information concerning seasonal variation and time trends. However, it will introduce uncertainties in mass closure studies, i.e. by overestimating EC and underestimating OC. Finally, TC obtained by VDI is comparable to TC obtained by thermal-optical methods. In fact, Melpitz reported the highest annual mean TC in PM$_{10}$ for 2008 (Figure 2.6). For PM$_{2.5}$, only the TC levels reported for Ispra were higher than that of Melpitz, however there is a substantial gap in the TC concentrations between these two sites.

The levels of EC, OC and TC were slightly reduced or unchanged for PM$_{10}$ in 2008 compared to 2007, whereas for PM$_{2.5}$ the levels were increased by approximately 20%.

Table 2.7:   Annual mean concentrations of EC, OC, and TC in PM$_{10}$, PM$_{2.5}$ at the German site Melpitz (DE0044R) for the period 2006 - 2008 ($\mu g\ C\ m^{-3}$).

Year	PM$_{10}$			PM$_{2.5}$			PM$_{10-2.5}$[1]		
	EC	OC	TC	EC	OC	TC	EC	OC	TC
2006	2.3	3.1	5.4	1.9	2.1	4.0	0.9	1.1	2.0
2007	1.6	2.7	4.3	1.1	1.5	2.6	0.6*	1.1*	1.8*
2008	1.3	2.7	4.0	1.3	1.8	3.1	0.3*	1.0*	1.0*

1) Annual mean concentrations of EC, OC and TC in PM$_{10-2.5}$ are based on concurrent 24 hour measurements of EC, OC and TC in PM$_{10}$ and PM$_{2.5}$ for which the difference between EC, OC and TC in PM$_{10}$ and PM$_{2.5}$ is ≥ 0.

The majority (75%) of the carbon content in PM$_{10}$, here measured as TC, was associated with fine aerosols (PM$_{2.5}$) supporting that carbonaceous aerosol typically is combustion derived or is the result of atmospheric secondary formation. This finding corresponds with that observed for 2006, but is substantially different from that of 2007, when only 60% of TC was accounted for by the fine fraction of PM$_{10}$. The pronounced seasonal variation of fine (high in winter) and coarse (high in summer) OC (and TC) observed for 2007 (see EMEP, 2009, Figure 2.19) was not as pronounced for 2008. This suggests a change in source strength of e.g. PBAP, and/or that artefacts associated with the VDI "thermal only" approach has been less profound. Nevertheless, changing to a thermal-optical method would minimize potential artefacts and would help further interpretation of the sources of the carbonaceous aerosol at this site, as well as making it possible to compare results for EC and OC with that of other sites.

2.4.4   Southern Europe

2.4.4.1   EC and OC levels at the Spanish sites Montseny (ES1778R) and Cambisábalos (ES0009R)

Measurements of EC and OC in PM$_{10}$ and PM$_{2.5}$ were performed at the two Spanish sites Montseny (ES1778R) and Campisábalos (ES0009R). Both sites are situated at relatively high altitude; i.e. 720 m asl for Montseny and 1360 m asl for Campisábalos. Montseny is situated 25 km from the Mediterranean coastline, whereas Campisábalos is a continental site. The annual mean concentration of EC (see Table 2.6) are in the lower range of what has been reported for the European rural background environment (e.g. by Yttri et al., 2007 and Puxbaum et al., 2007), and is comparable to that observed in the Scandinavian countries and certain high altitude European continental sites. The EC concentration increased by a substantial 30-40% in winter at Montseny. This seasonality of EC along with a substantially higher annual mean concentration of EC at Montseny compared to Campisábalos, might be attributed to air masses passing over the nearby city of Barcelona, situated no more than 40 km to the North-east of Montseny. The different seasonal variation of EC and OC (see text below) at Montseny cause a factor of two difference for the EC/TC ratio, being 22% on average in summer compared to 11% in summer.

The OC level at Montseny and Campisábalos are both considered low and are comparable, or slightly higher, than that of the upper range observed for

Scandinavia. OC has a pronounced seasonality, with concentrations increased by 60-70% in summer compared to winter (Figure 2.12). This is observed for both sites. For Montseny we find that not only $PM_{2.5}$ both also $PM_{10-2.5}$ contributes to the elevated levels in summer, while for Campisábalos the quality/capture of the dataset does not allow us to conclude upon this. The seasonal size distribution of OC could suggest a certain influence of PBAP to the coarse fraction of PM_{10}, along with a most likely dominating contribution of SOA to the fine fraction. Interestingly, the OC level at Campisábalos is 50 - 60% higher compared to Montseny, while the EC level is 40% less. The very low annual mean EC/TC ratio at Campisábalos, 6 - 7%, indicates that biogenic sources dominate. There is no pronounced correlation observed between EC and OC for the two sites, suggesting influence of various sources.
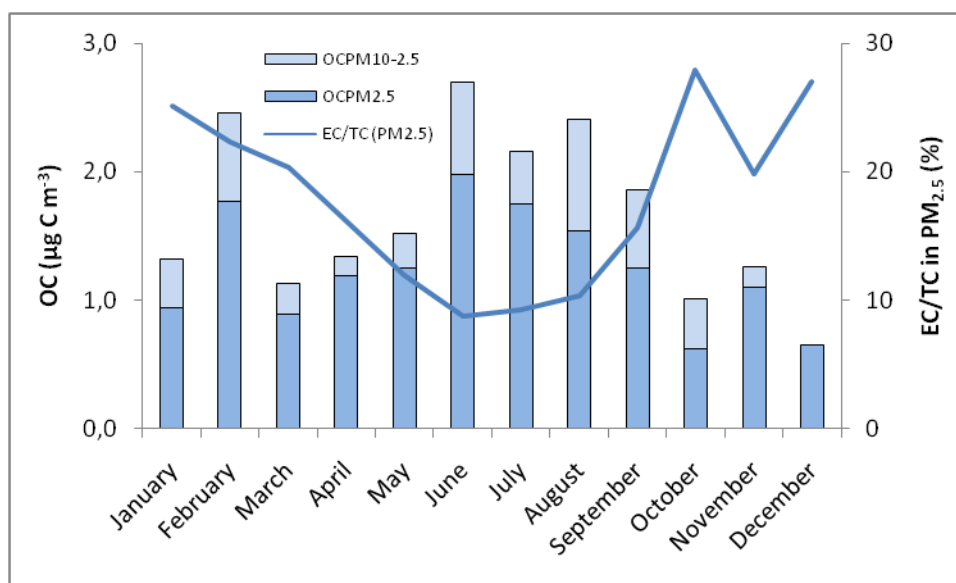
Figure 2.12: Seasonal variation of OC and the EC/TC ratio at the Spanish site Montseny (ES1778R) for 2008. Elevated concentration of both coarse ($PM_{10-2.5}$) and fine OC ($PM_{2.5}$) is observed in summer. The EC/TC ratio is a factor of two higher in winter compared to summer, caused both by increased EC levels in winter as well as by increased levels of OC in summer.

2.4.4.2 EC and OC levels at the French site Puy de Dome (FR0009R)

Measurements of EC and OC in $PM_{2.5}$ was performed at the site Puy de Dome (FR0030R) (1465 m asl) situated in a mountainous area in Central France. The annual mean EC concentration at Puy de Dome falls between that of the two Spanish sites, and is thus considered low, being comparable to levels reported for Scandinavia. The annual mean OC concentration is lower compared to the Spanish sites and even for two of the Scandinavian sites (See Table 2.6). The OC concentration increased by a factor of two in summer compared to winter, which could suggest and influence of secondary carbonaceous aerosols. On the other hand, EC increased by a factor of 1.7 in summer as well. Thus, it is likely that a substantial part of this seasonal variation is attributed to Puy de Dome being most

of the time in the free troposphere in winter, whereas during summer it is more likely to be influenced by emissions in the planetary boundary layer.

2.4.4.3   EC and OC levels at the Italian site Ispra (IT0004R)

The Italian site Ispra (IT0004R) (209 m asl) is situated in the Po Valley in the north-western part of Italy. The site is representative for the rural parts of the densely populated central Europe. The annual mean concentrations of EC, OC and TC observed at Ispra are much higher than that reported for other European rural background sites (see Table 2.6 and Yttri et al., 2007), and is attributed to the severe regional air pollution characterizing the Po Valley region. E.g. the annual mean TC concentrations is a factor of 3 higher at Ispra than for the site with the second highest TC level listed in Table 2.6. The carbonaceous aerosol at Ispra has a particularly pronounced seasonal variation with severely elevated levels in winter, having a profound influence on the annual mean. The highest monthly mean of TC (22 μg C m^{-3} for February) is a factor of seven higher than the month with the lowest mean concentration (3 μg C m^{-3} for July). Note that the summer time increase of OC seen for quite a few of the other regional background sites is not observed at Ispra, as it likely is being camouflaged by a substantial anthropogenic contribution.
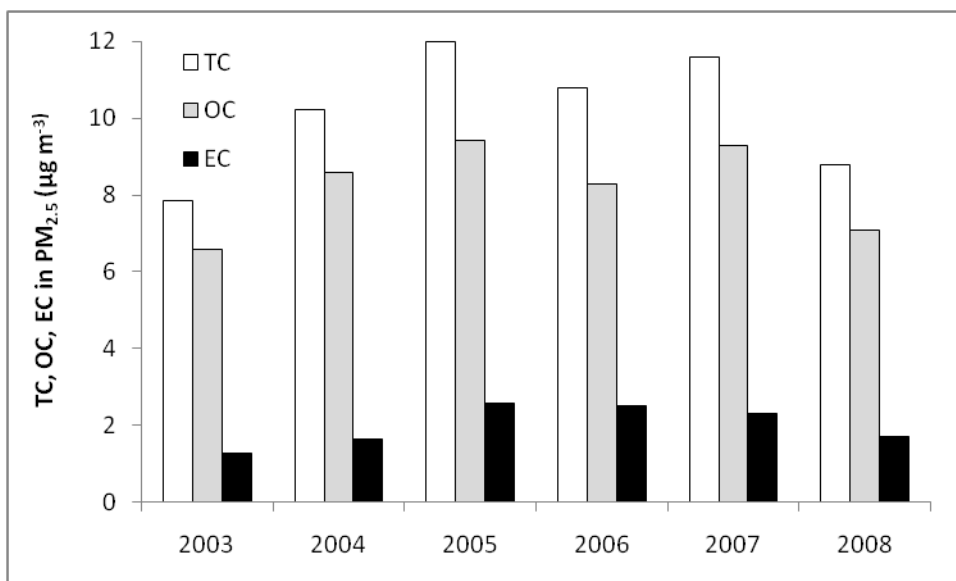
Figure 2.13: Annual mean concentrations of EC, OC and TC in PM$_{2.5}$ at the Italian site Ispra (IT0004R) for the period 2003 – 2008.

Ispra has a time series of EC, OC, and TC in PM$_{2.5}$ using thermal optical analysis going back to 2003 (Figure 2.13). During this period inter annual variations of 30% has been reported for TC for consecutive years. For 2008 there was a substantial 25% decrease in the carbonaceous aerosol concentration (here: EC, OC and TC) compared to the previous year, which is in the same size range as that observed for the PM$_{2.5}$ mass concentration (21% decrease).

2.4.4.4 Concluding remarks

The lack of a harmonized sampling- and analytical measurement protocol has been the main concern in our effort to establish a reliable picture of the regional distribution of the carbonaceous aerosol concentration within EMEP. For 2008, 7 out of 8 sites reported levels of EC and OC using the recently developed EUSAAR2 thermal protocol, being an important step towards harmonized and comparable data for EC and OC within EMEP. Fully comparable data require that also the sampling protocol is harmonized, which is currently not the case. Some challenges still remain before an "artefact-free" sampling train can be taken into service. There is a substantial variation (more than one order of magnitude) in the carbonaceous aerosol concentration within the European rural background environment, as well as with respect to its seasonality. This calls for a rapid increase in the number of sites measuring this variable on a continuous basis. The substantial increase in number of sites reporting EC, OC and TC for 2008 (8) compared to 2007 (4), is thus highly encouraging. Complementary analyses of e.g. organic tracers and ^{14}C, along with AMS-measurements are necessary to reveal the sources of particulate carbonaceous matter. With such analysis being the main focus of the joint EMEP/EUCAARI Intensive Measurement Periods, it is fair to argue that we are about to make substantial improvement in our understating of the sources contributing to the carbonaceous aerosol in the European rural background environment. Without such knowledge, effective abatement strategies cannot be cannot be initiated.

2.5 Organic aerosol modelling in EMEP: Recent Developments

By Robert Bergström and David Simpson

2.5.1 Introduction

The EMEP model for particulate carbonaceous matter (PCM) is an extension of the standard EMEP MSC-W photochemistry model. In the EMEP PCM model, a scheme for secondary organic aerosol (SOA) formation, from biogenic and anthropogenic VOCs, and gas/particle partitioning of semi-volatile organic compounds, using the volatility basis set (VBS) approach, are added to the modelled primary emissions of elemental carbon (EC) and organic aerosol (POA).

The new VBS based EMEP PCM model was introduced in Simpson et al. (2009), and during the last year it has been further developed and tested for longer time periods (2002-2003 and 2007-2008). In this chapter some new results are presented.

2.5.2 Emissions

Carbonaceous aerosol emissions from anthropogenic sources are taken from the emission inventory by Denier van der Gon et al. (2010), prepared as part of the EUCAARI project (Kulmala et al., 2009). The EC and OC emissions in the inventory are separated in three size classes but in the present EMEP PCM model only two classes are used, i.e. PM-fine (up to 2.5 μm) and PM-coarse (10-2.5 μm). Further details about the EC/OC emissions are given in Simpson et al. (2009).

Biogenic emissions of terpenes and isoprene are calculated by the model using the emissions algorithms of Guenther et al. (1995); for details see Simpson et al. (1999). Emissions from vegetation fires are taken from the Global Fire Emission Database (GFEDv2, van der Werf et al., 2006; Giglio et al., 2003; Tsyro et al., 2007). Other anthropogenic emissions, including VOC-emissions, are taken from the standard EMEP emission inventory.

2.5.3 EMEP-VBS PCM models, and results

Donahue and co-workers introduced the use of a volatility basis set (VBS) to help models cope with both the wide range of aerosol concentrations (C_{OA}) in the atmosphere and the ongoing oxidation of semi volatile organics in both the gas and particle phases (see, e.g., Donahue et al., 2006 and 2009). The VBS consists of a group of lumped compounds with fixed saturation concentrations (C^*, μg/m^3), comprising up to 9 bins separated by one order of magnitude each in C^* at 300 K. Using the VBS, different SOA-forming reactions can be mapped onto the same set of bins over the range of organic aerosol mass concentration typical of ambient conditions (0.1–100 μg m^{-3}) while maintaining mass balance for more volatile co-products as well. Aging reactions within the VBS can be added easily if the kinetics and volatility distribution of the products can be measured or estimated.

A number of different VBS-based models have been used for modelling organic aerosol in North America (e.g., Robinson et al., 2007; Lane et al., 2008 a,b; Shrivastava et al., 2008; Murphy and Pandis, 2009) and the present versions of the

EMEP PCM models for Europe are based on the VBS parameterisations used in the American studies.

Four versions of the EMEP PCM model are compared in this report. Different aspects of the VBS approach are tested. Various assumptions about aging reactions of OA-components in the gas phase are investigated. The model versions are summarised in Table 2.8.

Table 2.8: Summary of EMEP VBS versions.

Version	POA Emissions Partitioning?	Aging? (k_{OH} reaction rates [cm^3 molecule^{-1} s^{-1}])
VBS-NP	No (nonvolatile POA)	None
VBS-PAP	Yes	POA (4.0×10^{-11})
VBS-PAPA	Yes	POA (4.0×10^{-11}), ASOA (1.0×10^{-11})
VBS-PAPS	Yes	POA (4.0×10^{-11}), ASOA and BSOA (4.0×10^{-12})

The first model version, VBS-NP, uses the SOA scheme of Lane et al. (2008a), which includes SOA formation from anthropogenic VOC, isoprene, and terpene species, using four volatility bins. Primary organic aerosol (POA) emissions are assumed non-volatile, taken directly from the EUCAARI emission data-set.

The VBS-PAP (VBS-NP + partitioning and aging of POA emissions) model introduces three important changes to the treatment of emissions, following suggestions of Shrivastava et al. (2008):

i.   The emitted POA is distributed over different volatilities (9-bin VBS) and hence partitions between the gas and particulate phase. Essentially, this allows a large fraction of the POA to evaporate.

ii.   The POA emissions are assumed to be accompanied by emissions of low-vapour pressure (i.e. partitioning) gases, which are currently not captured in either the POA or the VOC inventories. Following Shrivastava et al. (2008) we assume that the total emissions of condensable material (including POA) amount to 2.5 times the POA inventory. We use the same partitioning coefficients as in Shrivastava et al. (2008) to calculate how much of this material is condensed at any given moment.

iii.   Aging reactions for the gaseous part of the POA emissions are included, similar to that done by Shrivastava et al. (2008). POA compounds in the gas phase are allowed to react with OH, with each reaction resulting in a shift of the compound to the next lower volatility bin.

The third model version, VBS-PAPA, is similar to VBS-PAP but also includes aging reactions for anthropogenic SOA (ASOA) in the gas phase, using an OH-reaction rate for ASOA of 1×10^{-11} cm^3 molecule^{-1} s^{-1}, based on Murphy and Pandis (2009).

The VBS-PAPS model includes gas phase aging of both anthropogenic and biogenic SOA as well as POA. This version uses an order of magnitude slower OH-reaction rate for SOA (4×10^{-12} cm^3 molecule^{-1} s^{-1}) than for POA, as suggested by Lane et al. (2008b).

Figure 2.14 shows model results for organic carbon (OC) concentrations in PM$_{10}$ for three of the stations participating in the EMEP EC/OC campaign in 2002-2003 (Yttri et al., 2007). The model treating the primary OA emissions as non-volatile (VBS-NP) gives similar results to the VBS-PAP scheme, which partitions the emissions between the gas and particle phase and include aging of the gaseous part. The aging reactions (and the assumed larger total emissions) compensate the fact that a lot of the POA evaporates at emission. VBS-PAP gives higher OM concentrations in the southern parts of the model domain (not shown), especially over the Mediterranean Sea, where the oxidation rate is higher than in the north. In some high emission areas (e.g. St. Petersburg and Paris) the VBS-PAP model gives lower yearly average OM concentrations than the VBS-NP model. Introducing aging reactions for SOA (the VBS-PAPA and VBS-PAPS schemes), gives much higher concentrations of OM than the two first schemes. Including aging reactions for biogenic SOA (VBS-PAPS) has a larger impact on OM concentrations than the effect of aging of anthropogenic SOA in most of Europe.

Model performances vary between stations. It seems clear that the VBS-PAPS version overestimates OC in summer at most locations. This observation is similar to what Lane et al. (2008b) found for rural areas in eastern USA; they showed that including aging reactions for SOA lead to serious overestimation of OC concentrations there and they suggest that although aging reactions for SOA components do occur the effect may not be a net increase in particle mass since decomposition reactions may compete with substitution reactions. The other model versions give lower OC concentrations, closer to observed levels.

For the winter months, all model versions give similar (fairly low) OC concentrations. For two of the measurement sites, Ispra (not shown) and Illmitz, the EMEP PCM models underestimate winter and early spring concentrations of OC severely. Similar underpredictions were noted by Simpson et al. (2007), and were shown to result from problems with significant contributions of wood-burning to OA, which were not accounted for in the model. It is not possible to say at this stage if such contributions are a local problem or reflect more wide-spread problems with the wood-burning inventories.
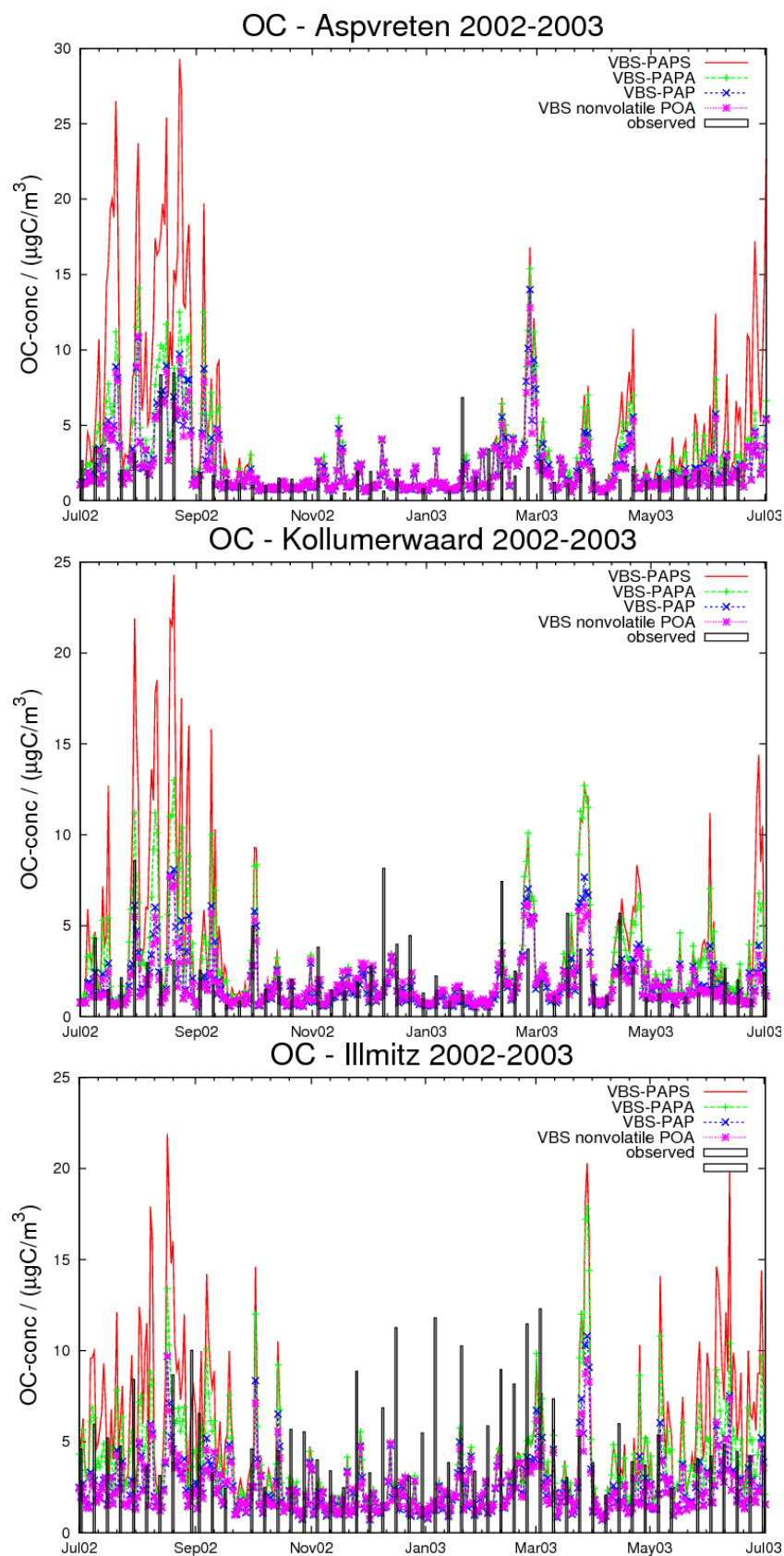
Figure 2.14: Daily average OC concentrations during the EMEP EC/OC campaign conducted in 2002-2003. Results are shown for three stations. EMEP-VBS model results and observed concentrations. Unit: µg C m^{-3}.

2.5.4 *Caveats, Conclusions and Future Work*

This chapter has presented an overview of ongoing activities and some preliminary results. The VBS models are computationally efficient and, with suitable choices reaction parameters for aging reactions for semi-volatile OA components, it seems possible to reproduce total OC measurements rather well, at least for parts of Europe.

However, large uncertainties still exists for SOA modelling (see Hallquist et al., 2009, for a discussion of the sources and formation mechanisms for SOA), and it is not yet clear if the models reproduce the measurements for the right reasons. The biogenic emissions are very uncertain and in the present version of the EMEP PCM model we do not include emissions of sesquiterpenes or any *primary* biological particles. The combined uncertainties of emissions and model parameters means that it, presently, is impossible to use "only" models to reliably describe the organic aerosol over Europe. Measurement data are crucial to constrain and validate the models and emissions. Field measurements of different types and at different locations are needed. Source-apportionment studies and chemically detailed measurements (such as AMS-measurements) are especially important.

The main future plans for the EMEP PCM model involve work making use of new data arising from recent field experiments, which include sufficient measurements to allow source-apportionment of the aerosol. Major data-sets involve the recent EMEP intensive measurement periods and data from the EU EUCAARI project (Kulmala et al., 2009).

Further details of the EMEP PCM model and comparisons to measurements will be presented in subsequent publications.

2.5.5 *Acknowledgements*

2.6 Mass closure at selected EMEP sites in 2008

Chemical speciation of the ambient aerosol is performed for a number of reasons, such as, screening for environmental toxins causing adverse humans health effects upon exposure or to wild life when deposited in various ecosystems, and for measuring levels of known climate forcing agents, such as BC. Chemical analysis of the ambient aerosol can also provide important information about the various sources contributing to the ambient aerosol loading, as well as about chemical and physical processes taking place in the atmosphere. By an extended chemical speciation, the various variables analyzed can be used as input in receptor models for a quantitative assessment of the contributing sources. This is important as the ambient aerosol pr. se is known to have adverse health effects on human health, cause visibility degradation, contributing to acidification and eutrophication of ecosystems, causing material and crop damage, amongst others.

The three levels of increasing sophistication upon which the EMEP monitoring strategy (UNECE, 2009) is built, provides a sufficient number of chemical species necessary for receptor modelling. However, the necessary diversity of chemical species is rarely available for an entire year, but rather for a few selected sites during intensive measurement periods such as the EIMPs (EMEP Intensive Monitoring Periods). Useful information about the ambient aerosol sources could also be obtained simply by compiling and graphically presenting the major aerosol constituents and fractions, know as mass closure. As a minimum, EC/OC and the secondary inorganic constituent (SIA) are required to attempt a mass closure, as they typically are the major contributors to the aerosol mass concentration. Further, sea salts and mineral dust ought to be included as well. In the recent EU Directive 2008/50/EC, chemical speciation of particulate matter with respect to EC/OC and the major anions and cations (including SIA) in the rural background environment are required to provide a better understanding of the sources contribution to the ambient aerosol loading, thus underlining the importance of performing such analysis.

Due to their influence on acidification and eutrophication, the SIA constituents are the species most widely analyzed within the EMEP monitoring network. Despite that we see an increase in the number of sites reporting EC and OC for 2008, such measurements are collocated with SIA only at limited number of sites. Obviously the capture and the quality of the data has to be sufficient for attempting mass closure, but the samples also ought to be collected concurrently in order to get the most out of such an approach. For 2008 we have attempted a mass closure for five sites. Our selection criteria, consisting of concurrent measurements of SIA, EC, OC, and sea salts on a daily or weekly basis, and which covers more than 6 months of 2008, would allow for annual and seasonal (winter and summer) mass closure of the ambient aerosol. In addition, the mass closure corresponding to the 95th percentile of the PM mass concentration, i.e. a proxy for the most severely polluted time periods, can be established. Unfortunately, these criteria were not all fulfilled at the five sites selected.

2.6.1 Mass closure of PM$_{10}$ at Birkenes (NO0001R), Norway, 2008

The mass closure observed for 2008 (see Figure 2.15) deviated somewhat from the average mass closure observed for the period 2001–2008 (see chapter 2.6.1.1);

i.e. the relative contribution of NH_4^+ (2.9%) for 2008 is not within the mean $\pm$ SD (6$\pm$2%) for the period 2001 – 2008. A similar finding was made for SO_4^{2-}, being 14% for 2008 compared to 19$\pm$3%, which is the long term mean. The sea salt contribution (18%) was substantially higher for 2008 compared to the long term mean, which is 13$\pm$3%.
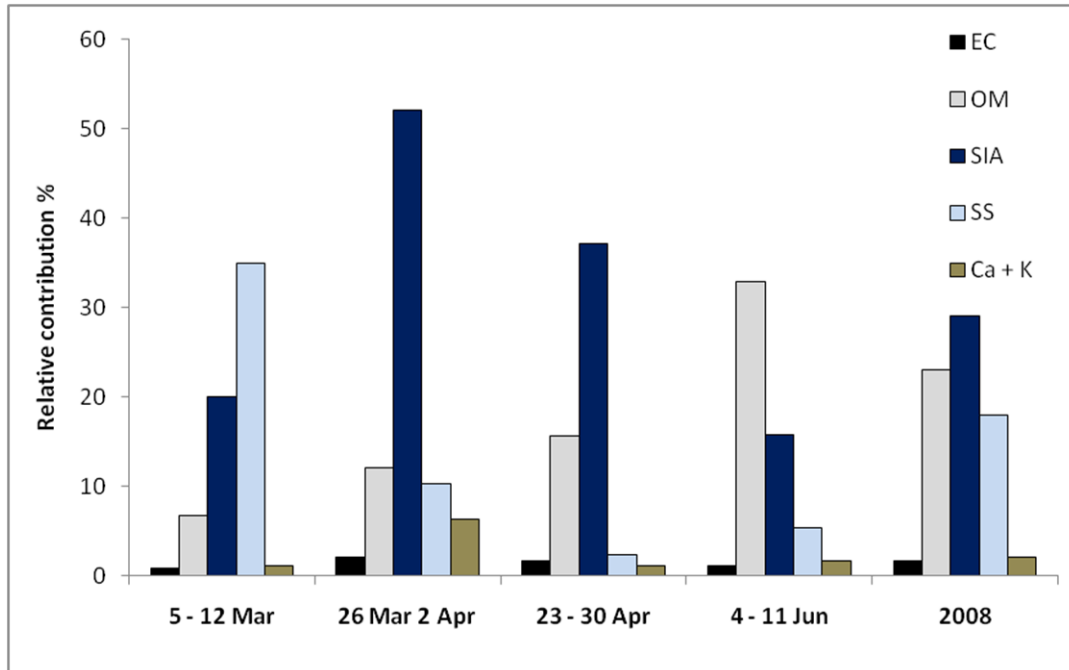

Figure 2.15: The annual mean relative contribution of EC (x1.1), OM (OM = OC x 1.7), SIA (SO_4^{2-}, NO_3^-, NH_4^+), sea salts and Ca^{2+}; K^+ to PM_{10} for 2008. The mass closure observed for weeks of elevated PM_{10} concentrations, i.e. corresponding to the 95th percentile of PM_{10}, is included as well.

The mass closure of PM_{10} has as a pronounced seasonal variation at Birkenes. The most characteristic feature is that of OM, which account for 19% of the aerosol mass concentration in winter and 36% in summer. This finding reflects the substantial (3x) increase in the OM concentration going from winter to summer. This increase can be attributed to OM both in the fine and the coarse fraction of PM_{10}, thus most likely reflecting the formation of Secondary Organic Aerosols (SOA) and Primary Biological Aerosol Particles (PBAP) emissions. A summer time increase was also observed for SO_4^{2-} and NH_4^+, but not nearly as pronounced as for OM. Sea salts, NO_3^-, the base cations and EC all make a more substantial contribution to PM_{10} in winter than for summer. This is most pronounced for the sea salts, which relative contribution to PM_{10} in winter are twice that seen for summer.

The mass closure seen for the most polluted time periods, i.e. the 95th percentile of PM_{10}, differ substantially. For one of these four weeks (5-12 of March) sea salts were the dominating species, underlining that the Birkenes site is situated no more than 20 km from the coast. SIA constituents dominated completely during the two weeks in spring (26 March-2 April and 23-30 April) for which PM_{10}

levels were found to be elevated, which is consistent with LRT. Birkenes typically experience an increased frequency of LRT episodes in spring. For the week 4-12 June the carbonaceous fraction of the aerosol contributed the most to the elevated PM_{10} concentration. The EC/TC ratio is no more than 5% for this week, indicating a substantial influence from natural sources. These findings made at Birkenes nicely illustrate how different sources, natural as well as anthropogenic, may be responsible for elevated ambient levels of PM. However, further speciation is needed, e.g. to look into the sources of the carbonaceous fraction of the aerosol, as well as for the potential contribution of mineral dust.

2.6.1.1 *Mass closure of PM at Birkenes for the period 2001 - 2008*

Birkenes has a time series of EC/OC, major anions and cations, PM_{10} and $PM_{2.5}$ measurements going back to 2001. For this time period OM is the major subfraction/species accounting for 26±3% of PM_{10} followed by SO_4^{2-} (19±3%), NO_3^- (13±2%), sea-salts (13±3%), NH_4^+ (6±2%) and EC (2±0.5%) (see Figure 2.15, left). A downward tendency is observed for the annual mean contribution of SO_4^{2-} to PM_{10}, as well as for NH_4^+ to PM_{10} for the actual period, corresponding to the reduced emissions of SO_2 and NH_3. On the other hand, an increase is observed for the relative contribution of sea salts to PM_{10}. Our analyses suggests that this is mainly attributed to decreased levels of fine mode SIA constituents rather than the observed increase of sea salts; i.e. the sea salt to $PM_{10-2.5}$ ratio remain relatively unchanged over this period. The relative contribution of nitrate to PM_{10} showed a noticeable increase for the six first years of the period but this has been followed by a pronounced decrease. For organic matter (OM = OC x 1.7) and EC (EC x 1.1), the relative contribution to PM_{10} are rather stable throughout the 8 year long period, despite that the levels of OC and EC has decreased somewhat. The relative contribution of SIA to PM_{10} (38±6%) is larger than that of the carbonaceous fraction (i.e. OM + EC) (28±3%) throughout the entire period. However this difference has decreased substantially over the last 3 years; being 18% in 2005 it was no more than 4% for 2008. 70% of the PM_{10} mass concentration observed at Birkenes for the period 2001 – 2008 can be accounted for by the chemical speciation performed. When applying conversion factors to account for elements associated with OC and EC that is not accounted for by thermal-optical analysis, 81% of the mass concentration can be explained (see Figure 2.15, right). The unexplained mass is likely attributed to mineral dust and the aerosol water content. For the period in question, the percentage of the mass concentrations that can be explained has decreased steadily. This is likely due to a combination of reduced levels of important SIA constituents and that mineral dust is not part of the current measurement program.

Only OC and EC are regularly analyzed for the $PM_{2.5}$ size fraction at Birkenes for the period 2001 - 2008, thus any attempt to establish a mass closure for $PM_{2.5}$ has to rely on a priori knowledge of the size distribution of the inorganic constituents (i.e. SIA, sea-salts). The result of such an attempt is provided in Figure 2.16 (right), showing that a larger fraction of $PM_{2.5}$ is likely to be accounted for by the chemical analyses performed. This finding is to be expected as most species and fractions analyzed typically reside in the fine fraction of PM_{10} and that species not analyzed, e.g. mineral dust, predominantly are associated with the coarse fraction of PM_{10}.
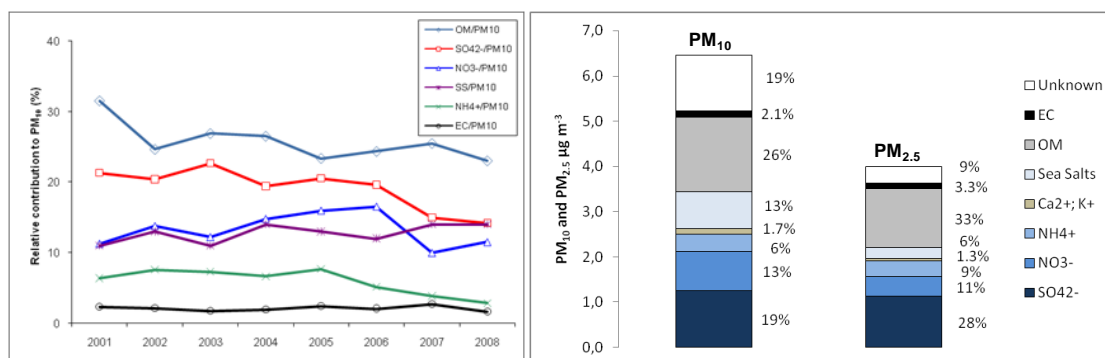
Figure 2.16: Relative contribution of organic matter (OM = OC x 1.7), SO$_4^{2-}$, NO$_3^-$, sea salts, NH$_4^+$, EC (x1.1) and Ca^{2+}; K$^+$ to PM$_{10}$ for the time period 2001 – 2008 (left). Average mass closure of PM$_{10}$ and PM$_{2.5}$ at Birkenes for the time period 2001 – 2008 (right).

2.6.2 Mass closure of PM$_{10}$ at Vavihill (SE0011), Sweden, 2008

Mass closure of PM$_{10}$ at Vavihill could only be attempted for a total of 17 samples, which were collected according to an irregular sampling time during the period of June – December, 2008. Obviously, any effort to establish an annual or seasonal mass closure for PM$_{10}$ would be severely biased. The available data indicates that organic matter (19%) and nitrate (19%) are the major contributors to PM$_{10}$ regardless of season. A mass closure for the period mid June – mid September, being fairly representative for summer, has been attempted (see Figure 2.17), showing that OM (19%) is the major sub fraction/species along with NO$_3^-$ (18%), followed by SO$_4^{2-}$ (17%) and NH$_4^+$ (14%). SIA (SO$_4^{2-}$, NO$_3^-$, NH$_4^+$) accounts for a substantial 50% of the PM$_{10}$ mass concentration for the mid June – mid September period, which is 2.5 times higher than that of the carbonaceous content (20%). This finding is completely the opposite of that observed for the other Scandinavian site Birkenes, for which the carbonaceous fraction (OM + EC) account for 38% of PM$_{10}$ in summer, whereas SIA amounts to 32% only. Proximity to major urban areas (within 25–45 km) (see chapter 2.4.2.1) and surrounding farm land, might explain some of the SIA dominance at Vavihill in summer. On the other hand, the OC data from Vavihill is based on denuded sampling, thus substantially reducing the positive sampling artifact of OC. Further, using a denuder without including a backup sorbent in the sampling train, which is the case at Vavihill, will likely increase the negative artifact, thus the OC measurements at this Swedish site might be "underestimated" compared to that of the Norwegian site Birkenes, which do not correct for neither positive nor negative artefacts.
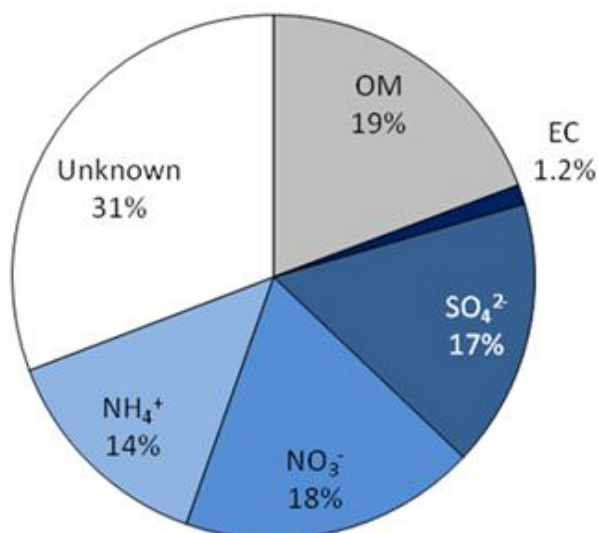
Figure 2.17: Mass closure of PM$_{10}$ at Vavihill for the period 10th June – 17th September 2008.

2.6.3 Mass closure of PM$_{10}$ at Campisábalos (ES0009R), Spain, 2008

Both EC/OC and the major cations and anions are reported for the Spanish site Campisábalos (ES0009R). However, the lack of concurrent measurements and a rather poor data capture severely hampers any effort to establish a reliable mass closure. A nearly complete mass closure without having accounted for e.g. mineral dust, which is an important contributor to the ambient aerosol at any Spanish site, underlines the current level of uncertainty. It also demonstrates the importance of high quality data sets being the result of a consistent sampling approach and a well reasoned monitoring strategy. Despite the abovementioned uncertainties, the results strongly indicates that the carbonaceous fraction is the major contributor to the aerosol loading on an annual basis, accounting for more than 60% of the PM$_{2.5}$ mass concentration. The very low EC/TC ratio (6-7%) suggests that the carbonaceous material predominantly is of biogenic origin. When attempting to perform mass closure for the summer and winter time periods, an increase in OM, EC and NO$_3^-$ is indicated when going from summer to winter, although levels of OM and EC are higher in summer than winter.

2.6.4 Mass closure of PM$_{10}$ and PM$_{2.5}$ at Melpitz (DE0044R), Germany, 2008

Concurrent measurements of EC/OC and the major cations and anions in PM$_{10}$ and PM$_{2.5}$ at a 24 hour time resolution are available for mass closure at the German site Melpitz. The mass closure for the two size fractions closely resembles each other, which is to be expected as 76% of the PM$_{10}$ mass concentration can be attributed to its fine fraction, OM (19% for PM$_{2.5}$ and 22% for PM$_{10}$) and NO$_3^-$ (17%) being the main contributors to both size fractions for 2008. The relative contribution of NO$_3^-$ was found to be increased by nearly a factor of 3 going from summer to winter, accounting for 25% of the winter time aerosol loading, thus being the major speciated aerosol compound (see Figure 2.18). This finding was observed for both PM$_{10}$ and PM$_{2.5}$ and is briefly explained by the thermal instability of NH$_4$NO$_3$, i.e. at low temperatures the equilibrium of the system shifts towards the particulate phase. A similar increase

was observed for the relative contribution of NH_4^+ to PM in winter, although not nearly as pronounced as seen for NO_3^-. Sea salts exhibited a similar seasonal variation as NO_3^- and NH_4^+, increasing by a factor of 4 going from summer to winter, thus accounting for 7% of PM_{10} and 4% of $PM_{2.5}$ in winter.
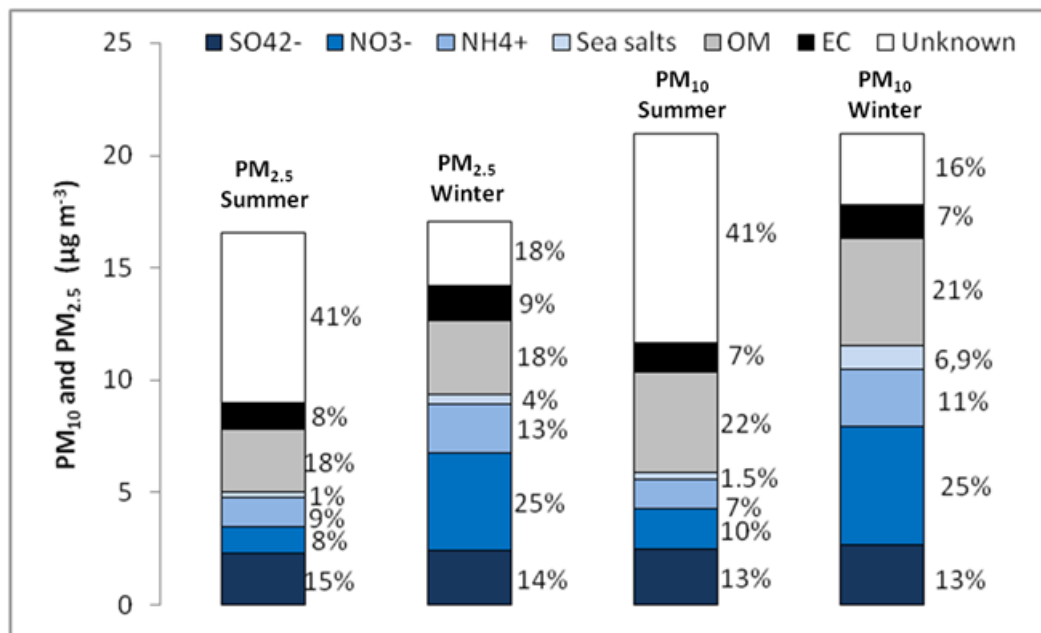

Figure 2.18: Relative contribution of organic matter (OM = OC x 1.7), SO_4^{2-}, NO_3^-, sea salts, NH_4^+ and EC (x1.1) to PM_{10} and $PM_{2.5}$ during summer and winter for 2008 at Melpitz (DE0044R), Germany.

The percentage of unaccounted PM mass is substantially higher in summer (41%) compared to winter (16% (PM_{10}) and 18% ($PM_{2.5}$)). Since this finding is observed for both PM_{10} and $PM_{2.5}$ and that the majority (76%) of PM_{10} is attributed to its fine fraction, mineral dust, which predominantly resides in the coarse fraction of PM_{10}, is not likely to explain this pattern. Thus, there appears to be some kind of systemic uncertainty or artifact, which either is independent of the particle size or which is associated with the fine fraction of PM. Here we can only speculate about the reason; e.g. too low factor used to convert OC to OM in summer (e.g. due to high SOA contribution) or a too high factor used in winter. The unaccounted mass could be somewhat overestimated in general, as the analytical method (VDI) used for quantification of EC and OC leads to an erroneous separation of the two carbonaceous sub fractions overestimating EC on behalf of OC. There is however no evidence available that this kind of error should be more pronounced in summer compared to winter.

For the most polluted days (here: the 95th percentile of the PM_{10} and the $PM_{2.5}$ mass concentration) there was an increase in the relative contribution of OM and EC compared to that of the annual mean, whereas there were minimal or no change for the other species. The increase was most pronounced for EC in $PM_{2.5}$ accounting for 12% during days of elevated $PM_{2.5}$ pollution compared to 8% for the annual mean, however the EC/TC ratio was not enriched compared to the annual mean.

At present, mass closure data are only available for the period 2006 – 2008 at Melpitz, which is too early for any trend analysis. The finding that the SIA contribution is larger than that of the carbonaceous fraction is however consistent for these three years, and it is observed for both PM_{10} and $PM_{2.5}$.

2.6.5   Mass closure of $PM_{2.5}$ at Ispra (IT0004R), Italy, 2008

The $PM_{2.5}$ mass closure observed at Ispra in 2008 does not differ to any extent from that of previous years (2003 - 2008), with OM (44%) accounting for the greatest contribution to the $PM_{2.5}$ mass concentration followed by SO_4^{2-} (16%), NO_3^- (12%), EC (10%) and NH_4^+ (9%). The rather high contribution of EC to the $PM_{2.5}$ mass loading differs from that observed at the other sites, underlining the substantial influence of primary PM air pollution from anthropogenic sources at the Ispra site. It is somewhat surprising that the unaccounted mass is no more than 9% when only EC/OC and SIA has been used as input in the mass closure attempt. Further, a denuder, but no back up sorbent, has been included in the sampling train suggesting that the level of OC reported is a conservative estimate. In addition, the factor used to convert OC to OM (i.e. 1.4) is rather low compared to that of the other sites. Although contributing mainly to the coarse fraction of PM_{10}, including mineral dust and sea salt to the mass closure would likely result in a complete closure of the PM mass or even overestimate it. At present, i.e. only accounting for SIA and the carbonaceous fraction, there are already quite a few incidences where the mass closure exceeded 100% of the $PM_{2.5}$ mass concentration on a daily basis (not included in Figure 2.19, right), which is rather difficult to explain. The carbonaceous fraction (53%) is found to be greater than that of SIA (38%) on an annual basis.

The relative contribution of the various species analyzed varied considerably according to season (See Figure 2.19, right). OM was the major contributor to $PM_{2.5}$ regardless of season, but was noticeably higher in winter (48%) compared to summer (38%). The relative contribution of NO_3^- was increased by a factor of two in winter (19%), whereas only a minor increase was observed for EC (10%). SO_4^{2-} and NH_4^+ both accounted for a larger fraction of the $PM_{2.5}$ mass concentration in summer than in winter. The increase was particularly pronounced for SO_4^{2-}, being the second largest speciated constituent of the summer time $PM_{2.5}$ with 25%. While the carbonaceous fraction and SIA made an equally large contribution to $PM_{2.5}$ in summer, the carbonaceous fraction (59%) dominated over SIA (36%) during winter.

The most polluted days (here: the 95th percentile of the $PM_{2.5}$ mass concentration) all occurred in January, February and March. OM (43%) and NO_3^- (31%) were the major constituents accounting for 75% of the total $PM_{2.5}$ mass concentration, however only NO_3^- was found to be increased compared to the annual (12%) and winter time mean (19%). It is also found that the EC/TC ratio is noticeably lower for these days (14%) compared to that of the annual mean (22%) and the winter time mean (21%). This finding could indicate an influence of residential wood burning, which typically has a low EC/TC ratio. During the two EMEP intensive measurement periods conducted in fall 2008 and winter 2009 the levels of levoglucosan, a tracer of residential wood burning, has been substantial, collaborating to this suggestion. Low ambient temperatures at these days could

also favour condensation of semi volatile species, contributing to a lower EC/TC ratio.

For Ispra there is a continuous time series of concurrent measurements of EC/OC and SIA at a daily time resolution going back to 2003. As for previous years, OM is the major contributor to the $PM_{2.5}$ mass concentration by a clear margin; in fact OM makes a larger contribution to $PM_{2.5}$ than the sum of SO_4^{2-}, NO_3^- and NH_4^+ for the years considered (2003-2008). SO_4^{2-} is the only species for which there is a continuous upward or downward tendency in the relative contribution, i.e. increasing from 13% in 2003 to 16% in 2008.
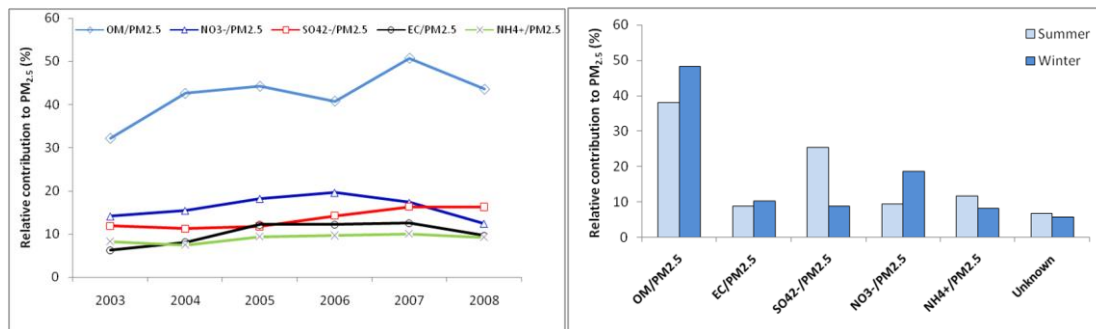
Figure 2.19: Relative contribution of organic matter (OM = OC x 1.4), SO_4^{2-}, NO_3^-, sea salts, NH_4^+, EC (x1.1) to $PM_{2.5}$ for the time period 2003 – 2008 (left). Relative contribution of speciated mass to $PM_{2.5}$ during summer and winter 2008 at Ispra (right).

3 EMEP Intensive Measurement Periods – Update

3.1 EMEP Intensive Measurement Periods – EIMP

By Karl Espen Yttri and Wenche Aas

The EMEP intensive measurement periods (EIMP) have become an important addition to the EMEP monitoring programme, both with respect to the scientific development and for capacity building; i.e. by extending the suite of measurement variables and measurement methods. The last intensive measurement periods were conducted in two periods; i.e. 17 September – 15 October 2008 and 25 February – 26 March 2009. The measurements were performed in close cooperation with ongoing activities in the EU funded projects EUSAAR and EUCAARI. The objectives and scope of these two EIMPs were:

- Chemical speciation of particulate matter with respect to its inorganic, mineral and carbonaceous content with daily/weekly (EMEP) and hourly (EUCAARI) time resolution
- Gas/particle phase distribution of inorganic nitrogen constituents
- Aerosol size distribution (EUCAARI/EUSAAR)
- Separation of the carbonaceous aerosol into
  - primary vs. secondary
  - biogenic vs. anthropogenic
- Attempts to quantify the aerosol water content (EUCAARI)
- Attempts to quantify the OC/OM ratio (EUCAARI)

A total of eighteen sites participated in the second EIMP, but not all sites had a full suite of measurements. Table 3.1 provides an overview of which measurements have been conducted at the various sites. Several EUSAAR sites performed additional measurements such as CPC and CCNC during these time periods, whereas additional measurement periods exists for a few selected sites; i.e. Puijo, San Pietro Capofiume and Jungfraujoch (EUCAARI). The final analyses from the intensive measurement periods are currently being undertaken and data processing are in progress. The general impression is that the measurements went quite smoothly and that the methodologies applied have been well harmonized and consistent in most cases. Recently, a subgroup to the TFMM has defined a new *Eurodelta* model inter comparison project that will start in fall 2010, which is based on the data obtained during the EIMPs, thus highlighting the great value of the EIMP activity.

Table 3.1: *Overview of sites participating in the Joint EMEP/EUCAARI intensive measurement periods, as well as the measurements performed.*

		EUCAARI (EMEP)		EMEP (+ some EUCAARI)						EUSAAR	
		Intensive hourly with AMS/MARGA(GRAGOR)	Water content	Carbonecous (PM_{10})			PM_{10} (or FP)		unbiased HNO_3 and NH_3	Size nr distrib	Absorption
				EC/OC	Levo	14C	Inorg	Mineral			
CH0002	Payerne	Q-AMS		X	X	X	X		DELTA denuder	SMPS	
CZ0003	Košetice		HTDMA	X	X	X	PM1			SMPS	
DK0041	Lille Valby			X	X	X		X	NH3	DMPS	
DE0044	Melpitz	ToF-AMS	HTDMA	X	X	X	X		NH3	DMPS	MAAP
ES1778	Montseny	ToF-AMS (spring09)		X	PM1 (FMI)		X	X		jan.09	MAAP
FI0050	Hyytiälä	ToF-AMS	HTDMA							DMPS	Aethal
FR0013	Peyrusse Vieille			Single			SIA				
FR0030	Puy de Dôme	ToF-AMS-CTCF	HTDMA	Denuder			X			SMPS	MAAP
GB0048	Auchencorth Moss	MARGA, Q-AMS		Spring 09							
GB0036	Harwell	GRAEGOR, ToF-AMS								SMPS	Aethal
GR0002	Finokalia	Q-AMS (spring09)		X	PM1 (FMI)		X	X		SMPS	Aethal
HU0002	K-Puzta	ToF-AMS (fall08)	HTDMA	X	X		SIA			SMPS	PSAP
IE0031	Mace Head	ToF-AMS	HTDMA	X	X	X				SMPS	MAAP/Aethal
IT0001	Montelibretti			X	X	X	X	X	Denuder		
IT0004	Ispra	WAD-SJAC	HTDMA	X	X	X	PM2.5			DMPS	MAAP/Aethal
NL0011	Cabauw	MARGA (AMS spring09)	HTDMA						NH3,HNO3,HCl	SMPS	MAAP
NO0001	Birkenes			X	X	X	X			DMPS	PSAP
SE0011	Vavihill	ToF-AMS	HTDMA	X	Lund	Lund	X			DMPS	PSAP

3.1.1 *The carbonaceous aerosol in the EIMPS – Update*

During the joint EMEP/EUCAARI intensive measurement periods conducted in 2008 and 2009 there has been a particular focus on the carbonaceous aerosol (see Chapter 2.5 in the 2009 EMEP Annual PM report (EMEP, 2009)). This has been attributed to the fact that the carbonaceous aerosol constitutes a substantial part of the ambient aerosol, it affects radiative forcing, contributes to adverse health effects and that it's sources are poorly resolved. Thus, our aim has been defined as to perform "*Source apportionment of the carbonaceous aerosol for Air-Quality, Climate, and Model Validation issues*". The AMS high time resolution measurement (EUCAARI), as well as the integrated filter samples analyzed with respect to EC/OC, selected organic tracers and $^{14}C/^{12}C$ (EMEP) will be particularly useful with respect to studying the sources of this ill defined fraction of the ambient aerosol. A presentation of the organic factor analysis obtained from the AMS results is planned for next year's EMEP Annual PM Report, and will be the topic of forthcoming peer reviewed papers, including in the EMEP special Issue in ACP. Some preliminary results concerning the bulk organics obtained by the AMS measurements are briefly presented in chapter 3.2, whereas a status report on the integrated samples can be found in chapter 3.1.2. These results are to be presented in peer reviewed papers, e.g. the EMEP special Issue in ACP, as well.

3.1.2 Source apportionment of the carbonaceous aerosol based on EC/OC, $^{14}C/^{12}C$, and organic tracer analysis

By Karl Espen Yttri, David Simpson, Marianne Glasius, Johan Genberg, Minna Aurela, Risto Hillamo

Our present knowledge concerning the carbonaceous aerosol in the European rural background environment mainly stems from the EMEP EC/OC campaign conducted in 2002/2003 (Yttri et al., 2007) and the CARBOSOL project in 2002 – 2004 (Legrand et al., 2007). In addition, a very few EMEP sites have reported levels of EC and OC for some years now. Within the EU funded project, EUSAAR we have been able to boost critical areas regarding sampling and analysis of the carbonaceous aerosol and a unified protocol has been developed. This is partly why we have made the carbonaceous aerosol a topic of the EMEP/EUCAARI intensives; i.e. to learn more about the carbonaceous aerosol, to provide necessary data for model validation and to boost the use of the EUSAAR 2 thermal program.

However, EC/OC measurements do not resolve the multitude of sources contributing to the ambient aerosol loading per se, but substantial quantitative and qualitative information about its sources can be obtained when combined with organic tracers and $^{14}C/^{12}C$ – analysis (Szidat et al., 2004; Szidat et al., 2009), followed by statistical analyses, as demonstrated by Gelenscer et al. (2007).
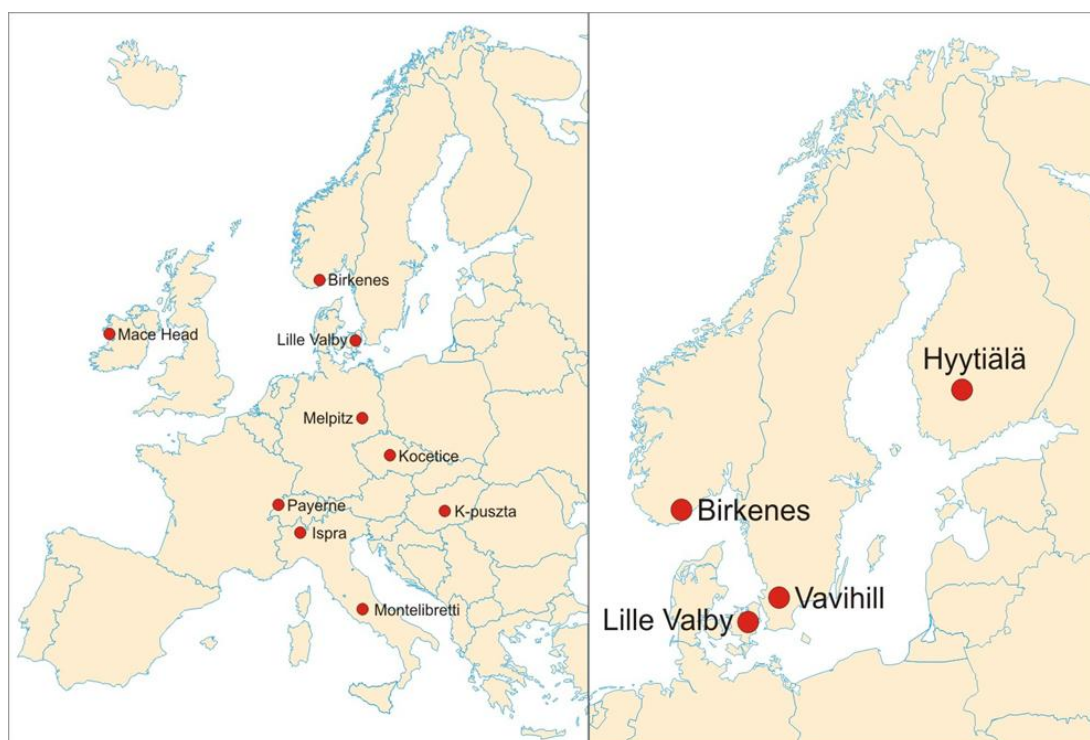
Figure 3.1: Left) Sampling sites participating in the EMEP/EUCAARI Intensive Measurement Periods in fall 2008 and winter 2009; Right) Sampling sites participating in the SONORA (Secondary Organic Aerosols in the Nordic Rural Background Environment) Intensive Sampling Period in Summer 2009.

A total of 9 sites have participated in such an intensified effort on the carbonaceous aerosol (See Figure 3.1, left), covering parts of Central, Eastern, Southern and the North-West of Europe. At these sites the following variables have been analyzed: EC, OC and TC according to a QBQ sampling principle and the EUSAAR2 thermal protocol, levoglucosan (which is a biomass burning tracer), and fM (fraction modern) which is the ^{14}C/^{12}C ratio of the sample related to that of a reference year.

The EC/OC and levoglucosan analyses have been finished for quite some time, whereas there is an unexpected delay for the ^{14}C-analysis, which is attributed to unforeseen analytical problems (Table 3.2). AMS ^{14}C/^{12}C is a highly challenging analysis to perform and in order to obtain sufficiently high quality data, which is needed for the statistical analyses, the remaining analyses cannot be initiated unless we are confident that they will be successful. At present, 5/9 samples have been analyzed for the fall 2008 period, whereas the corresponding figures for the winter 2009 period is 6/9 samples. The paper planned to cover these results has been initiated. Further, additional analysis of the carbonaceous aerosol is available for selected site, which might be useful to include in this paper. A brief presentation of some of the carbonaceous aerosol data collected during the EIMP in winter 2009 can be found in Chapter 2.5 in the 2009 EMEP Annual PM report (EMEP, 2009).

Table 3.2:   *Overview of chemical analyses performed on integrated filter samples collected during the EIMPs in fall 2008 (F.08) and winter 2009 (W.09).*

Site	Thermal-optical analysis		Levoglucosan analysis		^{14}C-analysis	
	F. 08	W. 09	F. 08	W. 09	F. 08	W. 09
Birkenes (NO)	X	X	X	X		X
Ispra (IT)	X	X	X	X		X
Kocetice (CZ)	X	X	X	X	X	X
K-puszta (HU)	X	X	X	X		
Lille Valby (DK)	X	X	X	X	X	X
Melpitz (DE)	X	X	X	X	X	X
Montelibretti (IT)	X	X	X	X		
Mace Head (IE)	X	X	X	X	X	
Payerne (CH)	X	X	X	X	X	X

A number of EMEP sites have been selected for an even more thorough investigation of the carbonaceous aerosol (See Figure 3.1, right), being the topic of the NMR funded project SONORA. These sites are all situated in the Nordic countries, where we expect to have a particularly strong and pronounced signal from natural sources, thus the campaign was conducted in August 2009 when there is an assumed maximum of BVOC emissions and SOA formation and a substantial release of PBAP (Primary Biological Aerosol Particles). The diversity of chemical analyses exceeds that of the EIMPs conducted in fall 2008 and winter 2009 including a range of sugars/sugar-alcohols, cellulose, pinic acid and organosulphates/nitrates in addition to EC/OC, levoglucosan, and ^{14}C/^{12}C-analysis. The chemical analyses to be conducted in SONORA are all finished and

the statistical analyses are in progress. Also the paper covering these results will be submitted to the EMEP Special Issue in ACP.

Preliminary results from the source apportionment of the carbonaceous aerosol at the Finnish site Hyytiälä are shown in Figure 3.2. The pronounced biogenic profile becomes obvious from the fact that approximately 80% of the aerosol's TC content can be attributed to OC_{nf}, which is a proxy for BSOA (Biogenic Secondary organic Aerosols), and PBAP (Primary Biological Aerosol Particles). A similar pattern is seen for the three other Nordic sites as well. While the Aerosol OC fraction is dominated by natural sources, the situation is vice versa for elemental carbon (EC). Approximately 80% of the EC can be attributed to combustion of fossil fuel, whereas the remaining 20% is attributed to combustion of wood. Any distinction between EC from wood burning for residential heating and EC originating from wild or agricultural fires has not been attempted at this stage. Nevertheless, EC appears to be almost exclusively of anthropogenic origin.
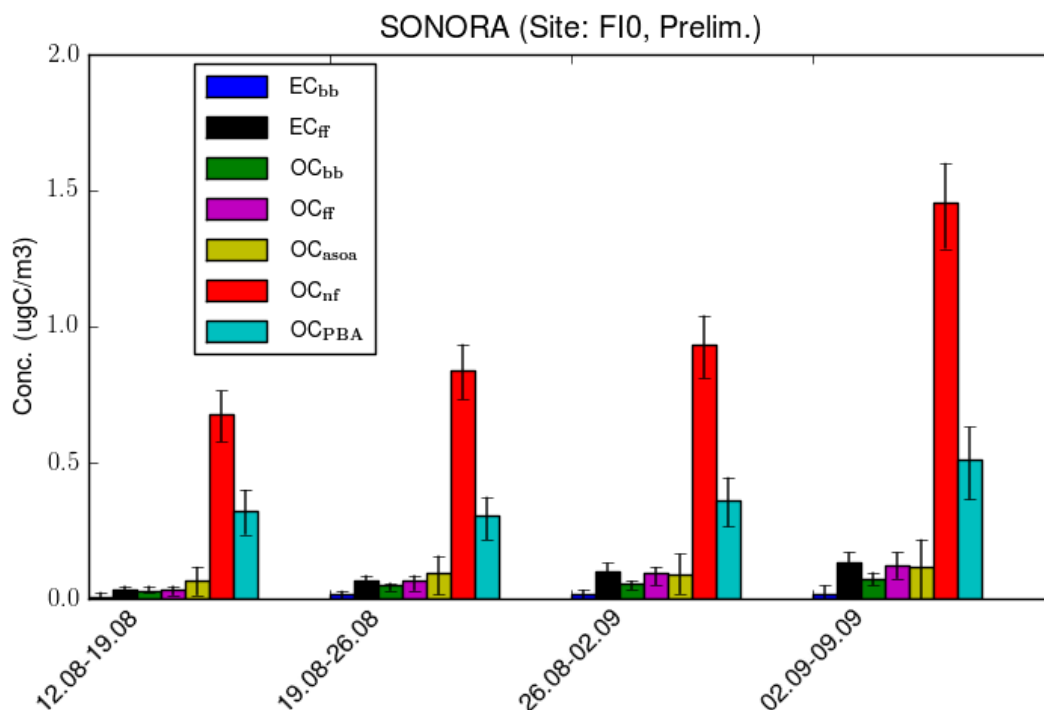
Figure 3.2: *Source apportionment of the carbonaceous aerosol at the Finnish rural background site Hyytiälä for the period 12th of August to 9th of September 2009. Uncertainty bars represent the 10th and 90th percentile of latin-hypercube statistical analysis, methodology similar to that used in Gelencser et al. (2007) and Szidat et al. (2009). Preliminary results.*

3.1.3   Acknowledgments

The SONORA Project was supported by the Nordic Council of Ministers.

3.2 Aerosol Mass Spectrometer Measurements during the EMEP / EUCAARI Intensive Measurement Periods 2008/09

By Eiko G. Nemitz

By joining forces between the national contributions of the Member States of the Convention to the EMEP Intensive Measurement Periods (EIMPs) with the European project EUCAARI IP, a significant European network of parallel Aerosol Mass Spectrometer measurements could be realised. The Aerodyne Aerosol Mass Spectrometer measures the non-refractory (NR) aerosol components (i.e. those that flash volatilise at 600 °C) in a size range that approaches that of PM_1 (referred to as $NR\text{-}PM_1$). The instruments were operated and analysed with standardised protocols ensuring maximum intercomparability between sites, providing the largest dataset of online aerosol chemical measurements with a unified methodology to date. Due to the high temporal resolution of the measurements (typically several minutes, block-averaged to hourly data), the measurement provides diurnal patterns of the aerosol concentrations, which is not typically available in EMEP aerosol chemical measurements, and which provides a powerful dataset to assess the performance of chemical transport models (such as the unified EMEP model) in terms of the parameters that affect aerosol concentrations at the sub-daily time-scale, such as emissions, boundary layer height, secondary aerosol formation, as well as thermodynamic response to temperature and relative humidity.

Figure xxx summarises preliminary results of the bulk concentrations of organic aerosol mass, sulphate, nitrate, chloride and ammonium during the three EIMPs (Apr/May 2008 – EUCAARI activity only; Joint EMEP/EUCAARI EIMP Sep/Oct 2008; Joint EMEP/EUCAARI EIMP Feb/Mar 2009) in the spatial European context. The time-series of the third campaign are exemplified in Figure 3.4.

In interpreting the results, it needs to be borne in mind that the dataset contains two high-altitude sites (Jungfraujoch, JFJ, CH; Puy de Dome, PDD, FR) and two urban sites (Barcelona, BAR, ES; Helsinki, HEL, FI). In general, concentrations were largest in central Europe, where the contribution of nitrate also exceeded that of sulphate, especially during the colder third EIMP. The exception is the two high altitude sites (JFJ and PDD) where concentrations were low. By contrast, concentrations are lower at the fringes of Europe such as the outer parts of the British Isles (MHD and to some extent BU), N. Scandinavia (SMR, PUI) and, during the last EIMP, also on Crete (FKL). Here sulphate makes a more important contribution, because nitrate volatilises during transport into remote areas characterised by ammonia and nitric acid and has virtually disappeared under the warm conditions in Crete. In addition, it is likely that the SMR, HEL, PUI and FKL are more affected by the comparably higher sulphate emissions in Eastern Europe.

The time-series (Figure 3.4) shows marked differences between sites. While concentrations in central Europe are fairly uniform, often following a diurnal pattern, concentrations at the fringes of Europe are highly episodic. Some of these episodes are linked between sites. The dataset includes the observation of major ammonium nitrate events, which are regularly observed over Europe in early

spring and have been linked to agricultural activities. For example, during 18-20 March such an event was first observed over the British Isles (CHB, MHD, BU) and then also picked up by the Dutch (CBW) and German (MPZ) sites.

These measurements represent a quantum leap forward in the European measurement database for the assessment of chemical transport models (CTMs). They will continue to challenge the different processes described in the CTMs, such as emissions, transport and thermodynamics.
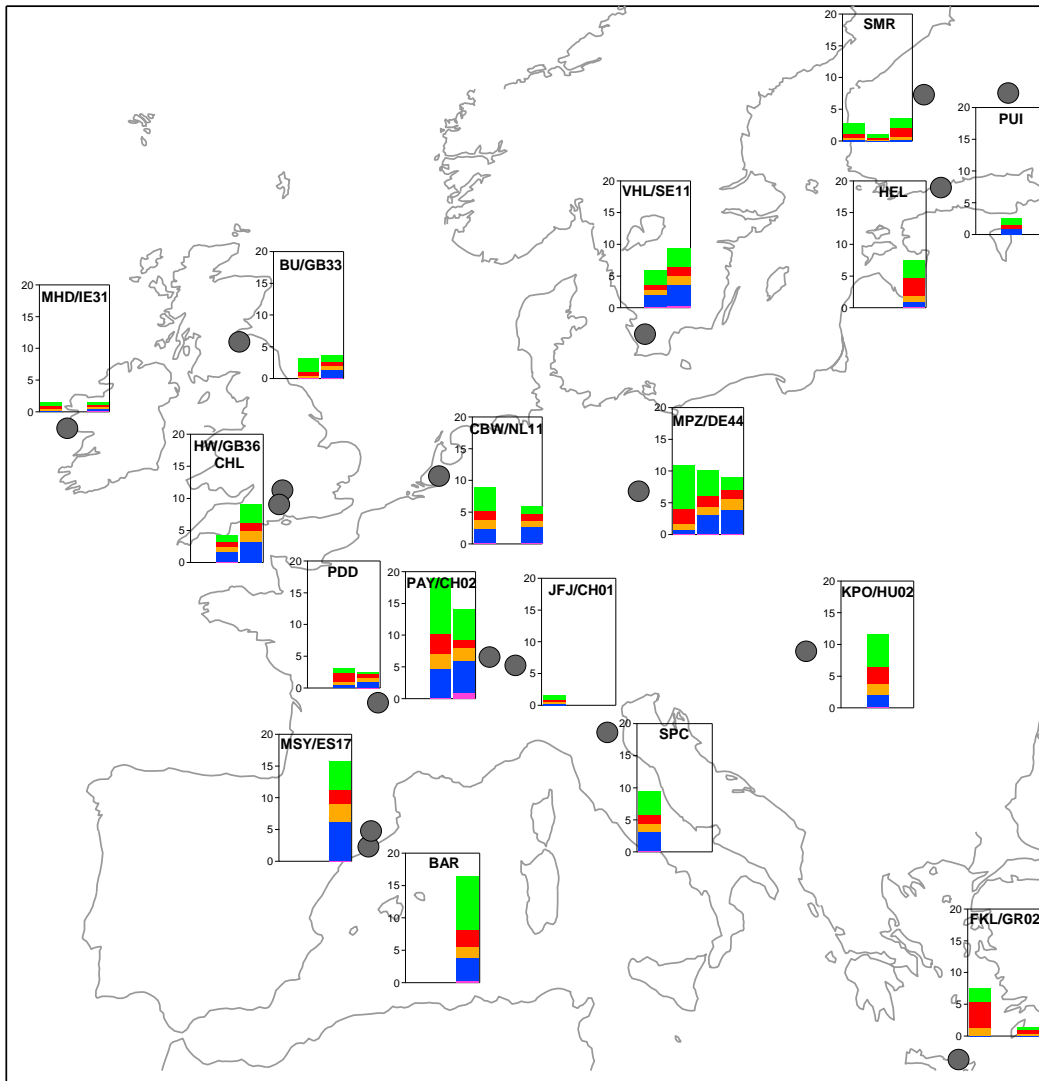

Figure 3.3:   Overview of the non-refractory submicron aerosol chemical composition. The three bars in each plot refer to the three EMEP/EUCAARI Intensive Measurement Periods (Apr/May 2008; Sep/Oct 2008; Feb/Mar 2009). Green=organic aerosol mass; red = sulphate; orange = ammonium; blue = nitrate; pink = chloride (preliminary data).
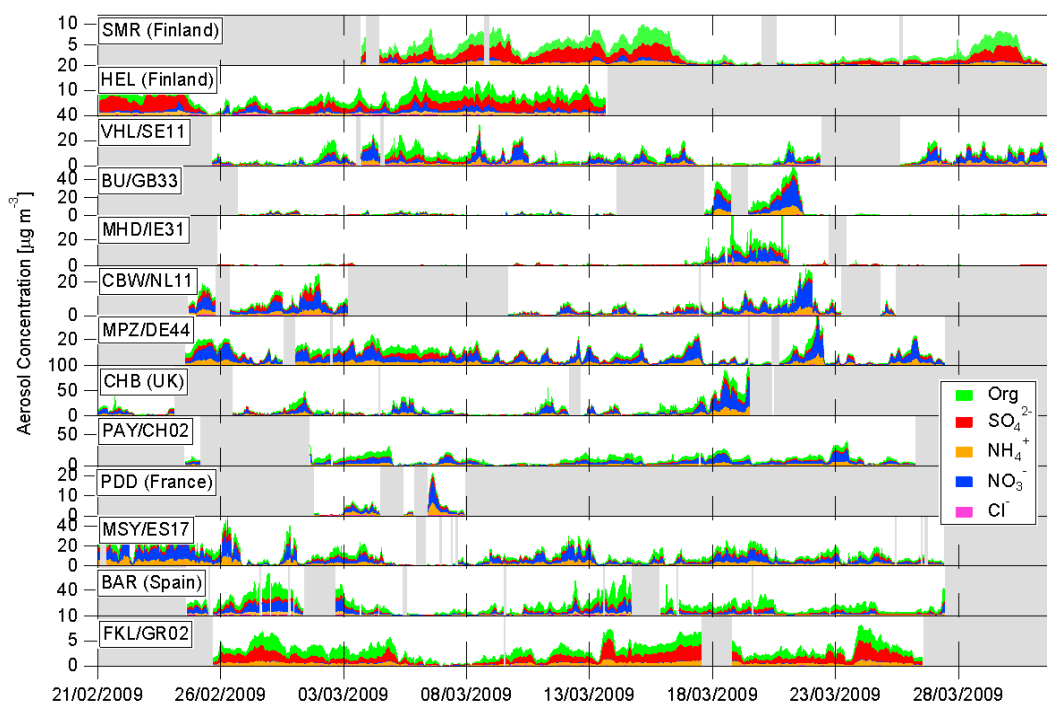
Figure 3.4: *Stacked time-series of non-refractory sub-micron aerosol composition as measured across the European Aerosol Mass Spectrometer network during the EMEP/EUCAARI Intensive Measurement Period in Feb/Mar 2009 (Preliminary data). Grey shaded areas identify gaps in the data. The time-series are ordered by latitude from North (top) to South (bottom).*

The data analysis is currently being finalised and the bulk concentrations will be made available via EBAS in due course, with the results of an ongoing factor analysis of the organic aerosol component into its components (e.g. primary hydrocarbon-like organic aerosol and secondary oxygenated organic aerosol) following later in this year (2010).

These data have been provided by the following participating groups: Eiko Nemitz, Chiara Di Marco and Gavin Phillips from the Centre for Ecology and Hydrology (UK); Andre Prevot, Peter De Carlo, Claudia Mohr, Valentin Lanz from the Paul Scherrer Institute (CH); Mikko Äijälä, Mikael Ehn, and Heikki Juninen from the University of Helsinki (FI); Karine Sellegri, Ralf Weigel and Evelyn Freney from the University of Clermont-Ferrand (FR); Petri Tiitta, Tomi Raatikainen and Ari Laaksonen from the University of Eastern Finland (FI); Laurent Poulain, Gerald Spindler and Hartmut Herrmann from the Institute for Tropospheric Research (DE); Amewu Mensah, Astrid Kiendler-Scharr and Thomas Mentel from the Jülich Research Centre (DE); Manuel Dall'Osto, Harald Berresheim, Darius Ceburnis, Jurgita Ovadnevaite and Colin O'Dowd from the National University Ireland, Galway (IR); James Allan, Gerard Capes, Hugh Coe, Gordon McFiggans and Tom Choularton from the University of Manchester (UK); Joakim Pagels, Axel Eriksson and Erik Swietlicki from Lund University (SE); Jose Jimenez, Donna Sueper, Mike Cubison, Amber Ortega and Sanna Saarikoski from the Univ. Colorado at Boulder (USA); Doug Worsnop and Sally

Ng from Aerodyne Research Inc. (USA); Tomi Raatikainen, Samara Carbone and Ari Laaksonen from the Finish Meteorological Institute (FI); Lea Hildebrand from Carnegie Mellon Univ. (USA); Spyros Pandis from the University of Patras (GR).

4 An overview of the complex Mediterranean aerosol phenomenology

By X. Querol, A. Alastuey, J. Pey and K.E. Yttri

4.1 Introduction

The Mediterranean Basin (MB) has a complex aerosol phenomenology caused by factors such as (Querol et al., 2009a): 1) high particle emissions from anthropogenic and natural sources, 2) enhanced formation of secondary aerosols due to the high concentrations of gaseous precursors, elevated relatively humidity and solar radiation, 3) a characteristic meteorology that favours the stagnation of pollutants on a regional scale, especially in the Western part of the MB (Millán et al., 1997; Gangoiti et al., 2001), and 4) low precipitation rates, which increase the atmospheric life time of the aerosol. Countries surrounding the Mediterranean Basin, along with Eastern Europe, show particularly high levels of regional background particulate matter (PM) compared to Northern and some central European regions (Querol et al., 1998; Rodriguez et al., 2002; Koçak et al., 2007a; Gerasopoulos et al., 2007). Both anthropogenic (e.g. transport sector, industrial processes, power generation, biomass burning, shipping, man-made forest fires) and natural (African dust, sea spray, wild fires, primary and secondary organic compounds) emissions contribute to these elevated PM levels. Shipping is considered a major regional anthropogenic source in the MB due to high traffic intensity in a relatively poorly ventilated basin. The combination of an elevated regional background PM loading and dust outbreaks is responsible for 70% of the PM_{10} daily limit value (2008/50/CE European directive) exceedances reported for the Western MB regional background environment (here: Spain) (Escudero et al., 2007a). Similar findings are reported for the Eastern MB, e.g. by Gerasopoulos et al. (2006) and Koçak et al. (2007a). The complexity of the MB aerosol phenomenology, which to a large extent is influenced by regional and long range transported PM, calls for a dense network of regional background monitoring sites. Unfortunately, this does not reflect the current situation, as the Eastern part of the MB severely lacks such measurements, and only Spain appears to have a sufficient number of monitoring sites.

4.2 Meteorological characteristics: Western and Eastern patterns

The atmospheric dynamic conditions of the Western MB is highly influenced by the following factors: 1) the Azores high-pressure system that diverge the low pressure systems to northern Europe in summer; 2) the coastal mountain ranges surrounding the shore that favour atmospheric stagnation; 3) the influence of the summer Iberian and Saharan thermal lows causing weak pressure gradients over the region; 4) the intense mountain and sea breeze activation along the coast driven by the high insolation and the typical low advective conditions; 5) the scarce summer precipitation, prolonging the atmospheric residential time of PM 6) the frequent arrival of Saharan dust air masses in summer as a result of the formation of a high-pressure system over North Africa at high altitude (~1500 m a.s.l.); and 7) the occurrence of high pollution episodes caused by the accumulation of regional pollution during intense and persistent winter-autumn anticyclonic episodes.

Similarly, the Eastern MB meteorology is controlled by the following factors: 1) during spring and early summer the development of Saharan depressions to the south of the Atlas Mountains take place (Moulin et al., 1998). These cyclones move eastwards and are responsible for the transport of large amounts of desert dust over the EMB; 2) during summer the EMB is influenced by the Azores anticyclone extended to the east and the cyclonic branch of the large South Asian thermal low. Additionally, a strong influence by the Indian Monsoon on the dry Mediterranean climate (Rodwell and Hoskins, 2001), combined with the complex orographic terrain of regions such as Greece, result in persistent northerly winds, called "Etesians". As a result, the EMB is influenced by advection from Europe in the lower troposphere, favouring the transport of particles from urban areas in Central and Eastern Europe as well as from areas experiencing intense agricultural burning, typically Eastern Europe and areas surrounding the Black Sea (Balis et al., 2003; Sciare et al., 2008).

4.3   Regional background

4.3.1   PM levels

Querol et al. (2009b) showed that annual mean PM_{10} levels increased from West to East and from North to South across the Mediterranean basin. That is, annual PM_{10} levels ranging from 15 µg m^{-3} to approximately 35 µg m^{-3} along the West to East transect (Figure 4.1), and from approximately 10 µg m^{-3} to 35 µg m^{-3} for the North to South gradient. The trends observed for the annual mean PM_{10} concentration along the East to West and North to South transects coincide with the spatial distribution of PM_{10} attributed to African dust. When applying the methodology proposed by Escudero et al. (2007), it was found that PM_{10} dust originating from Africa contributed with a substantial 9-10 µg m^{-3} in the regional background environment in EMB, 6 µg m^{-3} in the SWMB, 2-3 µg m^{-3} in the WMB and < 2 µg m^{-3} in the NMB. Further, African dust episodes were responsible for 20-26 exceedances of the daily limit value of 50 µg m^{-3} of PM_{10} at regional background sites in the EMB, 16 in the SWMB, 4 in the WMB and < 2 in the NMB. It is also likely that higher concentrations of sulphate and sea spray aerosols in the EMB contribute to the observed West to East gradient of PM_{10} (Querol et al., 2009a).

The seasonal and multi-year evolution of PM_{10} levels in the Western (Monagrega) and Eastern (Ayia Marina) MBs are presented in Figure 4.2 and Figure 4.3. A clear summer maximum is observed for the WMB, whereas a broader or bimodal pattern is seen for the EMB, depending on the relative contribution of anthropogenic and natural sources. The elevated summer time (June-July) concentrations observed for the WMB are associated with low precipitation, high resuspension due to soil dryness, increased formation of secondary aerosols, high frequency of African dust outbreaks, and recirculation of air masses that prevent air renovation (Querol et al., 1998, Viana et. al., 2002; Rodríguez et al., 2003; Escudero et al., 2005). For selected years, a secondary maximum can be observed in winter (November - March), which is caused by either anthropogenic pollution events (winter anticyclonic scenarios, Pérez et al., 2008 and Pey et al., 2010a) or by natural (African dust) sources. For the rest of the year, PM levels are relatively low owing to the high frequency of Atlantic advections and precipitation. In the EMB the seasonal maximum is usually recorded in spring (April - May) as a

consequence of frequent African dust episodes (Moulin et al., 1998) (Figure 4.2). This is particularly evident for PM_{10} and $PM_{2.5}$, while for PM_1 concentrations are higher in summer, which is in accordance with the seasonality of anthropogenic derived aerosols such as e.g. non-sea salt sulphate (Gerasopoulos et al., 2007; Koulouri et al., 2008).
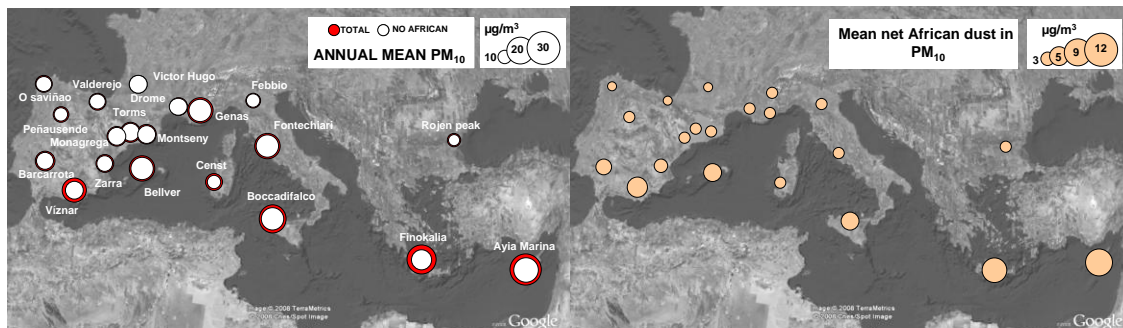

Figure 4.1: *Left: Annual mean PM_{10} levels at regional background sites in the MB with (red circle) and without (white circle) the contribution of African dust. Right: Annual mean contribution of African dust to the annual mean PM_{10} level. Modified from Querol et al. (2009b).*
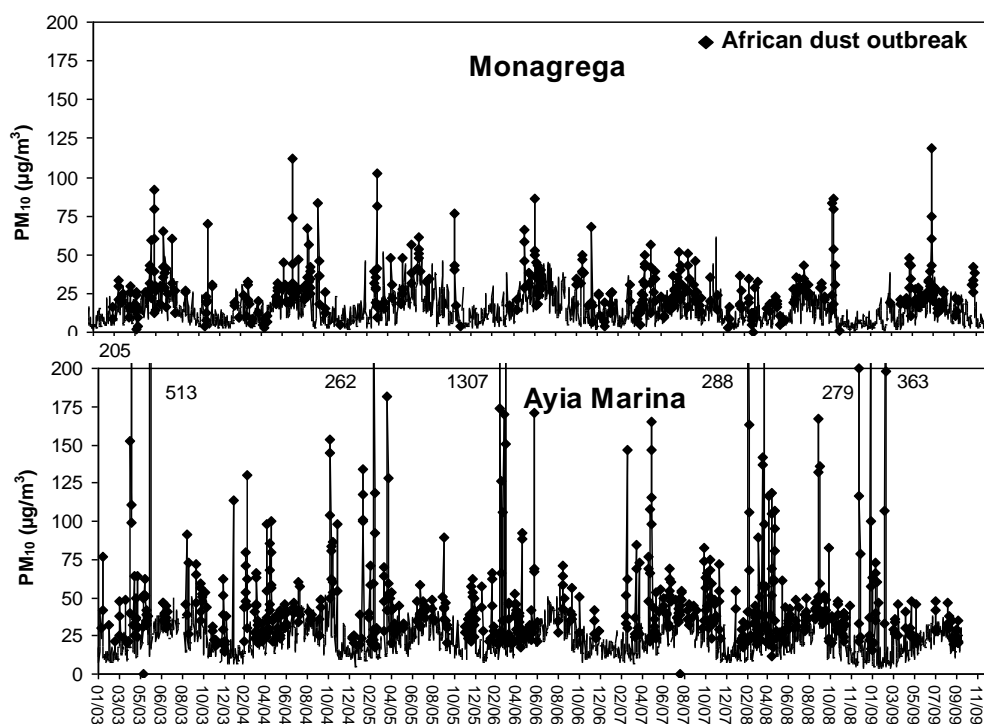
Figure 4.2: *Daily levels of PM_{10} (2003-2009) at Monagrega (E Spain) and Ayia Marina (Cyprus). Black diamonds indicate days with African dust outbreaks. Modified from Querol et al. (2009b).*
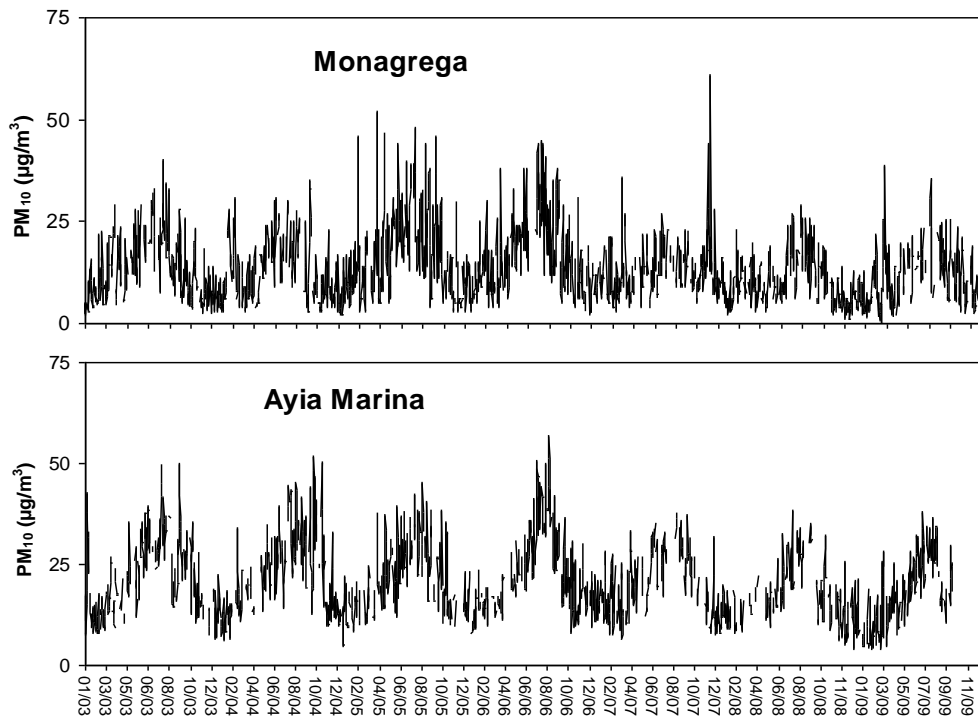
Figure 4.3: Daily levels (2003-2009) of PM$_{10}$ at Monagrega (E Spain) and Ayia Marina (Cyprus) for days without African dust outbreaks. Modified from Querol et al. (2009b)

The Mann-Kendall's Test and Sen's method using MAKESENS applied to the annual PM levels (Figure 4.4) at Montseny (WMB), reveals decreasing trends for PM$_{10}$, PM$_{2.5}$ and PM$_1$. The downward trend is significant for PM$_{2.5}$ and PM$_1$ (40% of reduction since 2002), while it is not for PM$_{10}$. The lack of significance for PM$_{10}$ is attributed to its coarse fraction (PM$_{10-2.5}$), which does not show any evidence of a downward trend. When excluding the contribution of African dust from these analyses, the decreasing trends become even more apparent. It should be noted that these decreasing trends observed at Montseny are not that apparent at other regional background sites located in the WMB. A decreasing tendency in the regional background for the entire MB, and in particular for the WMB, has also been deducted from the analysis of MODIS' aerosol optical depth, as presented by Papadimas et al. (2008).
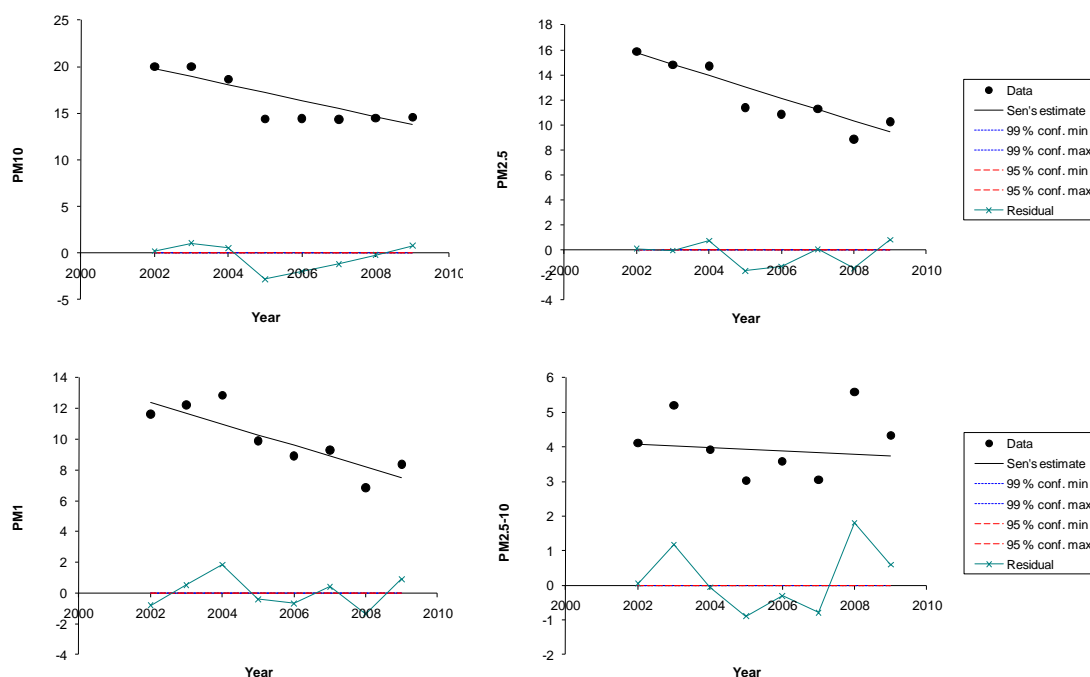
Figure 4.4:   Temporal trend of annual PM$_{10}$, PM$_{2.5}$, PM$_1$, and PM$_{2.5-10}$ levels at Montseny for the period 2002 – 2009 by means of Mann-Kendall's test and Sen's method using MAKESENS (Salmi et al., 2002).

4.3.2   Chemical composition

Mineral matter appears to be the major component of PM$_{10}$ at both the WMB (22%) and the EMB (38%) regional background sites, followed by sulphate, organic matter (OM), nitrate and ammonium Querol et al. (2009a). The high mineral matter content of PM$_{10}$ in the MB is characteristic for the region and deviates from rest of Europe. The influence of sea salts become increasingly important along a west to east transect, and is considered a major contributor to PM$_{10}$ in coastal areas, The relative contribution of mineral matter (8%) and sea salt (14%) to PM$_{2.5}$ is substantially less than for PM$_{10}$, as they typically reside in the coarse fraction of PM$_{10}$. The relative contribution of all other species and fractions are higher, though. 10-14% of PM$_{10}$ and 2-16% of PM$_{2.5}$ consists of unaccounted mass, which at least partly is attributed to moisture not eliminated during filter conditioning. When comparing the chemical composition of the MB with that of North and Central Europe, major gradients of mineral matter, nitrate, sulphate, organic and elemental carbon can be found.

The major chemical species of PM in the MB has a profound season variation, which is described in detail by Querol et al. (2009a), and in brief in the following text:
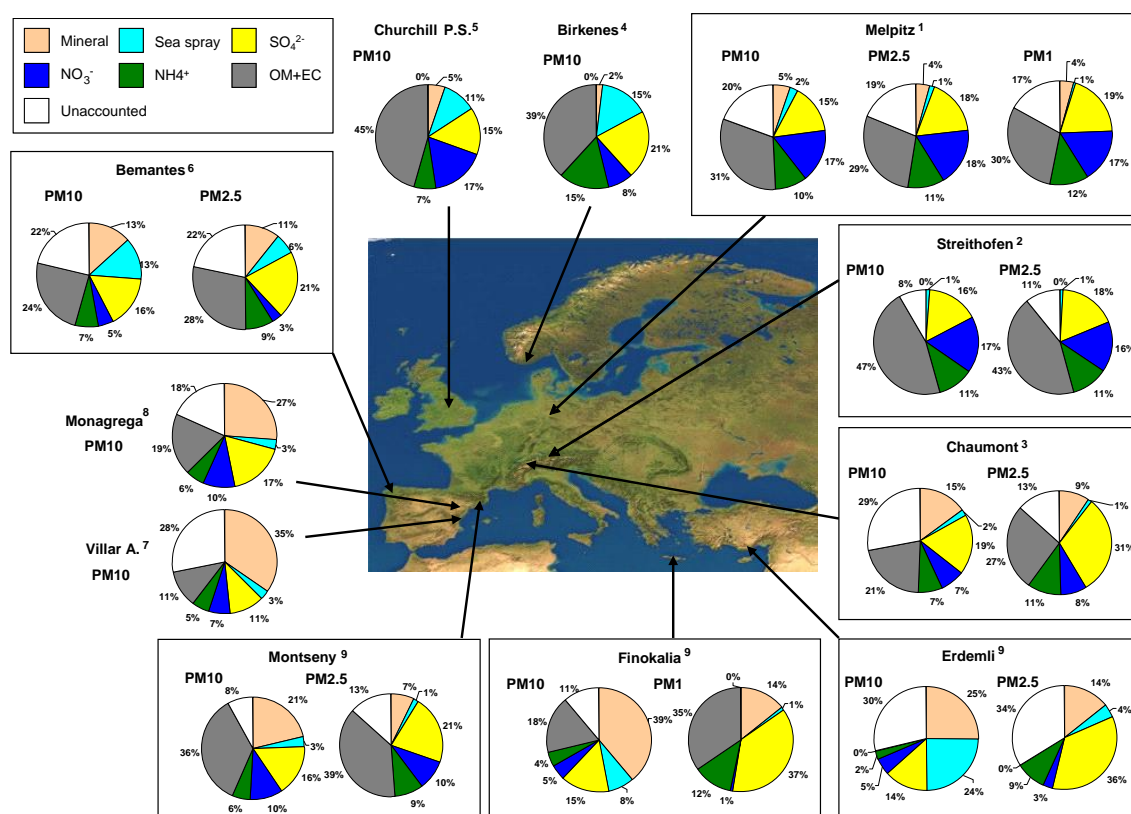
Figure 4.5:   Annual mean levels of PM$_{10}$ and PM$_{2.5}$ components measured at Montseny, Finokalia and Erdemli and a selection of European rural background sites. [1]Spindler et al. (2007); [2]Puxbaum et al. (2004); [3]Hueglin et al. (2005); [4]Yttri (2007); [5]Yin and Harrison (2008); [6]Salvador et al. (2007); [7]Viana et al. (2008); [8]Rodriguez et al. (2004); [8]Querol et al. (2009a). OM+ EC: organic matter + elemental carbon. Modified from Querol et al. (2009a).

Mineral matter in PM$_{10}$ and PM$_{2.5}$ exhibits a profound seasonal variability and high levels can be observed almost throughout the entire year, both in the WMB and the EMB (Figure 4.6). This can be attributed to resuspension of dust of local and regional origin caused by high convective dynamics and low precipitation, and the high frequency of African dust episodes occurring in spring and fall in the EMB and in spring and summer in the WMB (Pérez et al., 2008). The level of mineral matter in PM$_{2.5}$ usually accounts for less than 50% of that measured for PM$_{10}$, although this ratio varies throughout the year. In the WMB the lowest PM$_{2.5}$/PM$_{10}$ ratio for mineral matter is seen from late spring to midsummer (20-30%), whereas the highest is observed in winter (35-45%). For the EMB, the ratio remains rather low (15%) throughout the entire year, indicating the presence of coarser particles.

Nitrate levels in the WMB are profoundly increased in winter (Figure 4.6). The summer time decrease is due to the thermal instability of ammonium nitrate (Harrison and Pio, 1983; Querol et al., 2001), which is the most abundant nitrate species in this region. The rather low PM$_{2.5}$/PM$_{10}$ ratio (20%) observed for nitrate in summer compared to winter (90%) shows that a substantial part of nitrate is

present as coarse Ca and Na nitrate species. Episodes with peak nitrate concentrations of 15 µg m^{-3} on a daily basis are observed during winter on an annually basis and is associated with transport of aged air masses from the surrounding industrial/urban areas during anticyclonic conditions (Pérez et al., 2008, Pey et al., 2010a). The situation regarding nitrate is completely different for the EMB, as nitrate levels are higher in summer compared to winter. Size-segregated measurements show that the majority (>85%) of nitrate is confined in the coarse mode, strongly indicating that it is associated with alkaline ionic species following from the reaction between nitric acid and sea salt particles and mineral dust (Mamane and Gottlieb, 1992; Pakkanen et al., 1999; Metzger et al., 2006).

Sulphate levels increase from April-May to reach maximum level in mid summer (Figure 4.6). This seasonal pattern is observed for both the WMB and the EMB and is likely related to increased photochemical activity and low air mass renovation at the regional scale (Millán et al, 1997; Rodríguez et al., 2002), (Mihalopoulos et al., 2007). In the WMB, a secondary maxima of sulphate concentration are commonly recorded in winter, coinciding with the anticyclonic nitrate pollution episodes. A common feature for sulphate in the MB is that it predominantly resides in the fine aerosol fraction throughout the entire year. Some coarse sulphate is observed during African dust outbreaks, probably as $CaSO_4$.

Ammonium concentration shows different seasonal behaviour for the two basins. For the WMB, two periods of elevated concentrations are seen during winter, which mainly are attributed to the presence of ammonium nitrate, and to a lesser extent ammonium sulphate, whereas a third is observed in summer which is mainly associated with ammonium sulphate. Minimum levels are generally observed in April-May and September-October.

For the EMB, ammonium follows the seasonal variation of sulphate. The significant correlation between NH_4^+ and nss-SO_4^{2-} observed both at Erdemli and Finokalia, with the equivalent NH_4^+/nss-SO_4^{2-} slope being less than 1 (0.85 in Finokalia and 0.64-0.95 at Erdemli), suggests that NH_4^+ to a large extent neutralizes nss-SO_4^{2-}.

Sea-salt contribution to PM shows no uniform behaviour in the MB. At Montseny (WMB), sea salts show a distinct seasonal trend (Figure 4.6) with elevated concentration in summer, which probably is related to the increasing sea breeze circulation over the coast, which intensifies in the warm season. On the contrary, no clear trend is observed at Finokalia, while at Erdemli a maximum is seen during winter. At both the EMB sites the sea-salt concentration follow the variation of the wind speed. At both E and W MBs, chlorine/sodium ratios show a seasonal trend, with higher winter values (close to the typical marine ratio) and considerably lower values in summer. The lower summer ratios may be attributed to interaction of nitric acid with abundant sodium chloride, which causes loss of volatile hydrochloric acid. The $PM_{2.5}$/PM_{10} ratio for sea-spray had a rather constant ratio ranging from 0.4-0.6.

Total carbon reaches its' maximum concentration in summer in the WMB (Figure 4.6), coinciding with the lowest renovation of the atmosphere at a regional

scale (Rodríguez et al., 2002; Pérez et al., 2008), as well as with the higher formation of secondary organic aerosols from natural (biogenic) and anthropogenic precursor compounds. Elevated concentrations observed in late winter and late fall are associated with winter time anticyclonic pollution episodes. Carbonaceous aerosols typically reside in the fine fraction of the aerosol, as is also the case for the MB.
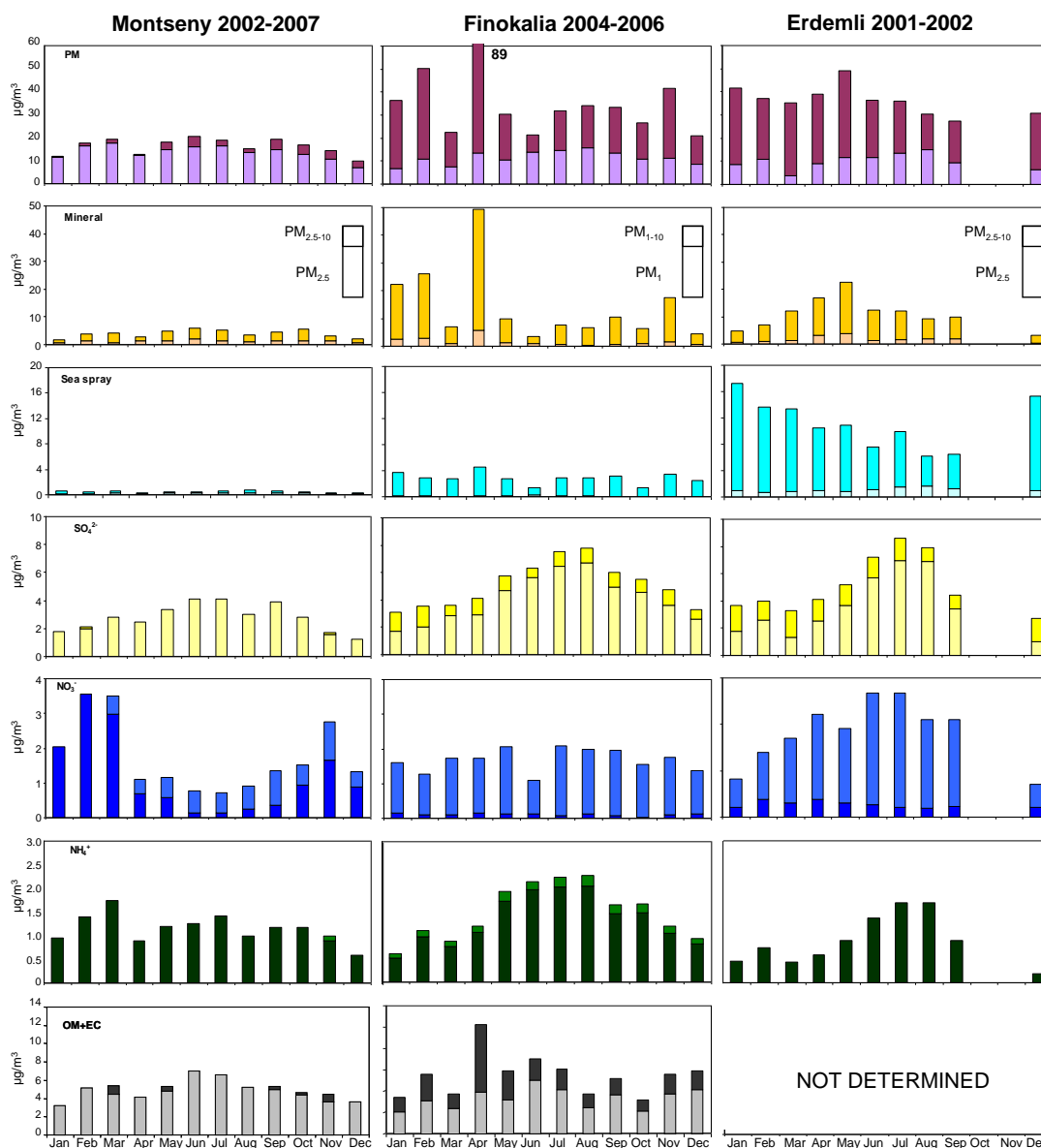

Figure 4.6: *Seasonal evolution of the PM mass concentration and its major species (mineral dust, sea spray, sulphate, nitrate, ammonium and organic matter + elemental carbon) in $PM_{2.5}$ and $PM_{2.5-10}$ (Montseny and Erdemli) and PM_1 and PM_{1-10} (Finokalia). Modified from Querol et al. (2009a).*

An annual mean OC/EC ratio close to 7 is observed for the WMB. The OC/EC ratio typically decreases in winter while it increases in summer, following from a number of factors of which SOA formation (summer) are likely to be of particular

importance. In the EMB the OC/EC ratio is lower ranging from 4 in PM_1 to 5.4 in PM_{10}. In addition, a statistically significant correlation occurs between fine OC and EC (slope equal to 4, r = 0.73), which does not change on a seasonal basis (r=0.65 for winter and 0.86 for summer). Maximum concentrations of OC and EC occur in summer (July - August for OC and in June for EC).

Long-term (5-year) measurements of Black Carbon (BC) and OC performed in the EMB (Crete Island, Sciare et al., 2008) have shown that long-range transport originating from agricultural waste burning in countries surrounding the Black Sea, causes elevated concentrations of EC and OC during two periods of the year, i.e. in March-April and July-September. The contribution of biomass burning to the concentrations of BC and OC is shown to be rather small (20% and 14%, respectively) on an annual basis, although this contribution could be much higher on a monthly basis and as well as having a high intra- and interannual variability. When removing the biomass burning influence, a profound seasonal variation is revealed for OC, which increases by almost a factor of two during May and June, whereas BC is found to be quite stable throughout the year.

4.4   Trace elements

Ambient air concentrations of trace elements across the MB region (Querol et al., 2009a) have showed that the levels of V and Ni are a factor of 3-9 higher than for most sites in Central Europe. A likely explanation might be the relatively high emissions from combustion of fuel-oil (power generation, industrial and shipping emissions).

4.5   Urban environments

Given the substantial impact of the regional background PM loading, the urban, industrial and harbour environments surrounding the MB share several of the features already described for the regional background sites. Nevertheless, some features are more specific for the urban environment, leading to a substantial urban increment, which appears to be more pronounced than for the rest of Europe, and which is characterized by the considerable influence of mineral dust (see Figure 4.7).
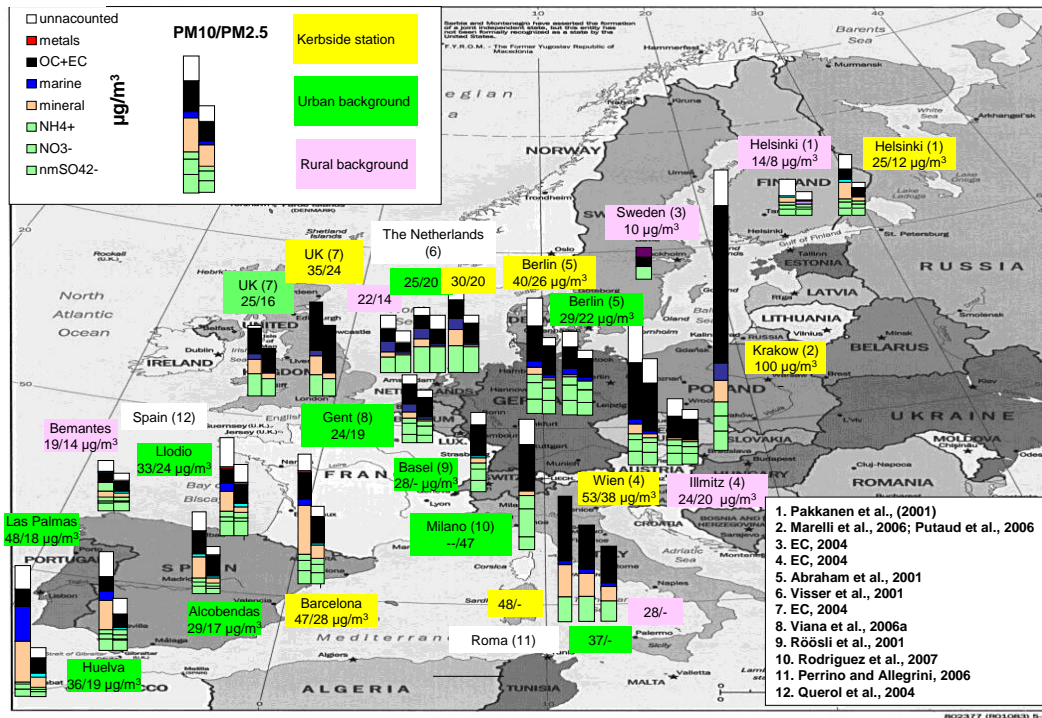
Figure 4.7:   Chemical speciation of PM_{10} and $PM_{2.5}$ reported by selected studies carried out in Europe.

One hallmark is the high population and traffic density for a number of the major cities in this region. For Barcelona the number of passenger cars pr km^2 is 4 times that of Berlin and London. The high car density causes high emissions within a restricted geographical area, which along with poor dispersion conditions (and a substantial regional contribution) lead to an accumulation of air pollutants. The majority (70%) of the light duty vehicles in the major Mediterranean cities is running on diesel. Consequently, tail pipe emissions of PM and NO_2 are enhanced, as is the NO_2/NO ratio of these emissions. Hence, there are difficulties in reaching the NO_2 and $PM_{2.5}$ (partly due to the fast formation of nitrate) target values for urban agglomerations in the region. A high number of building sites in many urban areas is a source of coarse fugitive dust, as is the case for non-exhaust vehicle emissions (abrasion of tires, brake pads and road pavement). Meteorological conditions favouring resuspension contributes to the finding that coarse PM, being dominated by mineral dust, is substantially higher for Mediterranean urban areas than for rest of Europe. Although there is a substantial $4 – 6$ µg m^{-3} contribution of African dust to PM_{10} in Southern Spain, most of the mineral dust in urban areas arises from anthropogenic urban sources (Figure 4.8).
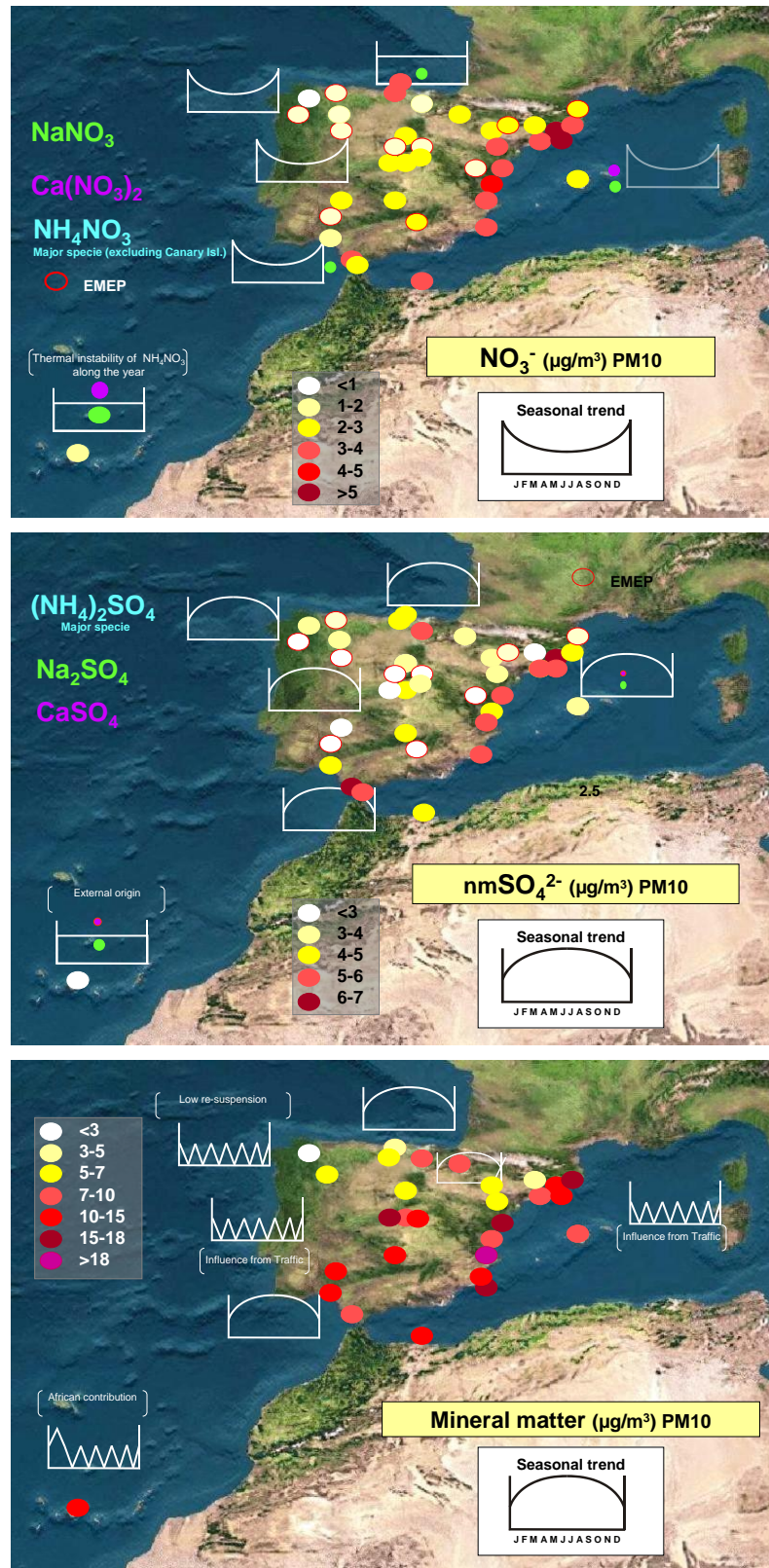
Figure 4.8: Mean annual levels of nitrate, sulphate and mineral matter at 35 Spanish sites. Source: Ministry of the Environment and Marine and Rural Affairs of Spain and Spanish Research Council (CSIC).

High and increasing emissions of ammonia in the Western Mediterranean due to farming have been demonstrated during recent years. Furthermore, preliminary results have shown that NH_3 levels in urban areas such as Barcelona are relatively high (1-8 $\mu g\ m^{-3}$), and that they are likely to be associated with vehicular and fugitive sewage emissions. Combined, this favours the formation of ammonium nitrate, which subsequently increases the PM levels. Figure 4.8 illustrates the factor of 3 higher nitrate levels (by a factor of 3 compared with central or Atlantic cities) along the Spanish Mediterranean coast compared to central and Atlantic cities.

The substantial shipping traffic taking place in the Mediterranean Basin and the subsequent need of major harbour areas close to urban agglomerates, combined with relatively poor dispersion conditions, favours high concentrations of ammonium sulphate, V and Ni (Pey et al., 2010b). The concentrations appear to be particularly in the high around the Gibraltar straight where ships leaving and entering the Mediterranean Basin converge (see Figure 4.8).

The general air pollution situation described above for Mediterranean urban areas, characterized by high PM and NO_2 levels, cause frequent exceedances of the daily limit values of PM and NO_2. Urban air quality assessments have concluded that for urban hotspots non-technological measures focusing on the decrease of traffic flow are necessary to approach the air quality targets for the above pollutants; I.e. technological measures are all important to improve air quality, but not enough to meet air quality requirements.

4.6   Conclusions

- There is a profound increase in the regional background annual mean PM_{10} and $PM_{2.5}$ levels along a West to East and North to South transect across the MB. For PM_1, no such gradient is observed. The observed gradients for PM_{10} and $PM_{2.5}$ are attributed to higher background levels of PM in the EMB, which is explained by the proximity to important source regions and the higher frequency of African dust outbreaks in the EMB compared to the WMB.

- Seasonal evolution of regional background PM levels in the WMB is characterized by a summer maximum which can be explained by scarce precipitation, favorable conditions for resuspension, increased photochemical activity and more frequent outbreaks of African dust. A broader pattern is observed for the EMB with maxima in spring due to the higher frequency of dust episodes.

- The Mediterranean regional background aerosol is characterized by relatively high levels of crustal material and sulphate, and lower levels of carbonaceous matter and nitrate than that of Central Europe. Features characteristic for the Mediterranean Region may account for these differences: a) **Crustal material**: lower atmospheric rain scavenging potential, high frequencies of African dust outbreaks, and high emissions (anthropogenic and natural). b) **Sulphate**: high SO_2 emissions, low ventilation of the atmospheric basin and higher photochemical activity. c) **OM+EC**: less use of biomass combustion in winter. d) **Nitrate**: high ambient temperature favoring the gas phase prevalence of nitrate.

- Coarse nitrate (Ca and Na species) prevails in the EMB in contrast to the dominance of fine nitrate (ammonium nitrate) in the WMB. A pronounce winter maximum is detected for nitrate in the WMB, which is explained by the occurrence of persistent antyciclonic conditions in winter. No seasonal trend is observed for nitrate in the EMB,

- Increasing leves of sulphate are observed for the entire MB from April-May and until midsummer. This is attributed to enhanced photochemical activity, low air mass renovation on a regional scale, increment of the summer mixing layer depth favoring the regional mixing of polluted air masses. The sulphate levels in the EMB appear to be somewhat higher than that of the WMB.

- A higher formation of secondary organic aerosols (SOA) in the WMB compared to the EMB may be deduced from the evaluation of the OC/EC ratios, however this remains highly uncertain.

- The high levels of V and Ni observed in the MB are likely the result of the large emissions from fuel-oil combustion across the basin, including power generation, industrial activities, and intensive shipping.

- PM levels in urban Mediterranean areas are generally higher than for Northern, Western and Central Europe. This has been attributed to certain particular features of the Mediterranean cities: i.e. a high population and car density, numerous construction and demolition activities, a vehicle fleet mainly running on diesel, substantial emissions from the harbors surrounding the cities, large emissions of ammonia from road traffic and sewage.

- The urban increment of PM appears to be particularly high compared to Central Europe.

4.7 Acknowledgements

5 Recent advances of EC/BC with respect to emissions, modelling, and measurements

5.1 Introduction

EC accounts for only a minor fraction (i.e. $3.4 \pm 1.1\%$) of the annual mean PM_{10} concentration in the European rural background environment (Yttri et al., 2007) (see Figure 5.1). Compared to the World Health Organization Air Quality Guidelines (WHO AQG) for PM_{10} of 20 µg m^{-3} pr. year, EC contribute less than 4% on average, whereas it constitutes less than 2% of the EU PM_{10} annual limit value of 40 µg m^{-3}. Hence, effort to reduce emissions of EC does not appear to be an effective way of reducing the adverse health effects caused by the ambient PM_{10} *mass concentration*, upon which the current legislation is founded. However, recent epidemiological studies have demonstrated that EC, and associated compounds, have the highest risk factors concerning cardiovascular and respiratory hospitalization (Peng et al., 2009; Bell et al., 2009). This strengthens the general advice given by the World Health Organization that combustion-derived primary particles are particularly important, as they "*are often rich in transition metals and organic compounds, and also have a relatively high surface area*". In addition, such particles have a substantial LRT potential due to their small size. Consequently, any reduction in EC emissions actually appears to go beyond the resulting reduction in the ambient PM_{10} mass concentration loading. Further, it is fair to argue that the carbonaceous aerosol is currently the most important with respect to aerosol effect on climate and that this mainly is attributed to its black carbon (BC) fraction. BC is regarded by e.g. Ramanathan and Carmichael (2008) to be the second most important contributor to global warming after CO_2, although the magnitude of the BC climate effect has been somewhat debated (e.g. Forster et al., 2007).
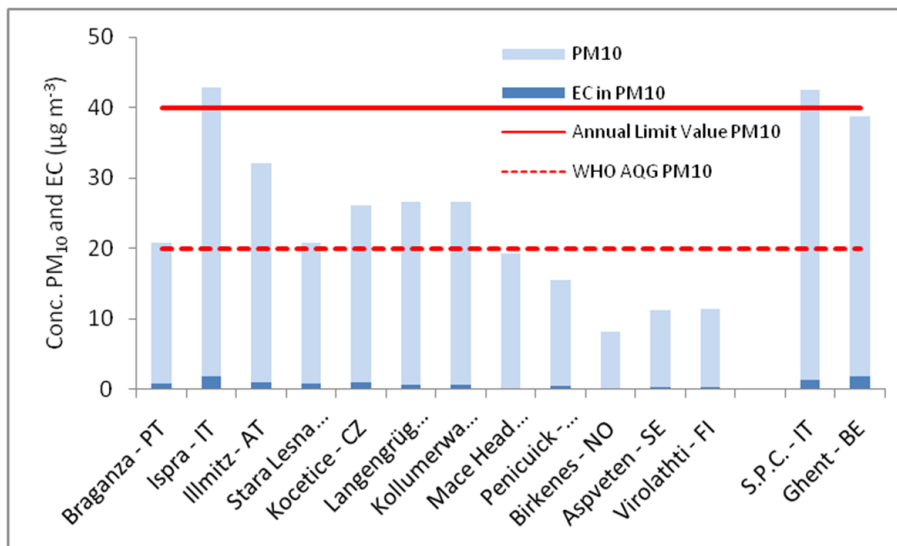

Figure 5.1: *Annual mean concentrations of PM_{10} and EC at twelve rural background (EMEP) sites and two urban background sites. Data from the EMEP EC/OC campaign conducted in 2002-2003 (Yttri et al., 2007). The EU annual limit value for PM_{10} and the World Health Organization Air Quality Guidelines for PM_{10} have been included for comparison.*

Due to the effect of BC on human health and as a climate forcing agent, the Executive Body of the UNECE Convention on Long-range Transboundary Air Pollution has called an Ad Hoc Expert Group on BC, chaired jointly by Norway and the United States, to identify options for potential revisions to the Convention's 1999 Gothenburg Protocol that would enable the Parties to mitigate BC as a component of PM for health purposes while also achieving climate co-benefits. The Group's work will contribute to improved coordination of black and organic carbon (OC)-related activities, with the aim of achieving emission reductions that will improve public health and also benefit the climate in the near term in the UNECE region (http://www.unece.org/press/pr2010/10env_p20e.htm).

In the present chapter there is a focus on the effort taking place with respect to improving emissions of BC, and OC, within EMEP, as well as an update on the EMEP model performance with respect to EC. Further, an outline of how to solve the EC/BC conundrum through model/observation integration has been included. Finally, an analysis of which are the most important source regions of the Arctic BC loading is included. This final chapter also addresses the long term trend of BC in the Arctic and attempts to disentangle its variation according to changes in the atmospheric circulation and emission strength.

For further details concerning the finalized version of the EUSAAR-2 thermal protocol for analysis of EC and OC, the interested reader is directed to the recently published peer reviewed paper by Cavalli et al. (2010).

5.2   Emissions of carbonaceous aerosols

By Zbigniew Klimont, Kaarle Kupiainen and Markus Amann

5.2.1   GAINS model development with respect to BC

The parties to the Convention do not have an obligation to report BC emissions and there are only few national BC inventories currently available. The GAINS model (developed at the International Institute for Applied Systems Analysis (IIASA) in Laxenburg, Austria; http://gains.iiasa.ac./gains) is being further developed by the EMEP Center for Integrated Assessment Modelling (CIAM), hosted by IIASA, to include estimates of black carbon (and organic carbon). In fact the research version of the carbonaceous module has been in use for a few years already (Kupiainen and Klimont, 2004 and 2007). Within the Expert Group work the key data and current results from the model were provided recently to the national experts (specifically experts nominated to participate in the BCEG) for discussion and potential use in their work for developing own national BC estimates. By the end of 2010 it is envisaged that the on-line version of the GAINS model including carbonaceous aerosols will be available and used for estimating the country or region specific emissions and mitigation potential. This first public release will include the results of the ongoing interaction with the national experts within the mandate of the BCEG.

Figure 5.2 presents a two-basket approach for extending the GAINS model to include analysis of near-term climate impacts in parallel to the existing ecosystem and health elements. This framework will allow for consideration of the co-control between short-lived climate forcers and long-lived substances.

Furthermore, optimizing for specific radiative forcing while maintaining air quality constraints might lead to increasing robustness of health impact strategies due to preferential treatment of black carbon vs. other (secondary) $PM_{2.5}$ components.
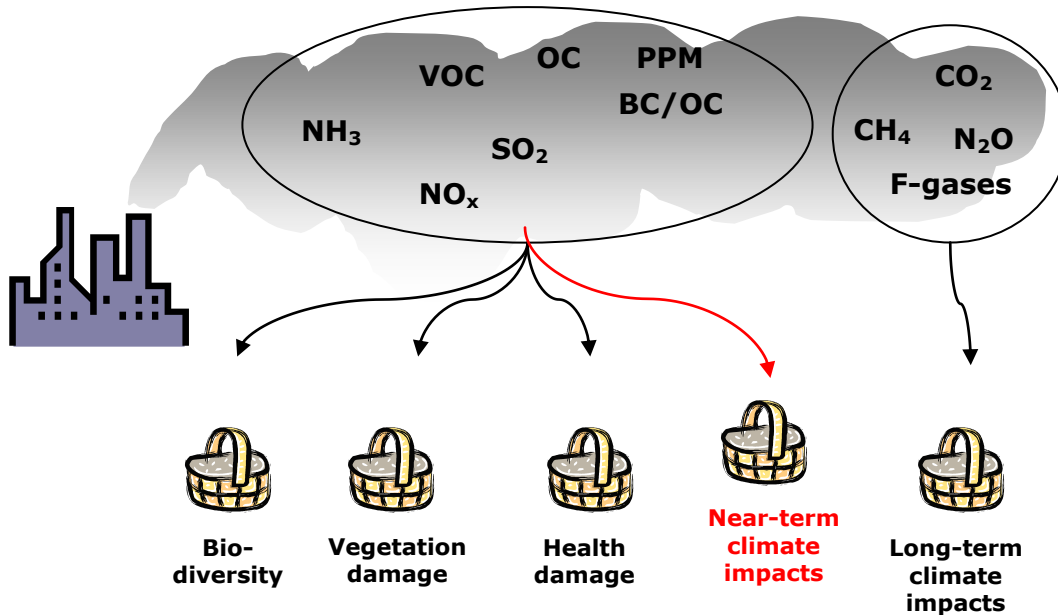

Figure 5.2: *A two-baskets approach in GAINS for climate impacts analysis and integration of air quality impacts.*

5.2.2 Overview of BC/OC emissions in the UNECE area

GAINS covers currently nearly all (51 of 56) of the UNECE member countries, only Andorra, Lichtenstein, Monaco, San Marino, and Israel not being included at present. Russia is split into a European and an Asian part, whereas Serbia and Montenegro, as well as Tajikistan, Turkmenistan, and Uzbekistan are represented as single regions.

Following the publication of the European inventory (Kupiainen and Klimont, 2007) based on the research version of the GAINS BC model (Kupiainen and Klimont, 2004), CIAM has been continuing the development and update of the tool. The current activity data for the UNECE countries is based on the work done under the recent revision of the Gothenburg Protocol; 16 countries have provided updates of the national energy balances and projections so far while for the remaining countries either the latest PRIMES model scenario or the IEA WEO 2009 scenario (IEA, 2009) is used.

The current (2005) and future (2030) baseline (current legislation - CLE) BC emissions are presented in Figure 5.3. Total BC and OC emissions for 2005 in the UNECE region are estimated at 1.0 and 1.4 Tg, respectively. For BC, the majority of the emissions originate from the residential and transport sectors, i.e., 30 and 50 percent. However, the importance of specific sectors varies between the regions, e.g., in the EU-15 and US the transport emissions are more important,

over 60 percent of the total BC, than in other regions, e.g. in Russia (see Figure 5.3). In Russia a major part of anthropogenic BC is estimated to come from oil and gas flaring and open burning of agricultural residues. However, these sectors belong to the most uncertain since both activity and emission factors are very scarce; as a matter of fact there are no established BC emission factors for flaring and only recently a research group in Canada undertook an effort to estimate them and validate numbers in use. The GAINS data for oil and gas flaring has been recently reviewed making use of the NOAA NGDC study (Elvidge et al., 2009). The data has been allocated to GAINS regions according to the spatial information provided at the study website (http://www.ngdc.noaa.gov/dmsp/interest/gas_flares.html).

Since the model is under development and a discussion with national experts has been initiated only recently, we are not attempting here a comparison of existing estimates for a few countries with the results of the current GAINS implementation. However, ongoing discussion with e.g., US experts, indicates that careful evaluation is needed as differences for specific sectors might be very large owing to different sources of emission factors or varying methodological approach. The final report of the BCEG group will discuss a number of these issues by the end of 2010.
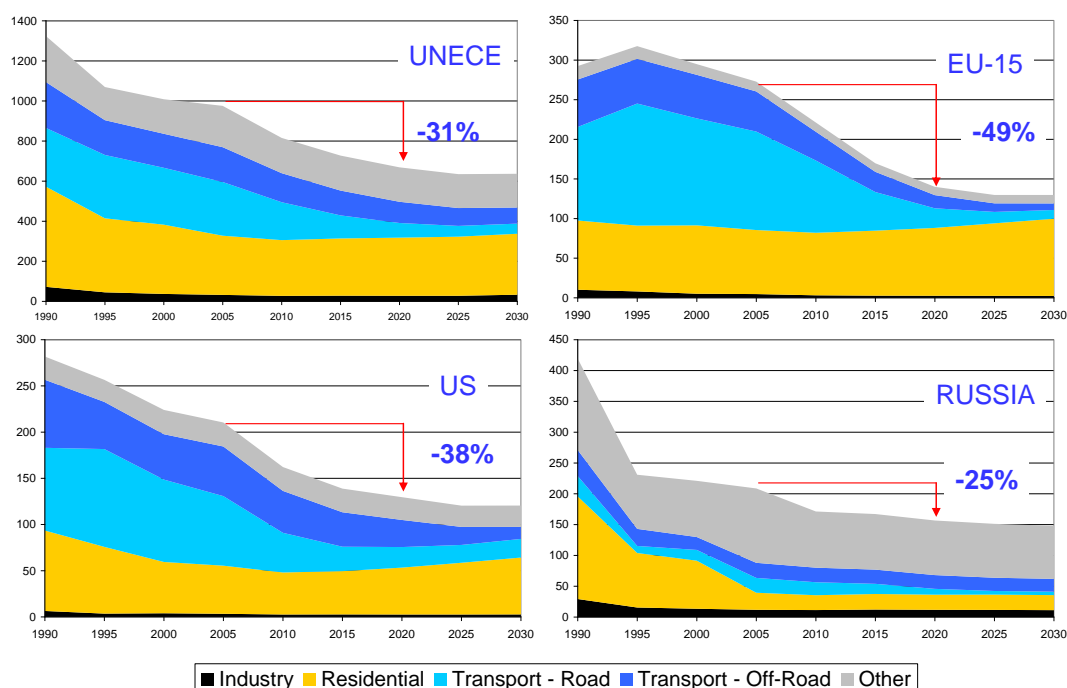

Figure 5.3: *Sectoral structure and development of BC emissions [kt] in selected UNECE regions in the CLE scenario; indicated reductions refer to the change between 2005 and 2020* – Source: *GAINS model.*

Figure 5.4 shows the sectoral emissions of BC and OC in Europe for 2000 and 2005, as estimated currently by GAINS vs. the 2000 values from Kupiainen and Klimont (2007). The current assessment is lower than that of Kupiainen and Klimont (2007), in particular for BC from road transport and OC from residential combustion. The main reasons for the differences are the updated activity data and

control strategies during the ongoing work on the revision of the Gothenburg Protocol, as well as updates of emission factors and other model parameters, e.g. revision of the transport sector emission factors in light of the COPERT4 data (http://lat.eng.auth.gr/copert/); mostly for the EU27 countries. Estimates presented in this graph, as well as in Figure 5.3, do not specifically consider high emitting vehicles (super-emitters); which is a topic for discussion in chapter 5.2.3.
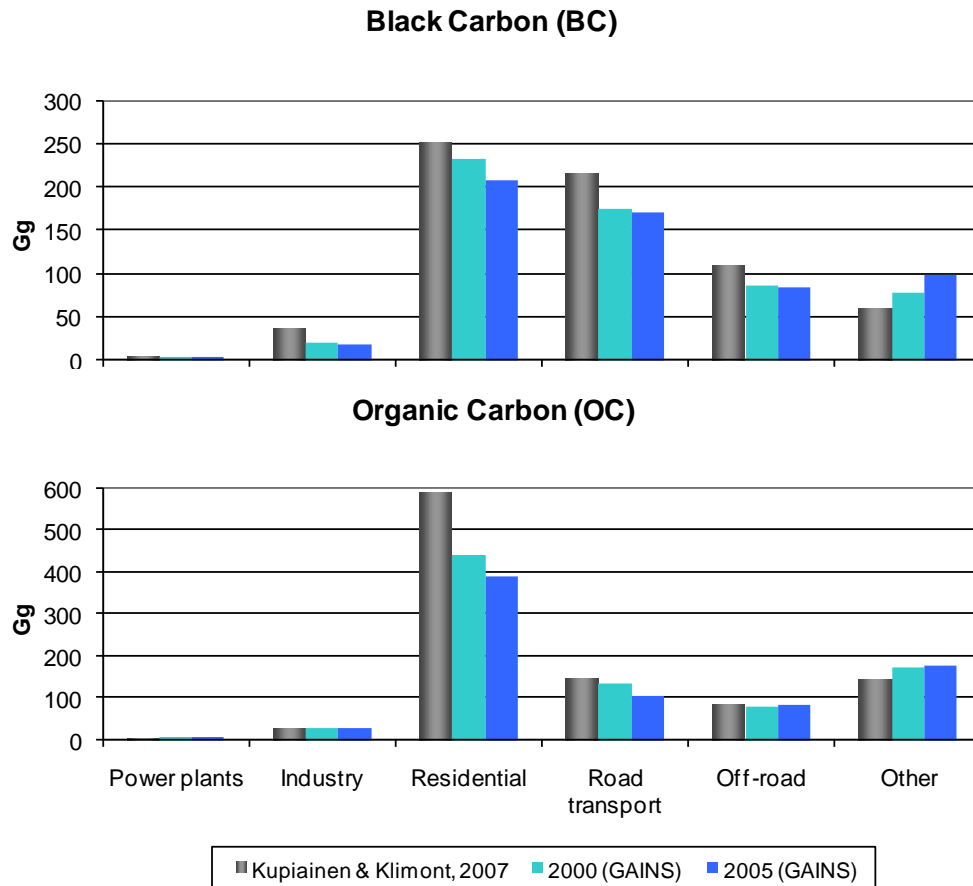
Black Carbon (BC)

Organic Carbon (OC)

Figure 5.4: Sectoral emissions of BC and OC in Europe for 2000 and 2005.

Figure 5.3 also shows expected future development of BC emissions in the considered regions assuming successful implementation of the current legislation (CLE). Although there is no specific legislation targeting carbonaceous aerosols, the existing and proposed PM and SO_2 regulation is expected to bring significant reductions of primary BC and OC. While residential combustion is, and will remain in the future a key BC emitting sector, the transport sector (especially road) is expected to decline by about 70 percent by 2020, provided current policies (DPF technology) will bring expected reductions. The highest reductions are expected in the EU-15, where the BC emissions could decline by 49 percent by 2020. This is more than for example in the US (-38%) and Russia (-25%). However, emissions from off road transportation are not reduced as strongly, which will increase this sector's relative importance in the future. Considering the fact that there is limited information available about key parameters of the off road transport sector, and because the equipment operates often in harsh

conditions, and have long lifetimes, careful monitoring of existing legislation and strengthening of policies in this area seem necessary.

The 2005 UNECE emissions of BC and OC as constituents of $PM_{2.5}$ by SNAP sectors are presented in Figure 5.5. Industrial sources (SNAP1, 3-6) have very low shares of carbonaceous particles and therefore are likely to be much less important from the perspective of BC reduction. Residential combustion (SNAP2) and transport sources (SNAP7-8), in turn, have high shares of carbonaceous emissions and therefore are priority source sectors. Transport sources also have a lower OC/BC-ratio compared to residential burning. SNAP9 and 10 include waste flaring and agricultural burning sources, which might be of relevance for specific regions.
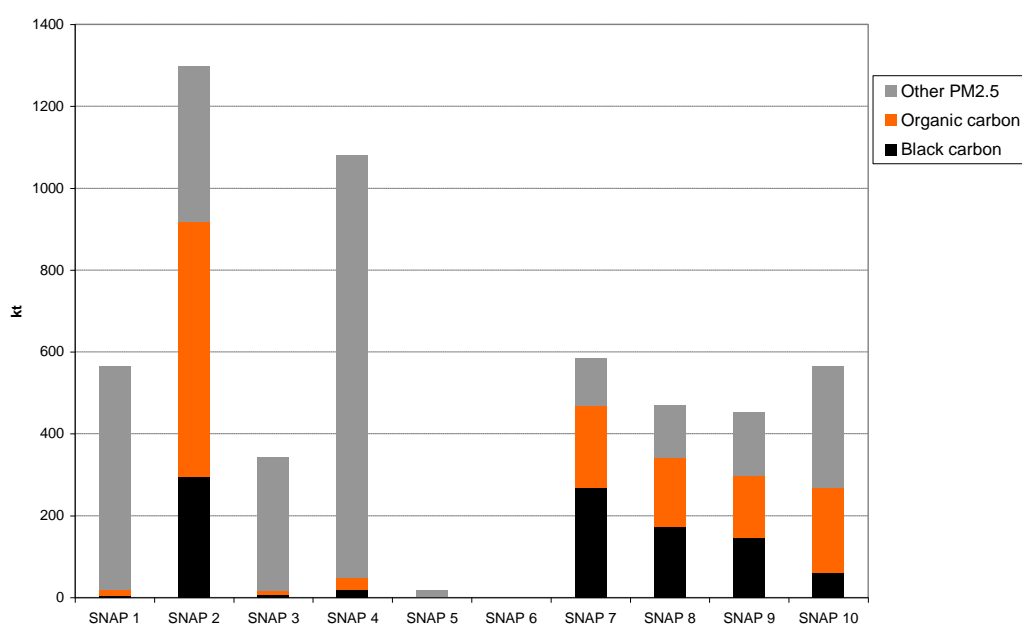

Figure 5.5: *Emissions of BC/OC/$PM_{2.5}$in the UNECE for 2005 by SNAP sector; Source: GAINS model.*

While Figure 5.5 indicates the importance of BC and OC in $PM_{2.5}$ at the total UNECE emission level, Figure 5.6 shows the average BC/$PM_{2.5}$ and OC/$PM_{2.5}$ ratios for the period 2000-2005, as estimated by GAINS by key sectors for the entire UNECE area, as well as the variation between countries. The error bars represent the low and high boundaries of the ratios calculated for the UNECE countries. National specific shares vary substantially owing to different importance of sectors and their different emission characteristics (as demonstrated in Figure 5.5). E.g., while the total residential sector emissions are dominated by biomass burning, characterized by higher shares of OC and BC in $PM_{2.5}$ (Figure 5.5), some UNECE countries still use significant amounts of coal leading to higher share of BC in $PM_{2.5}$ for this sector in certain countries (Figure 5.6). Similarly, for road transport the share of BC in $PM_{2.5}$ will strongly depend on the share of diesel fuel and the level of control. The regional differences point to potential problems in using for example simplified approaches to estimate total

PM$_{2.5}$ emissions, e.g., by using BC and OC only, not accounting for organic matter (OM=~1.4*OC). Such an approach might lead to a significant under-estimation of the fine PM emissions regionally. Furthermore, the use of BC and OC shares of PM$_{2.5}$ to derive source specific emission factors need to be done with caution as specific technology mixes (combustion devices, vehicles types, driving habits, fuels, age, etc.) might differ substantially from one region to the other.
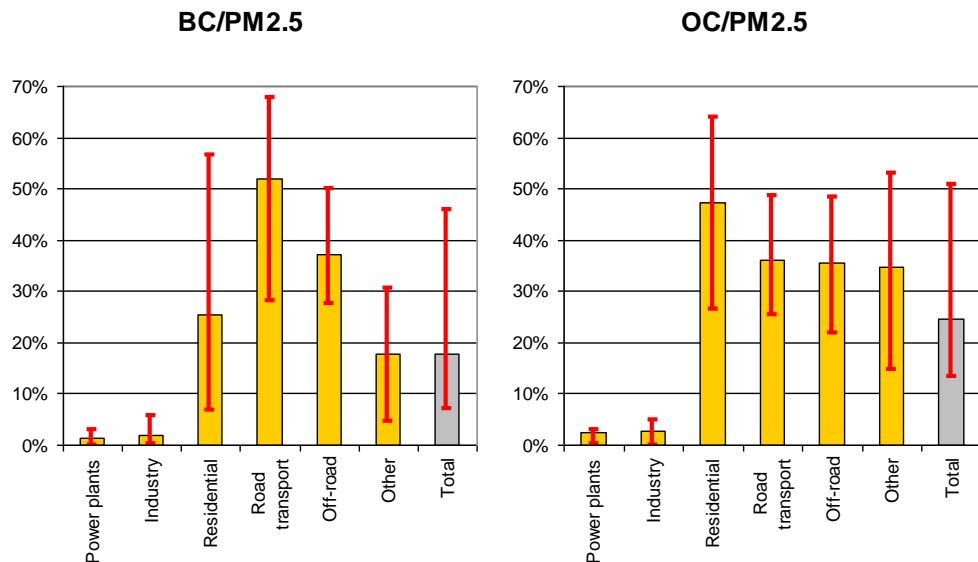

Figure 5.6:   *Share of BC and OC emissions in PM$_{2.5}$ (years 2000-2005) by sector and*
total for the entire UNECE region, as well as variation between all
countries (low-high).
Source: *Preliminary GAINS estimates; 'Industry' equals sum of SNAP*
3,4,5,6 and 'Other' the sum of SNAP 9 and 10.

Figure 5.7 provides an overview of the regional distribution of BC and OC emissions in Europe in 2005. According to Figure 5.3, a substantial decrease of BC is expected within 2030 (according to CLE).
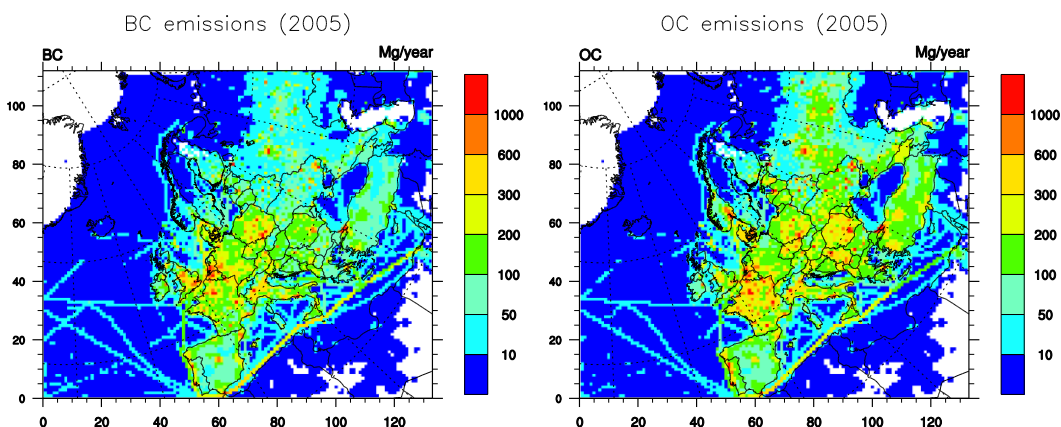

Figure 5.7:   *Spatial resolution of BC and OC emissions for 2005, as used in the*
EMEP model.

5.2.3 Introduction of high-emitters in GAINS

As indicated previously, the current GAINS algorithm does not specifically consider high emitting vehicles, e.g., Figure 5.3–Figure 5.5. However, CIAM is working on the implementation of such a feature and this section introduces the basic concept, as well as it shows some preliminary results.

On-road measurement studies of vehicle emissions have revealed that a relatively small fraction of the vehicle fleet is responsible for a relatively large share of the emissions. These vehicles are referred to as high emitters, super-emitters, gross emitters, smokers or excess emitters.

In GAINS these high emitters are defined as vehicles that have emissions above a certain emission threshold or cut-off. As a consequence two sets of information were introduced to the model:

- The amplification factor, which is the ratio between the high and normal emitter emission factors, and
- Country and region specific shares of high emitters in the vehicle fleet.

The technology specific amplification factors (e.g. for EURO 1 to 4) were created based on existing on-road studies mainly from the United States (Durbin et al., 1999; Yanowitz et al., 1999; Hsu & Mullen 2007; Ban-Weiss et al., 2009) and using the 95th percentile as the cut-off. The derived BC and OC amplification factors are shown for light and heavy duty vehicles in Table 5.1 and apply to all countries and regions. The values are currently the same for both BC and OC. This is in line with observations by Subramanian et al. (2009). However, Lawson (2010) showed that the OC/BC ratio might be different for high emitters than for normal vehicles.

Table 5.1:   BC and OC amplification factors for light and heavy duty vehicles.

	Light duty		Heavy duty	
	Diesel	gasoline	diesel	gasoline
No control	3	6	3	4
Euro1	3	6	3	4
Euro2	5	6	5	4
Euro3	5	10	5	10
Euro4	5	10	5	10

The next step was to study what share of the vehicle fleet corresponds to the amplification factors. A share of five percent was used for the United States based on the above mentioned measurement studies and was assumed to be representative also for Canada and the EU-27. However, deriving similar shares for the other UNECE countries and regions turned out to be a challenging task, since we found no studies with appropriate data. For the time being a high emitter share of 10 percent is used for other UNECE countries also taking into account earlier studies that include high emitters into emission models (Bond et al., 2004).

Preliminary estimate of contribution of high emitting vehicles to BC emissions in the 2005 and 2030 baseline in selected regions is shown in Figure 5.8. The high emitting vehicles are estimated to increase the transport emissions in the UNECE region by about 10 and 15 percent in 2005 and 2030, respectively. The country specific increments vary due to differences in vehicle age distribution, fuel use and the estimated share of high emitters in the fleet. As indicated in Figure 5.8, the overall reduction in transport and high emitter emissions is estimated to be more pronounced in the EU-15 than in the US and Russia. The high emitter emission estimates are preliminary and the data will be updated in the course of 2010.
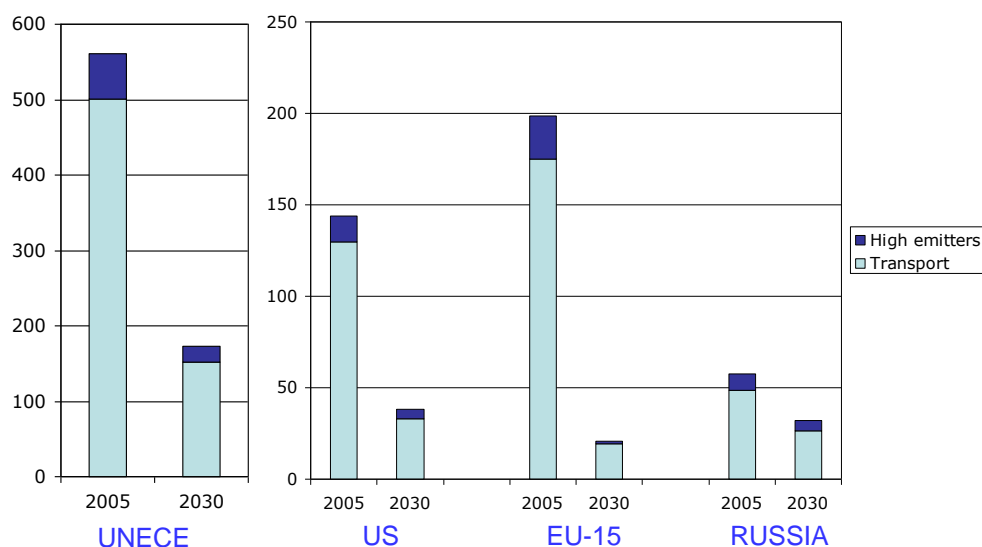

Figure 5.8: *Preliminary estimate of contribution of high emitting vehicles to BC emissions from the transport sector [kt] in 2005 and 2030 baseline for selected regions;*
Source: *preliminary GAINS calculation.*

5.3 EMEP modelling of Elemental Carbon

By Svetlana Tsyro and Karl Espen Yttri

Elemental carbon (EC) is directly emitted in the air during combustion of fossil and biomass fuels and vegetation fires. Though EC is a minor constituent of PM_{10} and $PM_{2.5}$, it was important to have it included in EMEP model calculations e.g. for PM mass balance. Moreover, EC can crudely be considered as a tracer of primary PM from combustion sources and used for testing the accuracy (preliminary evaluation) of emission data (Tsyro et al., 2007). The recent growth of interest in assessing the atmospheric burden and deposition of EC is primarily related to its climate effects, and is particular relevant for the Arctic areas (see chapter 5.4).

Model calculated concentrations of EC using the EMEP model have previously been evaluated by Tsyro et al. (2007) and Simpson et al. (2007) using data from the EMEP EC/OC campaign (2002 - 2003) (Yttri et al., 2007), EC/OC data from the CARBOSOL project (2002-2004) (Pio et al., 2007), and data from the EMEP intensive measurement periods in 2006 and 2007 (EMEP, 2008). In the above-mentioned studies, the model was found to overestimate EC in northern Europe, notably in winter, while considerably underestimating EC in central and southern Europe, particularly in summer.

Recently, more EC measurements have become available both within the EMEP intensive measurement periods conducted in 2008 and 2009, and as part of the regular monitoring taking place within the EMEP monitoring network. Black Carbon (BC) derived from absorption coefficient measurements using optical instrumentation can also be used for model validation purposes. Such measurements have lately become more readily available through the EU funded EUSAAR (European Supersites for Atmospheric Aerosol Research) project, and finally the estimates of EC emissions have been improved. In the current work, we have used new BC emission estimates from the GAINS model by IIASA, as well as a new EC/OC emission inventory by TNO (Visschedijk et al., 2009; Denier van der Gon et al., 2010) within the EMEP model to calculate EC concentrations for 2008. The model results have been evaluated against observations from three EMEP monitoring sites for the whole year of 2008 and against measurements from the EMEP intensive measurement period conducted in fall (17 September – 17 October) 2008. The main results of the current work is summarised in chapter 5.3.2.

5.3.1 Methods

The terms elemental carbon (EC) and black carbon (BC) are often used alternatively in atmospheric chemistry literature. The choice and use of these synonyms is operationally justified and reflects the method of determination and purpose of study. Within the EMEP measurement framework, using a thermal method with optical correction for charring is recommended for determination of EC. By definition, thermal-optical methods determine EC concentrations (Gelencsér, 2004) differently from optical methods which yield concentrations of

light absorbing carbon, i.e. BC. For consistency, the term "elemental carbon" (or EC) will be used through this chapter.

Emissions Based on GAINS-estimated anthropogenic emissions of EC and $PM_{2.5}$, the EC fraction of $PM_{2.5}$ emissions ($EC/PM_{2.5}$) have been derived for all European countries for each SNAP 1 activity sector for the year 2005. From the EMEP emission database, emissions of $PM_{2.5}$ and PM_{10} are only available at present, as the chemical speciation of PM emissions is not reported. Therefore for these model calculations, EC emissions for 2008 have then been calculated by multiplying $PM_{2.5}$ emissions for 2008 by the derived $EC/PM_{2.5}$ fractions (denoted "new"). For comparison, also model calculations using the previously employed ("old" henceforth) $EC/PM_{2.5}$ fractions are presented in this section. The old $EC/PM_{2.5}$ fractions were based on emissions of fine carbonaceous particles for the year 2000 from Kupiainen and Klimont (2006). Similarly, these old $EC/PM_{2.5}$ fractions has also been multiplied by the EMEP $PM_{2.5}$ emissions for 2008 to calculated "old" EC emissions for 2008.

Emissions of coarse EC have been calculated by multiplying EMEP emissions for 2008 of coarse PM by the EC fractions in coarse PM, based on preliminary estimates provided by IIASA back in 2005. Note that the same emissions of coarse EC have been used in both model runs with IIASA's data.

According to the latest estimates from the GAINS model, residential combustion was the largest single sector, contributing with about 43% to the total European EC emissions in 2005. The second most important source of EC was road transport, contributing with 35%, followed by other mobile sources and machinery (15%). There is a substantial variation in the importance amongst the various parts of Europe, though. The relative contributions from residential combustion and traffic varied according to season. This was particularly pronounced for the residential combustion sector, totally dominating for a number of countries in winter.

In addition, we have also made a model run using emissions of anthropogenic EC from a European inventory constructed by TNO, partly within the frame of the EU FP 7 project EUCAARI, for the year 2005 (Visschedijk et al., 2009; Denier van der Gon et al., 2010). In this estimate, the size-differentiated PM emission estimates (PM_{10}, $PM_{2.5}$, PM_1) from IIASA's GAINS model were combined with EC fractions from literature reviews, resulting in EC emission estimates for GAINS' 230 source categories and three particle size classes (i.e. EC_1, $EC_{1-2.5}$ and $EC_{2.5-10}$). The emissions were gridded on a $1/8°x1/16°$ resolution (i.e. approximately 7 x 7 km). For the present model runs, the TNO EC emissions have been interpolated to the EMEP 50 x 50 km^2 grid. Also, EC_1 and $EC_{1-2.5}$ have been added to derive $EC_{2.5}$ emissions for consistency with the IIASA's data.

Figure 5.9 compares the three EC emission datasets used for the model runs for each SNAP1 sector. The larger EC emissions from residential combustion (sector 2) derived from new IIASA data compared to IIASA old and TNO data, is noticeable. For road traffic (sector 7), the TNO estimate for EC is larger than both estimates from IIASA, whereas EC emissions from sector 8 (other mobile sources and machinery) are quite similar for the three datasets. It can also be noted that for

all minor EC sources (i.e. sectors energy production (1), production processes (4), waste incineration (9) and agriculture (10)) TNO emissions are larger than those from IIASA's estimates.

Model In the EMEP model, 20% of the emitted EC is assumed to be hydrophilic, whereas 80% is hydrophobic. In order to adequately describe the lifetime of EC in the atmosphere, the model accounts for EC ageing processes, i.e. changing of EC's hygroscopic properties, which determine the efficiency of its wet scavenging. The EC ageing rates, as dependent on season, time of the day and altitude, from Riemer et al. (2004) are used to describe the transformation of the hydrophobic EC to hydrophilic EC (Tsyro et al., 2007). In the EMEP model, the hydrophobic EC is assumed not to be washed out from clouds.
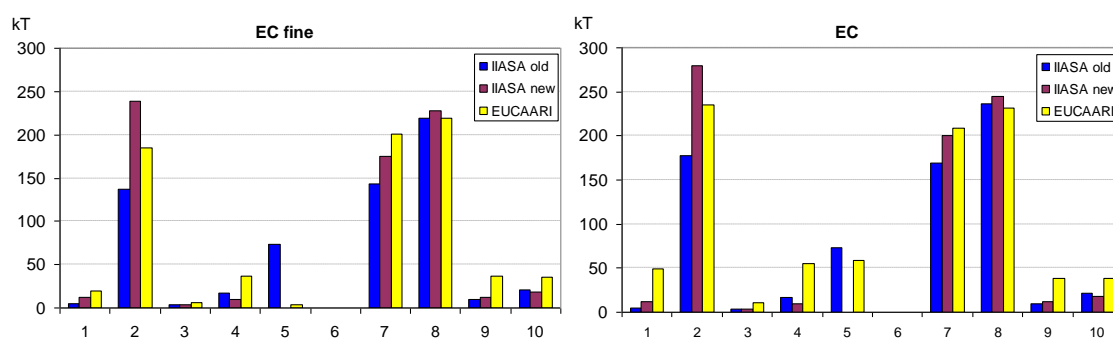

Figure 5.9: *Comparison of EC emissions for 2008 used for the model runs, which are based on IIASA old and new estimates and EC emissions for 2005 from the TNO/EUCAARI inventory for SNAP1 sectors (abscissa axis). Shown are $EC_{2.5}$ (left panel) and EC_{10} (right panel).*

Measurements Model calculated EC concentrations from both model runs have been compared with measurements of weekly PM_{10} EC concentrations measured during the EMEP intensive measurement period taking place from the 17th of September to 17th of October, 2008. These measurements are discussed more thoroughly in the paper by Yttri et al. (in preparation). In addition, annual measurements of EC concentrations in PM_{10} and $PM_{2.5}$ at Melpitz (DE0044R) and Birkenes (NO0001R) and EC concentrations in $PM_{2.5}$ at Ispra (IT0004R) for 2008 have been included in the comparison. The EC measurements were performed at a daily time resolution at DE0044R and IT0004R and weekly at NO0001R.

5.3.2 Results

5.3.2.1 EC concentrations for 2008

Model calculated annual mean concentrations of EC for 2008 are presented in Figure 5.10. The EC map on the left panel is from the model run with the new IIASA EC emission estimates, whereas the EC map on the right panel corresponds to the old emissions. In general, the most pronounced changes when using the new EC emission factors compared to the old ones are higher EC concentrations in the eastern and southern parts of France, west of Germany, Poland and Romania. On the other hand, the EC concentrations are lower in Ukraine, Russia and the EECCA area when the new emissions are used.

Model calculated EC concentration using TNO emissions are quite similar to those obtained using the new IIASA emissions in Western Europe, whereas they appear to be higher in Ukraine and central Russia. Also enhanced EC concentrations related to large EC emissions in cities are more pronounced when TNO data are used in the model calculations.
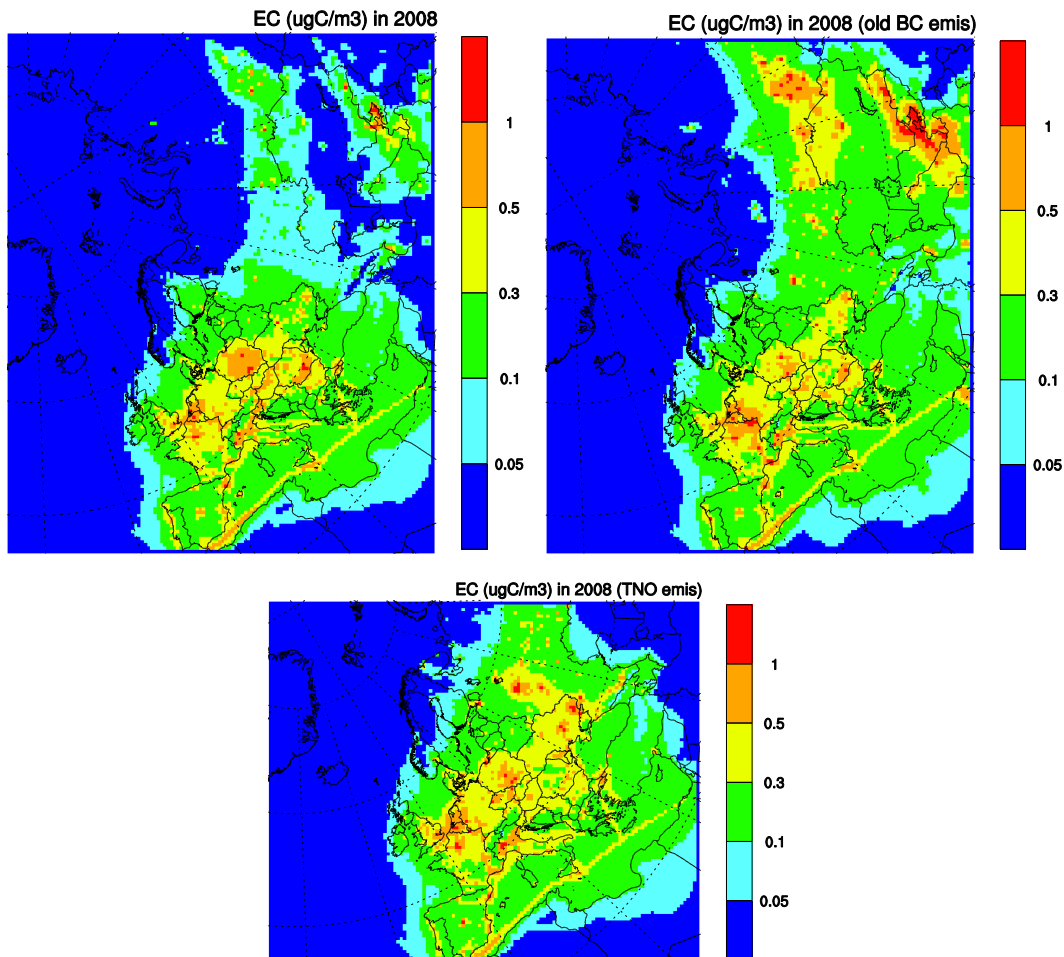

Figure 5.10: Annual mean concentrations of EC in 2008, calculated with the EMEP model using new (upper left panel) and old (upper right panel) EC emission estimates from the GAINS model at IIASA, and EC emissions from EUCAARI inventory (lower panel).

5.3.2.2   Comparison of modelled and observed EC concentrations

EMEP intensive measurement period – Fall 2008

Comparison of calculated EC concentrations using the EMEP model with measured EC concentrations from the EMEP intensive measurement period in fall 2008 are presented in Figure 5.11. Modelled EC calculated with the new IIASA EC emissions is denoted "ModN", whereas EC obtained with the old emissions are denoted "ModO". Shown in Figure 5.11 are the mean EC concentrations for each of the weekly samples, whereas mean values for the entire intensive period observed and calculated EC concentrations and model biases are given in Table 5.2.
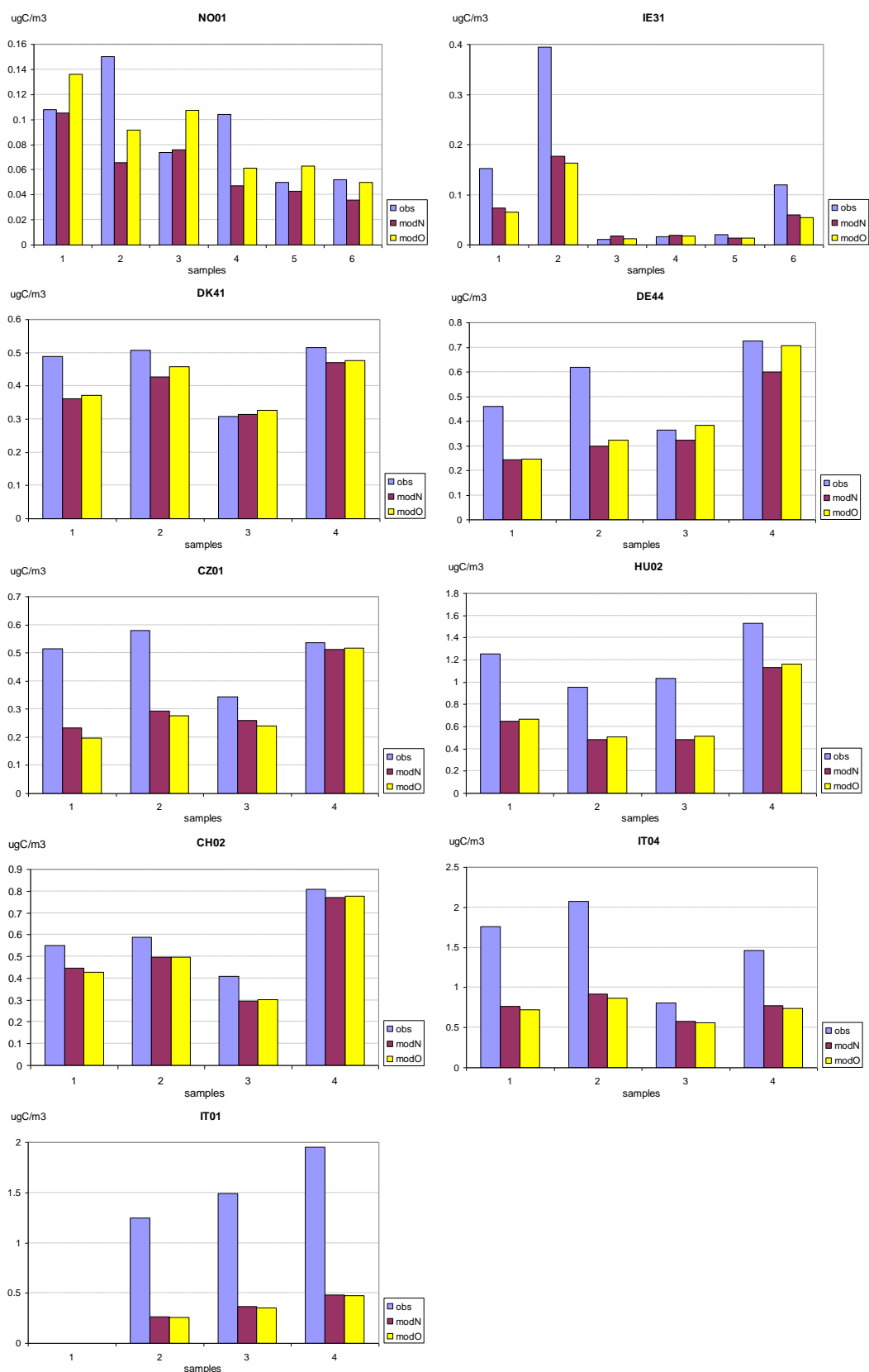
Figure 5.11: Observed (obs) and calculated EC concentrations for the EMEP intensive measurement period (17 September-17 October, 2008). For calculated EC: modN and modO are from model runs using IIASA's new EC and the old EC emissions respectively. "Samples" 1 - 4 on the x-axes corresponds to the weekly samples collected during the one month sampling period.

104

Table 5.2: Comparison of model calculated EC concentrations using the new and the old IIASA emission estimates with that of the observed EC concentrations observed during the EMEP intensive measurement period: mean concentration and relative bias are shown.

Site	Obs. mean	Model mean		Relative bias (%)	
		new EC emis	old EC emis	new EC emis	old EC emis
NO0001	0.09	0.06	0.09	-31	-5
IE0031	0.12	0.06	0.05	-50	-54
DK0041	0.46	0.39	0.41	-14	-10
DE0044	0.54	0.37	0.42	-32	-23
CZ0001	0.49	0.32	0.31	-34	-38
HU0002	1.19	0.69	0.71	-43	-40
CH0002	0.59	0.50	0.50	-15	-15
IT0004	1.53	0.76	0.72	-50	-53
IT0001	1.57	0.37	0.36	-76	-77

The model underestimates the observed EC concentrations for all sites in both runs, using new and old emissions. The underestimation is largest for the two Italian sites (76% at IT0001R and 50% at IT0004R), which are likely influenced by local sources unaccounted for by the model. September/October typically represents the start of the winter time increase of EC, which is particularly pronounced for the Ispra (IT0004R) site situated in Northern Italy. Nevertheless, the wood burning tracer levoglucosan is found to be present in samples collected at both sites, and in quite high concentrations at the IT0004R site (Yttri et al., in prep.), suggesting that the contribution of residential heating to the ambient EC level might be substantial already this early. Road traffic emissions are likely to be a major contributor to the EC concentrations, as well. The model under-estimation of EC is rather large (50%) also at Mace Head (IE0031). Likely explanations for this finding might be an underestimation of the trans-continental transport of EC from Northern America, as well as from Europe. The trans-continental contribution should in future be accounted for through describing the boundary conditions of EC. Concerning transport of EC from continental Europe, a too efficient EC removal from the atmosphere and an underestimation of European EC emissions might be likely explanations.

The differences in EC concentrations calculated with the new and the old EC emissions are in general rather small. The largest relative difference is found for Birkenes (NO0001R), where using the old emission data yields systematically higher EC. However, the EC concentrations are very low at Birkenes, hence the difference do not account for more than 0.04 μg C m^{-3}. Also for Melpitz (DE0044R), EC calculated with the old emissions are somewhat higher and closer to the observed levels compared to that of the new IIASA EC emissions.

In general, the model manages to reproduce observed temporal variation of EC concentrations, with the exception of NO0001R and DE0044R. For IE0031R and NO0001R, the model fails to predict enhanced EC concentrations in the second measurement week (September 24 – October 1). Trajectory analysis show that during that week, the transport to those sites originated from polluted regions in the UK and Central Europe for the 24th to 27th of September, while clean Atlantic

air masses influenced the sites from the 28th of September to the 1st of October. Thus, averaged over the whole week, EC concentrations are moderately high in the model results. For the whole measurement period, the relative model bias is -44 % and -43 %, whereas the spatial-temporal correlations are 0.8 and 0.77 using the new and the old IIASA EC emissions respectively.

EC levels from the regular EMEP monitoring

Figure 5.12 presents model calculated and observed time-series for EC in PM$_{10}$ and PM$_{2.5}$. Only model results obtained using the new IIASA EC emissions are included, as the differences between them and results using the old EC emissions are relatively small and can hardly be seen on the time-series.

For Melpitz (DE0044R) and Ispra (IT0004R), the daily time-series of observed and modelled EC are compared. On average, the model underestimates observed EC concentrations for both sites in 2008. At Melpitz, the model underestimates EC both for PM$_{10}$ and PM$_{2.5}$ through the whole year. It should be noted that the analytical method used to quantify EC in ambient samples collected at Melpitz severely overestimates EC, as it does not account for charring during analysis. Consequently, the model bias is less pronounced then observed from Figure 5.12.

At Ispra, model calculated EC in PM$_{2.5}$ is considerably lower than observations in winter, while quite close to measured EC concentrations in summer. However, the model is able to reproduce the seasonal variation observed for EC at this site. Elevated levoglucosan concentrations at Ispra observed during the EMEP intensive measurement periods in fall 2008, and in particular during winter 2009, suggest a substantial influence of residential wood burning. The discrepancies observed for the model calculated levels of EC and that observed during winter might thus be accounted for by missing wood-burning contributions.

The correlation between modelled and observed concentrations of EC is 0.66 for PM$_{10}$ and 0.64 for PM$_{2.5}$ at DE0044R. For IT0004R the correlation is found to be much lower (0.31). The model bias is about the same for the calculations with the old and new IIASA EC emissions. The correlation between calculated and measured EC has however improved using the new EC emissions compared to the old ones.

Figure 5.12 also shows the weekly time-series of observed and calculated EC concentrations for 2008 for Birkenes (NO0001R). For NO0001R, only EC in PM$_{10}$ is shown as the time-series for EC in PM$_{2.5}$ are almost identical, indicating a negligible contribution of coarse EC at NO0001R. A quite good agreement between modelled and measured EC is found for NO0001R. The calculated EC is practically unbiased on average and the correlation is 0.67. There is practically no difference in model calculated EC concentrations using the new and the old IIASA EC emissions (not shown) for NO0001R.
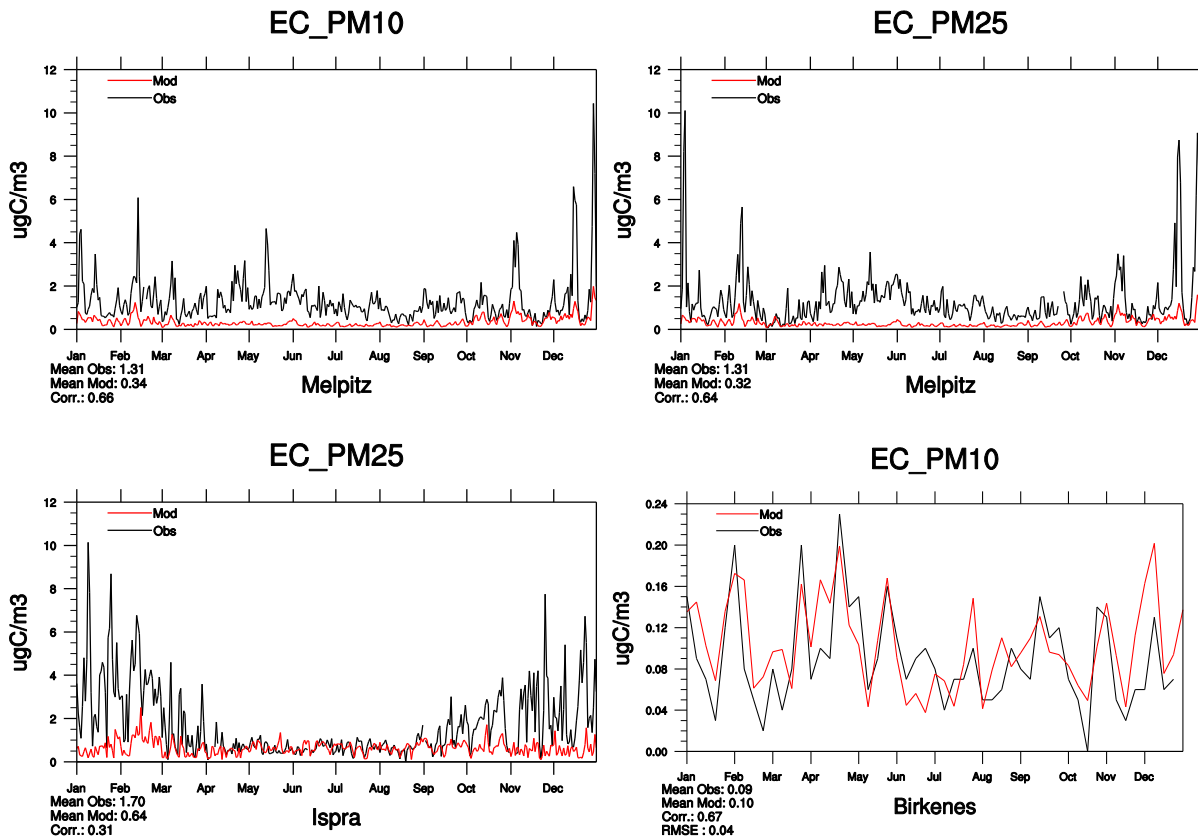
Figure 5.12: *Time-series for observed and model calculated EC for 2008: daily for Melpitz (DE0044R) and Ispra (IT0004R) and weekly for Birkenes (NO0001R). Only results obtained using the new EC emissions are shown as only minor differences are observed when compared to that obtained with the old emissions.*

Zooming in on the period from 17 September to 29 October, when EC measurements were performed as a part of the intensive period, we find approximately the same level of model underestimation of EC as shown in Figure 5.11. However, the measurements from the regular EMEP monitoring do not show the increase in weekly concentrations in the week between 26 September and 1 October, which is registered in the intensive data. Conversely, weekly EC concentrations decrease between 17 September and 22 October in both observation data and model calculations.

Summarising the results for considered EMEP monitoring sites, Table 5.3 shows the relative bias and correlation for EC calculated with old and new IIASA EC emissions and with TNO EC emissions compared to observations in 2008. Calculated with TNO emissions, model underestimation of observations is somewhat smaller, while the results with respect to correlation are variable.

Table 5.3:   Annual mean relative bias and correlation for EC calculated with old and new IIASA EC emissions and with TNO EC emissions compared to observations of EC from EMEP sites in 2008.

		Relative bias			Correlation		
		old IIASA	new IIASA	TNO	old IIASA	new IIASA	TNO
DE0044	EC_{10}	-74	-74	-68	0.55	0.66	0.67
	$EC_{2.5}$	-76	-76	-73	0.51	0.64	0.66
IT0004	$EC_{2.5}$	-64	-62	-58	0.25	0.31	0.24
NO0001	EC_{10}	11	11	0	0.67	0.67	0.66
	$EC_{2.5}$	-11	-11	0	0.68	0.73	0.68

Most of the results presented here show that the EMEP model tends to underestimate the observed EC concentrations. This is typically explained by a combination of several factors, notably emission uncertainties, inaccuracy of meteorological data, model deficiencies and measurement artefacts. Concerning emission uncertainties, one can be referred to Visschedijk et al. (2009). The sensitivity of EC model calculations to several uncertain parameters (EC ageing, wet and dry deposition, dispersion) was investigated by Tsyro et al. (2007). In that work, it was found that the model still underestimated EC concentrations for selected sites when both wet and dry deposition of EC was switched of (we have not performed similar test in the present work). Another aspect to check is how the model performs for other primary pollutants, which could say something about the accuracy of model description of pollutant dispersion from the sources. Thus, we have compared model results with observations of other primary components, namely SO_2 and NO_2, for the same sites as EC observations are available. This includes the sites NO0001R, CZ0001R, HU0002R, IT0001R and IT0004R. The model overestimates SO_2 concentrations at all five sites and NO_2 concentrations for NO0001R and HU0002R. It somewhat underestimates NO_2 for CZ0003R (by 26%) and IT0004R (by 37%), but the underestimation is larger for IT0001R (66%). These results indicate that at least for some of the sites, one should not rule out the possibility that model underestimation might occur due to too efficient turbulent upward mixing of pollutants.

5.3.3   Summary

Model calculated EC concentrations for 2008 have been compared with EMEP intensive measurements data obtained during fall 2008 and with EC observations from selected EMEP monitoring sites for the entire year of 2008. For the model calculations, new estimates of EC emissions from the GAINS model at IIASA and a new inventory of EC/OC emissions for 2005 by TNO/EUCAARI have been employed. The results have also been compared to model calculation using EC emissions from 2000 provided by IIASA.

The model underestimates weekly averaged EC concentrations from the intensive measurements by 44% on average. The relative bias ranges between -14% for DK0041R to 76% for IT0001R. In general, the model reproduces the week-to-week variation of EC concentrations. Results from model runs using the new and old IIASA EC emissions do not show significant differences, with the exception

108

of NO0001R and DE0044R, for which the old emissions cause a less underestimation of EC.

For daily EC observations for DE0044R and IT0004R, the model mainly underestimates EC concentrations, particularly during winter. The contrast in the model performance is particularly pronounced for the IT0004R site, for which the model hugely underestimates the EC levels in winter, while reproducing rather well the EC levels in summer. High levels of the wood burning tracer levoglucosan in fall and winter suggests that the winter time discrepancy at least partly might be attributed to missing wood burning contributions. The use of new IIASA EC emissions caused a slight improvement in the correlation between calculated and observed EC. Furthermore, the model is doing a fairly good job in reproducing weekly EC concentrations measured at NO0001R in 2008, both in terms of bias and correlation. Calculated with TNO emissions, model results show somewhat smaller underestimation of measured EC concentrations, while with respect to correlation the results are variable.

Model underestimation of EC found in this study could probably be caused both by uncertainties in emissions and in modelling pollutant dispersion, as well as by analytical artefacts. Effort should be made to further elucidate the differences observed when comparing model calculated and observed levels of EC.

5.3.4 Acknowledgement

5.4 BC in the Arctic

By David Hirdman

There is a pronounced seasonal variability in the source regions of the BC affecting the Arctic troposphere, but an overall downward long-term trend is observed. For all seasons except summer, long-range transport from Northern Eurasia is the major source of BC at the three Arctic observatories Zeppelin, Alert and Barrow. During summer the picture is more complex, with regional sources dominating, including e.g. boreal forest fires (Hirdman et al., 2010a)

Pollutants with a short atmospheric life time and black carbon (BC) in particular, have recently received attention as potentially significant climate forcers, especially in the Arctic. To enable the development of emission reduction strategies for this region it is essential to know where the emissions currently affecting this area the most are to be found. Furthermore, it is important to localize those regions in which new emissions would pose the greatest/least damage to this vulnerable environment.

By combining measurement data of equivalent BC (EBC) from the three Arctic observatories Zeppelin (Svalbard, Norway), Alert (Canada) and Barrow (Alaska, USA) with calculations from the Lagrangian particle dispersion model FLEXPART, the source and sink regions of BC has been identified. In brief, this was done by associating the highest (R_{90}) and the lowest (R_{10}) 10% of the measurement data, respectively, with the corresponding atmospheric transport simulated by FLEXPART. We have with this method identified the most important source regions contributing to the BC loading in the Arctic troposphere and how these changes with season.

A trend analysis was performed based on the times series available for BC at the three observatories, using a clustering approach identifying the most dominant regimes of the atmospheric transport and how the frequency of these transport regimes change with season, as well as over time. Our analysis show that there has been a general downward trend in the BC measured at Zeppelin as for Alert and Barrow (Hirdman et al., 2010b), and that only a minor fraction of the decrease of BC in the Arctic troposphere can be explained by a long-term change in the atmospheric circulation and that the decrease is largely attributed to decreasing emissions in Northern Eurasia. Despite the overall downward trend of BC observed at the Arctic observatories, there is recent evidence of increased winter time BC emissions in the eastern parts of Northern Eurasia over the last decade. This area corresponds to that shown in Figure 5.14d, which is enlarged to include more Southern altitude in winter.
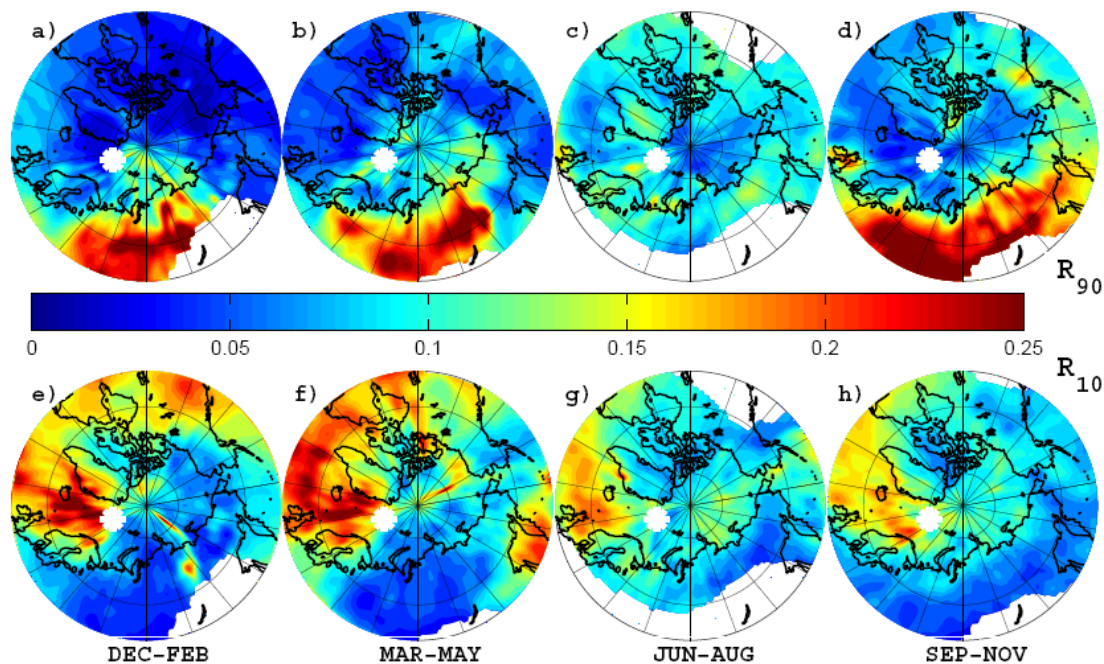
Figure 5.13: Fields of R$_{90}$ (top row) and R$_{10}$ (bottom row) for measurements of EBC at the Zeppelin station during the years 2002-2007, for December-February (far left column), March-May (middle left column), June-August (middle right column) and September-November (far right column). The location of the Zeppelin station is marked by a white asterisk. White areas have been excluded from the analysis because total sensitivity, S$_T$, is too low.

Figure 5.13 shows the potential source regions for BC measured at the Zeppelin observatory during the different seasons of the year. The top row indicates source regions corresponding to the highest 10% of the measured BC concentrations and the bottom row to the lowest 10% of the data. A region with a value above 0.1 means that there is an increased surface sensitivity associated with the highest or the lowest 10% of the BC concentrations measured at the station and thus a strong possibility to find the emission source (top row) or sinks (bottom row) within these regions. The top row of panels confirms that Northern Eurasia is the dominating source region for Zeppelin in all seasons but summer. The bottom row shows that the transport associated with the lowest BC concentrations mainly arrive from the North Atlantic Ocean.
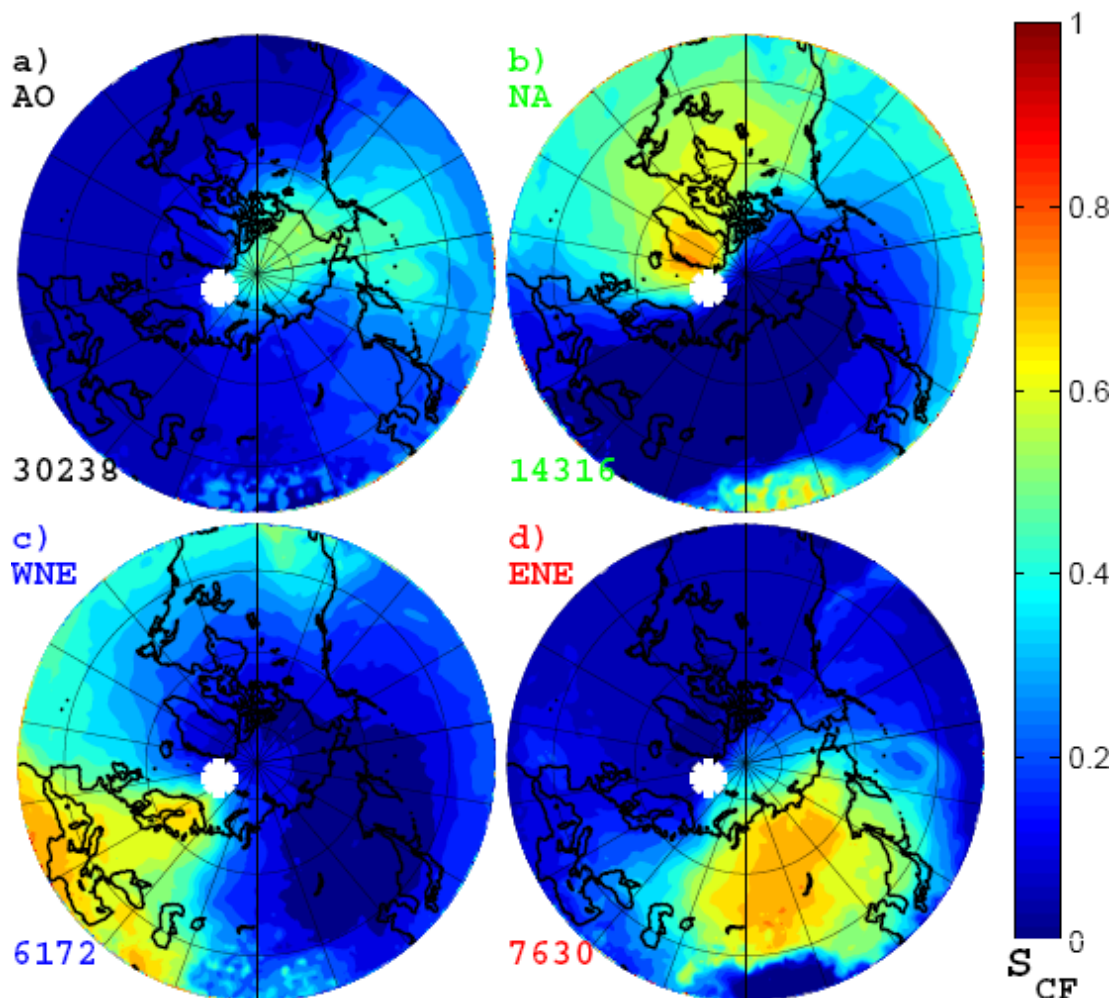
Figure 5.14: show the four clusters of atmospheric transport identified at Zeppelin. The clusters all have distinctive regions of influence, namely the Arctic Ocean (AO), North America and the North Atlantic Ocean (NA), western parts of Northern Eurasia (WNE), and eastern parts Northern Eurasia (ENE). Finally, Figure 3 displays to what extent trends in transport (dashed black line with black circles) may explain the overall trend of the BC measurements (solid black line) for the three Arctic stations Alert (top panel), Barrow (middle panel), and Zeppelin (bottom panel).
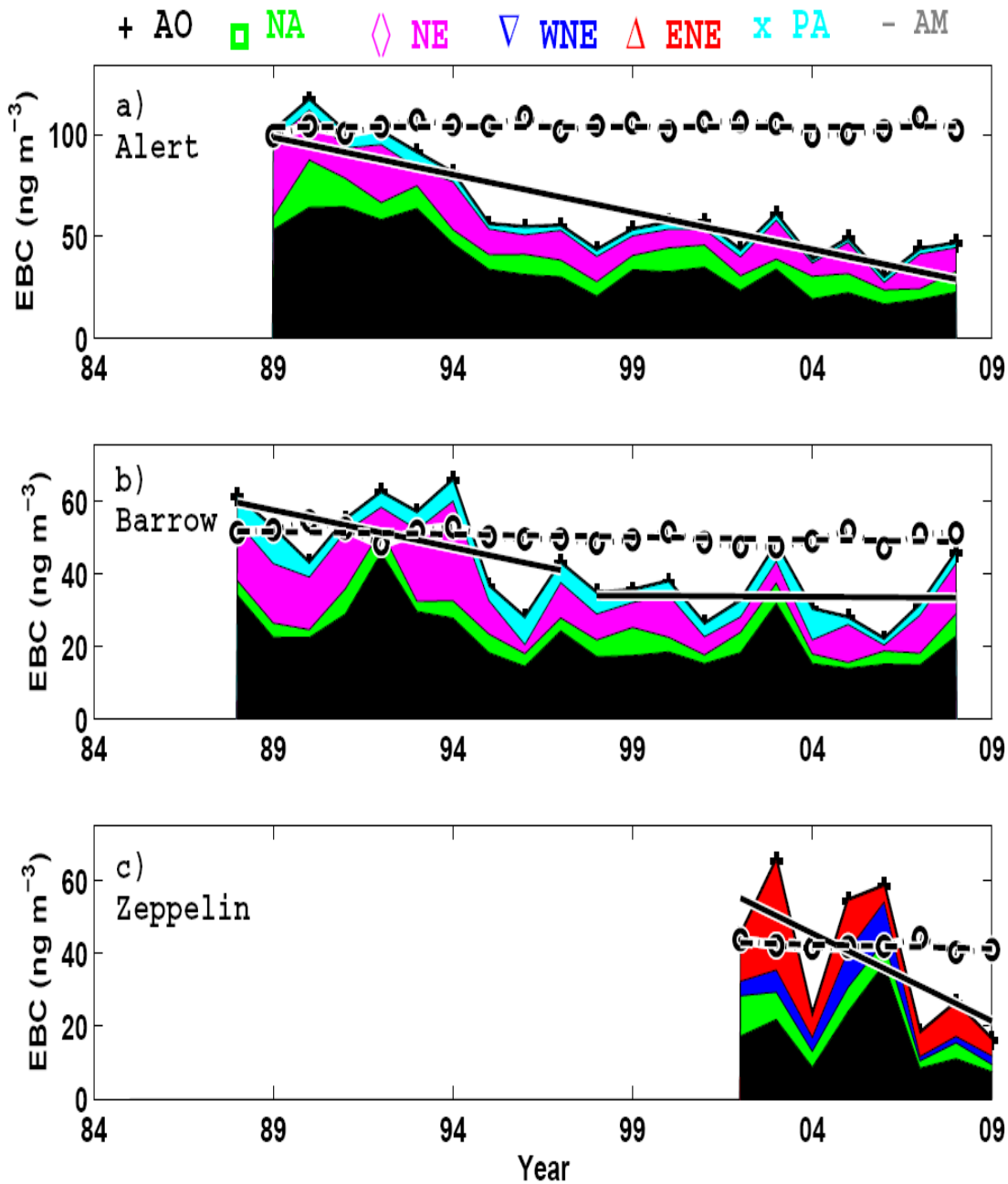
*Figure 5.15: The annual mean BC concentrations measured at the Alert (a),
Barrow (b), and Zeppelin (c) observatories and split into
contributions from the four transport clusters. The solid line shows
the linear trend through the measured concentrations. The circles
show the annual mean BC concentrations when the cluster-mean
concentrations are held constant over time (means over the first
three years). This line is influenced only by changes in the
frequencies of the four clusters. The dashed line shows the linear
trend of these data.*

5.5   Solving the EC/BC conundrum through model/observation integration

By Markus Fiebig

The objective of the EU funded project EUSAAR (European Supersites for Atmospheric Aerosol Research) is to integrate measurements of atmospheric aerosol properties at a number of European regional background supersites, which is to serve as an integrated atmospheric observing system for both air quality and climate studies. Measurements of non-regulated aerosol properties of interest to air quality and global climate, i.e. chemical, physical and optical properties, are currently performed outside of coordinated protocols and thus require particular focus. One variable for which there is a profound need of coordinated action is that of monitoring of soot particle bound black/elemental carbon.

Already in the early days of air quality monitoring, it became apparent that airborne particles containing fractally agglomerated carbon spherules, originating from incomplete combustion of hydrocarbons, colloquially referred to as "soot", have both significant effects on human health and the atmospheric radiation budget influencing climate. Of the experimental approaches developed for measuring "soot" concentrations in ambient air, two became widely used: 1) the *integrating plate* technique (Lin et al., 1973); 2) the *thermal-optical method* (Birch and Cary, 1996).

The integrating plate technique uses the fact that "soot" is highly absorbing for electromagnetic radiation in the visible spectral range with a uniform spectral signature. The aerosol particles are sampled on a semi-transparent, non-absorbing filter medium. While the filter is loaded with particles, the decrease in optical transmissivity of the filter is measured using monochromatic, also with independent measurements at several distinct wavelengths, or white light. This allows for online analysis of the data. Even though this method should actually measure the extinction of the particle sample, the scattering of the particle/filter system is dominated by the non-absorbing filter. The transmissivity change is thus sensitive mainly to the aerosol particle absorption coefficient σ_{ap}. The absorption coefficient is the relevant property for quantifying aerosol absorption with respect to the direct aerosol climate effect. For converting σ_{ap} into a mass concentration, which is commonly used by models, a mass absorption cross-section needs to be assumed. The resulting mass concentration is termed the black carbon (BC) concentration, since it is based on an optical absorption measurement.

The thermal-optical method makes use of the fact that the agglomerated carbon spherules typical for soot are refractory to high temperatures. The aerosol particle is sampled on a quartz filter and subsequently analysed offline or semi-continuously. The filter sample is heated in an oven using a pre-defined, temperature programme. During the first mode of the analysis carbon is evolved in an inert helium atmosphere, quantifying organic carbon (OC) present in the sample, whereas in mode two helium is replaced by a helium/O_2 mixture quantifying the initial EC in the sample, as well as the pyrolyzed EC coming from charring of OC during mode one. The evolved carbon is oxidized to CO_2 and then reduced to CH_4 and quantified with a flame ionization detector. To discriminate between OC and EC, including pyrolyzed EC, the change in reflectance/

transmittance of a laser monitoring the filter during the raise of temperature throughout the entire analysis is recorded. Thermal-optical analysis assumes that OC does not absorb light at the specific wavelength of the laser, and that EC is the only light absorbing carbon.

Both methods have their inherent advantages and shortcomings. With the thermal optical method OC may be subject to charring, thus overestimating the samples content of EC. To some extent this is corrected for by the continuous monitoring of the filter transmission during analysis. However, the definition of the point separating OC and EC remains somewhat arbitrary, and depends significantly on the temperature programme used (Cavalli et al., 2010). The integrating plate technique poses a challenge due to its cross-sensitivity to particle scattering (e.g. Bond et al., 1999; Virkkula et al., 2005). Thus parallel measurements of σ_{sp}, or an instrument measuring not just the filter transmissivity, but also its reflectivity (Multi-Angle Absorption Photometer MAAP, Petzold et al. (2005)), is needed for correction. Furthermore, there may be other absorbing components in the particle phase such as ferrous oxide or humic-like substances (HULIS) that interfere (Hitzenberger et al., 2008). Modern instruments based on this principle measure σ_{ap} spectrally to obtain information on the absorbing component. Another concern is the mass absorption cross-section needed for converting σ_{ap} into a BC mass concentration. This quantity is known to vary between $5 - 20$ m^{2}g^{-1} depending on the aerosol type (Liousse et al., 1993). This poses a problem also when using this data in climate models, since a model usually carries the BC mass, but needs to convert it into σ_{ap} for calculating the BC climate effect. Since this method actually measures the absorption coefficient, which is the relevant property for quantifying the effect of "soot" on the radiation budget, instruments based on the integrating plate technique are used in the climate change monitoring community.

With this background, it should be readily understandable that the two mentioned techniques, despite having been developed for measuring a "soot" concentration, measure sufficiently different properties so that EC and BC are not directly comparable. However, the past years have seen significant progress towards improving this situation, namely through the EUSAAR project. On the EC side, EUSAAR has developed a temperature protocol minimising ambiguities when distinguishing EC from OC (Cavalli et al., 2010). With respect to BC, EUSAAR has been working on improved correction schemes largely eliminating the cross-sensitivity of the integrating plate method to particle scattering, especially also for spectral measurements of σ_{ap} (Müller et al., 2010). It turned out that a large fraction of the previous uncertainty of the mass absorption cross-section was due to this artifact. The remaining uncertainty of the mass absorption cross-section is due to the a priori unknown size of the "soot" carbon spherules and the unknown morphology of the particles containing them (Bond et al., 2006).

The key to solving the EC/BC conundrum lies in integrating the observations through models. EMEP is in the unique position of now encompassing EC and BC measurements as well as models, and is thus suited for addressing this task. The EC mass measurements can be compared directly with the respective masses carried by the model. The modern aerosol model also "knows" the history of a given aerosol particle population, i.e. its oxidation status and how the absorbing carbon fraction is distributed with particle size. This is precisely the information

needed to calculate the mass absorption cross-section for a given location and time. This will allow to convert the carbon mass carried by the model directly to a σ_{ap} value, which then can be compared to filter based aerosol absorption measurements conducted at the EUSAAR sites. EMEP/EUSAAR sites running parallel measurements of EC and BC will be essential for validating the aerosol model and the scheme for calculating the mass absorption cross-section. This way, both types of observations can be utilised simultaneously to constrain the model. This approach will mobilise the synergy potential contained in merging air quality and climate questions within EMEP. EC measurements will be used not only for air quality purposes, but also for targeting the climate challenge, and vice versa with BC measurements.

6   Observation of aerosols from space

By Aasmund Fahre Vik, Ann-Mari Fjæraa and Kerstin Stebel

6.1   Introduction

EMEP-CCC and MSC-W have for a number of years been involved in activities related to satellite based observation of aerosols and some of the findings have been presented in previous EMEP reports (EMEP, 2009; 2008; 2006; 2005). There has been a particular focus on the use of satellite based products for EMEP purposes and work has included validation against EMEP ground based measurements and the EMEP MSC-W chemical transport model.

Through close collaboration with the German Space Agency, DLR, EMEP-CCC has for a number of years evaluated the SYNAER (SYNergetic AErosol Retrieval product) data product (EMEP, 2009) and contributed to its further development. A main result of this work has been an improvement in the bias and the correlation between the SYNAER product and ground based EMEP PM_{10} and $PM_{2.5}$ mass concentration measurements. No further work has been done on the SYNAER data the last year, but EMEP-CCC is planning to continue evaluating SYNAER data in the future. Especially the aerosol optical depth product and its usability for EMEP assessment purposes will be further studied.

6.2   New satellites and sensors

Observation of aerosol from space has been a reality for decades already, but it was initially seen as a bi-product to other and more mature satellite products. Two examples: Surface images from the American Landsat imaging satellite series needed to be corrected for atmospheric aerosol content and an estimation of the particle content was necessary in order to provide the final terrain data products. The American TOMS (Total Ozone Mapping Spectrometer) mission is another example: While originally being designed for studying the development of the stratospheric ozone layer, the instrument (or series of instruments rather) have capabilities to measure total columns also of atmospheric aerosol content. An aerosol index is now one of the daily updated standard products. While TOMS and Landsat are examples of aerosol products that effectively are bi-products of other main variables, most satellite based aerosol measurements are in fact not performed by dedicated aerosol missions. The American CALIPSO (Cloud-Aerosol LIDAR and Infrared Pathfinder Satellite Observation) mission is one of the few exceptions since most of the other widely used aerosol products originate from multi-purpose instruments capable of measuring several environmental parameters such as land/ocean surface temperature, vegetation indices, snow and ice-cover, surface fires, ocean biology (e.g. algae concentrations), etc. – besides aerosol products used by atmospheric scientists. The advantage of these satellite missions is the beneficial cost/benefit ratio due to the multipurpose nature of the satellites, but the tradeoffs that take place in the design phase to make one instrument useful for many applications have been limiting the usability of the satellite products. With the coming of a new generation of satellites, this is about to change.

6.2.1 Aerosol research missions

The European Earth Explorer series follows the multipurpose Envisat (Environmental Satellite) satellite and the new satellites are now much more specialized and targeted against a limited number of scientific objectives. Two upcoming missions, ADM-AEOLUS (Atmospheric Dynamics Mission) and EarthCARE (The Earth Clouds, Aerosols and Radiation Explorer) are both built around space borne LIDARs targeting measurements of wind and aerosol profiles respectively. Especially the EarthCARE satellite, expected to be launched in 2013/2014, is potentially interesting for the transboundary air pollution research community. The LIDAR is a more powerful and advanced instrument compared to the existing CALIPSO mission and is able to measure polarized aerosol backscatter profiles with a vertical resolution down to 100m. In addition to the LIDAR, the satellite carries assisting instruments that properly detects and identifies clouds. With a surface footprint of less than 30 m, unwanted multiple scattering effects are minimized, and measurements between clouds during partly clouded conditions are possible. Current satellites are often limited exactly by such conditions. Space borne aerosol LIDARs are also able to measure during nighttime. EarthCARE will provide global 3D measurements of aerosol optical properties and is expected to provide a valuable supplement to existing EMEP monitoring capabilities – especially for improving the knowledge of climate relevant radiative forcing and its coupling to transboundary air pollution. An artist impression of the EarthCARE satellite is shown in Figure 6.1.

Figure 6.1:   Artist's impression of EarthCARE (Earth Clouds, Aerosols and Radiation Explorer) satellite. Credits: European Space Agency (ESA).

6.2.2 *Operational satellite missions*

The satellite research missions enable dedicated and target measurements of the aerosol, but they often lack the spatial and temporal coverage and resolution that is required for atmospheric monitoring purposes. Research missions are often associated with testing of unproven technology and instruments are commonly set to operate in a multitude of different measurement modes – strongly limiting the ability to perform continuous and repeatable observations. So-called operational missions are normally based on known technology (a similar instrument has been in space before) and the measurement modes are much more limited. Operational missions focus on reliable delivery of measurements with known quality. Until recently, most satellite instruments capable of measuring atmospheric aerosols were multipurpose instruments and only the research instruments (such as MODIS, AATSR, etc.) were able to provide aerosol information with a sufficient accuracy and spatial resolution. Instruments with a larger spatial and temporal coverage were always targeted towards operational measurements of meteorological parameters (cloud coverage, temperature, humidity, etc.) and were rarely suitable for aerosol characterization. With the launch of the European MetOp satellite in October 2006, the situation has improved somewhat and it is expected that aerosol products from this mission will become more available in the years to come (the usage is still not large). The MetOp series consist of three satellites, each containing 12 instruments, and the next two satellites (exact copies that are already built) are planned for launch in 2012 and 2016/2017. This guarantees a continuous provision of well characterized data until at least 2020. The availability of data from the same instrument over such a long time-period is very important for long-term trends studies. The SYNAER product presented in earlier EMEP reports (EMEP, 2009) is expected to become operationally available utilizing instruments onboard MetOp (AVHRR and GOME-2) in the near future.

Another important series of operational satellites are those belonging to the European GMES (Global Monitoring for Environment and Security) program. The so-called Sentinel 4 and 5 satellites are targeting atmospheric composition monitoring (sentinel 1 to 3 have other foci) and are built to ensure reliable observations for the GMES services. Especially the Geo-stationary Sentinel 4 satellite that is planned for launch in 2018 is expected to provide better aerosol products for Europe. A Sentinel 5 precursor satellite is planned for launch in 2014, but will mainly be focusing on atmospheric trace gases.

6.3   New products and services

The development and evolution of satellite product services has been a major paradigm shift in Europe occurring during the past five to ten years. Previous use of satellite data was based on users applying satellite data directly for scientific or regulatory purposes and a significant understanding of the satellite technology was often necessary for interpretation and adaption of results. This easily became an obstacle and a limiting factor for widespread use of the space infrastructure and EU and ESA therefore decided to improve the situation through their common GMES program. The program was initiated about 10 years ago and focused on developing services and specialized products adapted to different users needs.

Service providers were set to provide a bridge between the satellite agencies and potential users of the data.

GMES services are currently provided by the EU FP7 funded project MACC (Monitoring Atmospheric Composition and Climate), which provides so-called core services and products on European and Global scale. The EMEP program and all its thematic centers are identified as core users of the MACC products, and NILU, acting as EMEPs Chemical Coordinating Center, have recently signed a Service Level Agreement (SLA) with the German Space Agency (DLR). This SLA regulates the provision (DLR) and use (NILU) of the SYNAER AOD product for EMEP assessment and reporting purposes. The provider agrees to deliver a product following the users requirements and the user agrees to utilize the product and to evaluate its feasibility/suitability for its purpose. Such agreements may be important in the future and is probably necessary for the adoption of satellite based data into legislative Air Quality monitoring. In addition to provision of satellite data, the MACC project has a strong focus on regional scale Air Quality modeling. EMEP MSC-W is contributing to this activity.

PASODOBLE (Promote air quality services integrating observations development of basic localized information for Europe) is another EU FP7 funded GMES service-providing project that recently started up. The project is providing so-called downstream services and delivers (often based on the input from MACC) atmospheric products for national, regional and local scale Air Quality management. The focus is, as such, not directly relevant for EMEP since it is strictly avoiding provision of services to European scale users, but some of the products and services of the project may still be of importance to the convention. One such example is the Saharan dust monitoring service that is utilizing infrared measurement techniques to retrieve mineral dust mass loading originating from Saharan dust being transported into Mediterranean areas severely impairing air quality in this region. The service will be delivered by NILU and is to be utilized by national environmental agencies to document exceedances of PM_{10} and $PM_{2.5}$ threshold levels due to natural sources (reporting for the CAFE directive). For EMEP purposes, it may be interesting to use the products for studying the transport events and to assess the suitability of existing monitoring and modeling capabilities. The dust service will consist of satellite derived mass loading products similar to that shown below in Figure 6.2, but will also feature a gap filling product (satellite measurements have gaps in space and time) based on the NILU FLEXPART model.

Another interesting service, one that became very relevant during May 2010, is the Volcanic ash products delivered by the ESA funded SAVAA (Support to Aviation for Volcanic Ash Avoidance) project. This project will develop products based on infrared satellite sensors to derive volcanic ash mass loading. Utilizing special optical properties of volcanic ash, the service is able to distinguish these potentially hazardous (to aviation) particles from other aerosol types. The service is targeted at aviation support for volcanic ash avoidance, but the products may also be useful for EMEP purposes.
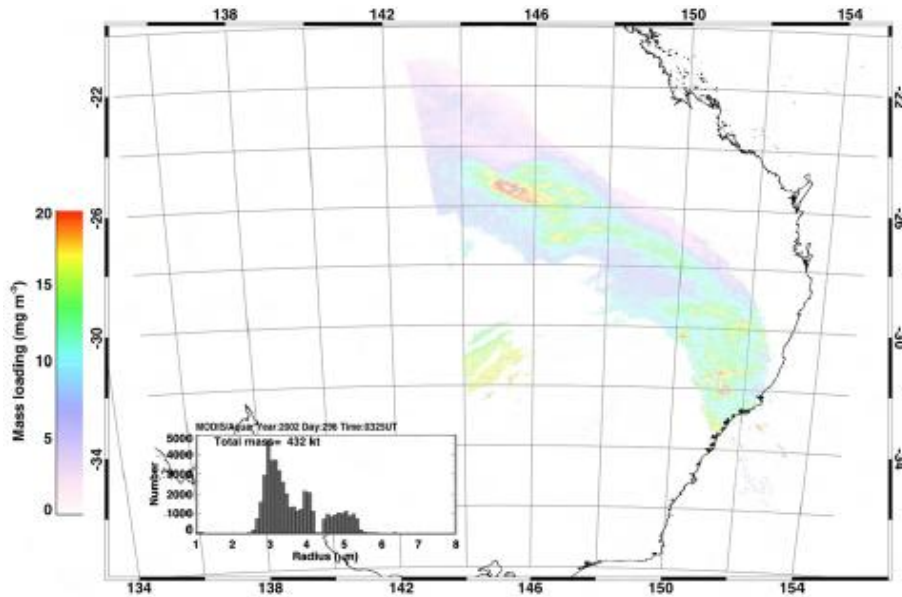
Figure 6.2: *PASODOBLE service example: Mass loading (mg m^{-3}) and dust particle size retrievals (μm) are retrieved using satellite infrared data, a microphysical particle model and radiative transfer calculations. The figure shows dust over eastern Australia using the NASA MODIS/Terra instrument. Similar products will be made available for the Mediterranean area. Credits: Fred Prata, NILU.*
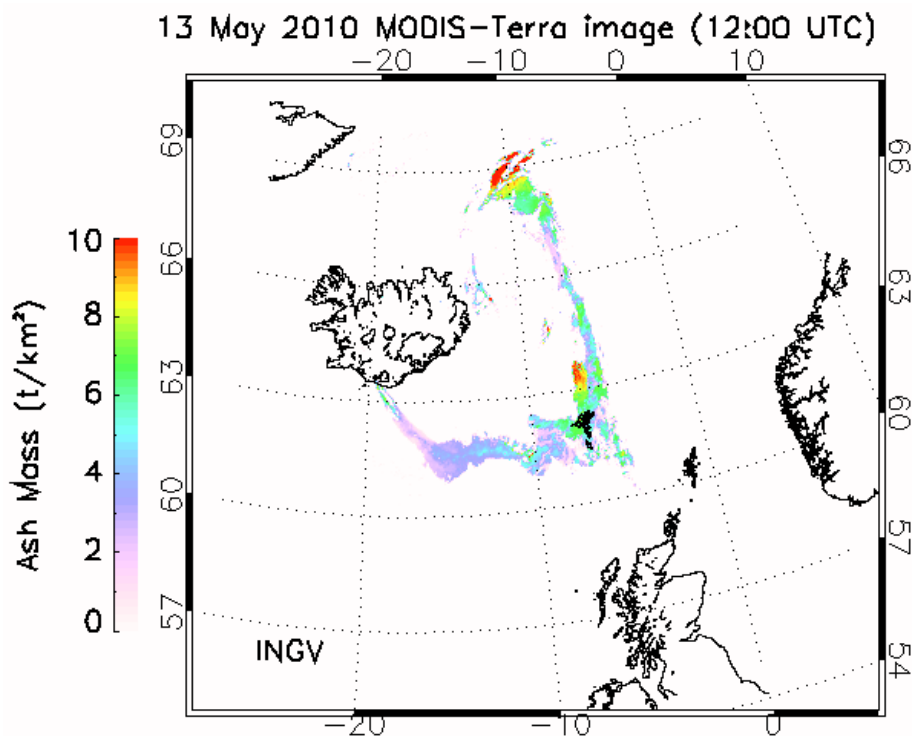

Figure 6.3: *Retrieval of volcanic ash mass loading from the NASA MODIS/Terra satellite during the eruption of the Eyjafjalla volcano in May 2010. The service is provided by the ESA funded SAVAA project. Credits: INGV.*

6.4 Saharan Dust over the Mediterranean Sea

As a case study we have included an example of a Saharan dust outburst over the eastern Mediterranean. The number of EMEP monitoring stations in this area is limited and the satellite data and earth observation data products can provide valuable information in addition to the EMEP monitoring network. Figure 4 shows a RGB-image of a dust plume originating from desert areas in Northern Africa during March 2008, taken by NASA's Terra and Aqua Satellites. Such storms are common as hot air over the vast African desert is pulled toward the cooler winter air in the north. The strong winds that result carry Saharan dust into the Mediterranean and across Europe. We clearly see the dust hitting the island of Cyprus, moving from south to north and from west towards east (the two satellite measurements are separated in time by 26 hours and 20 minutes). Figure 5 shows hourly averaged PM_{10} mass concentrations from the Ayia Marina station on Cyprus for March 2008, from which the influence of the sandstorm during the period 18 – 23 March is quite apparent. The dust plume seen moving over the island on the two satellite images in Figure 6.4 gives a clear signature in the PM_{10} mass concentration measurements around noon on the 25th of March, with hourly maximum PM_{10} levels close to 1000 µg m^{-3}. The visualized field of the Aerosol Optical Depth at 550 nm from MODIS Terra on 23-24 March 2008 is shown in Figure 6.6. The AOD plot is a collection of measurements done on the two days, but the pattern is still closely matching the image shown in Figure 6.4. One clearly sees the enhanced aerosol levels west of Cyprus. Figure 6.7 is similar to Figure 6.6 differing only in the time period; i.e. 25 - 28 of March.

The actual dust episode is a typical example of transport of Saharan dust into the Mediterranean region, a phenomenon that takes place several times each year, and which occasionally transport mineral particles as far as to Northern Europe. As can be seen in the images of Figure 6.4, it is only partly cloudy during the episode and it is therefore possible to calculate AOD values from the satellite measurements. This is not always the case during such events and it is expected that services such as those provided through the PASODOBLE project can provide additional satellite products and modeled gap-filling data on this matter.

**Terra
2008/084
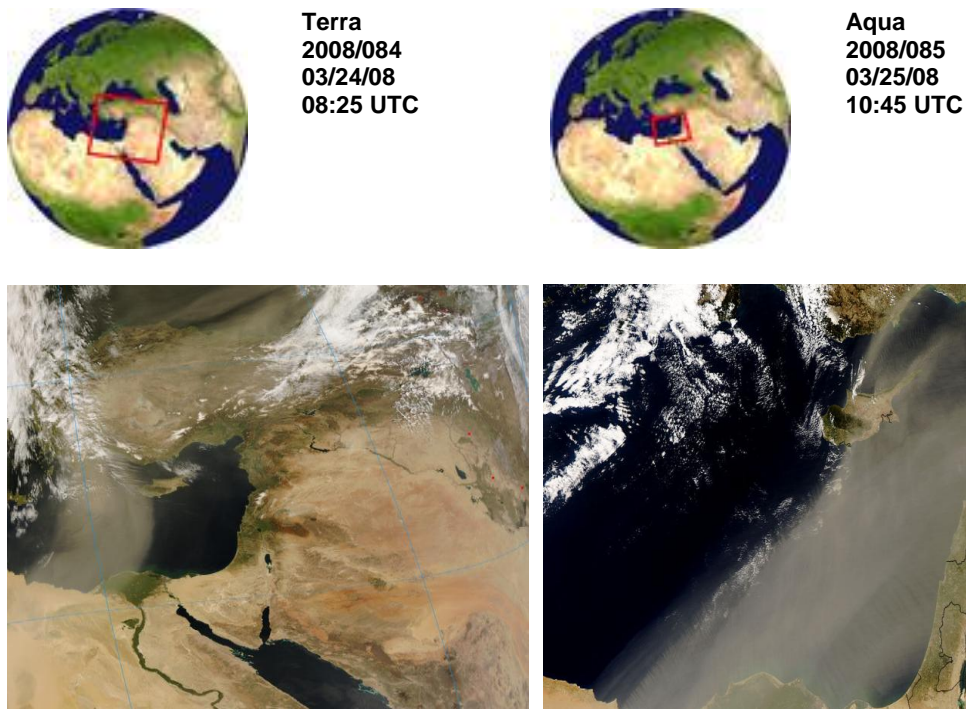03/24/08
08:25 UTC**

**Aqua
2008/085
03/25/08
10:45 UTC**

Figure 6.4: *NASA's Terra and Aqua Satellites captured these images of dust plumes streaming from the desert of Northern Africa out over the Mediterranean Sea in March 2008.*
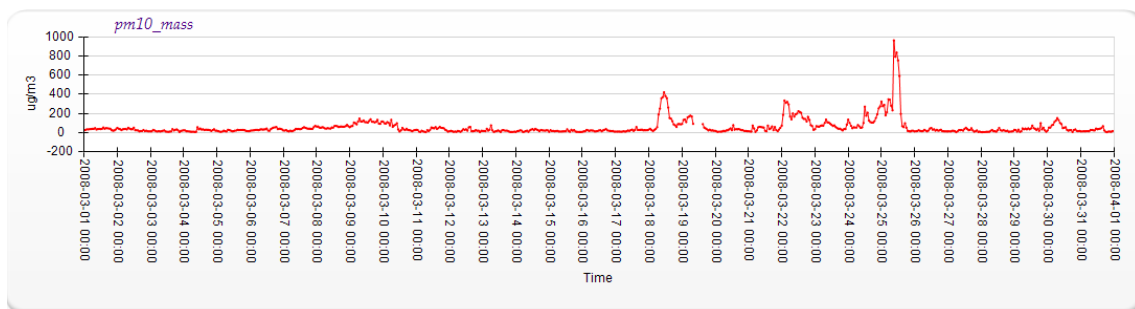
Figure 6.5: *Time series of hourly PM_{10} mass concentration from the Ayia Marina monitoring station on Cyprus in March 2008.*

Figure 6.6: *Aerosol Optical Depth at 550 nm from MODIS Terra on 23-24 March 2008. Measurements were performed at 08:25 UTC on the two days. Visualizations was produced with the Giovanni online data system, developed and maintained by the NASA GES DISC.*

Figure 6.7: *Aerosol Optical Depth at 550 nm from MODIS Terra on 25.-28.March 2008. Measurements were performed at 10:45 UTC on all days. Visualization was produced with the Giovanni online data system, developed and maintained by the NASA GES DISC.*

7 References

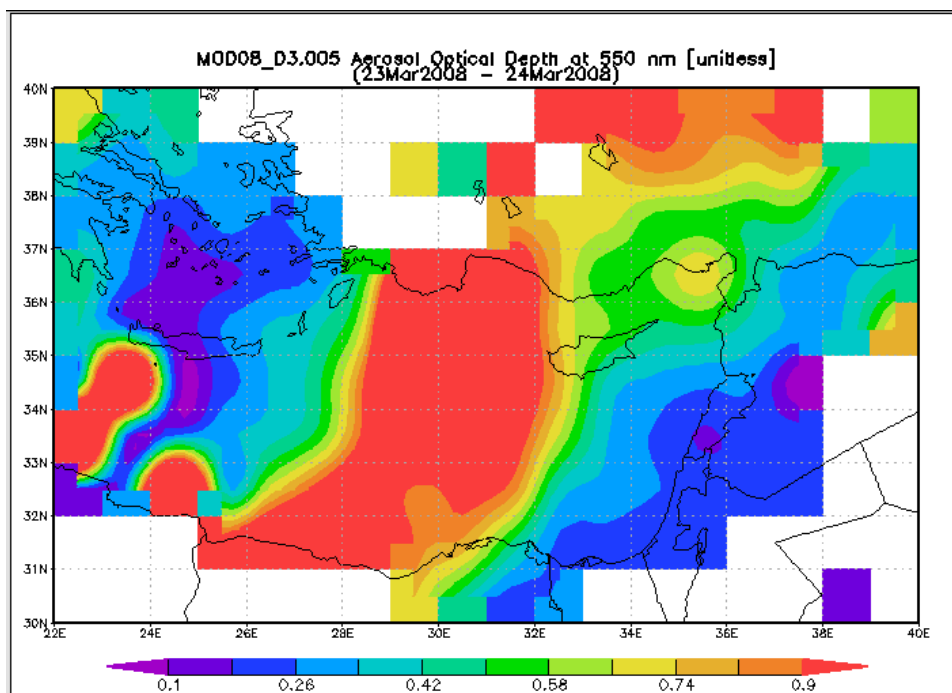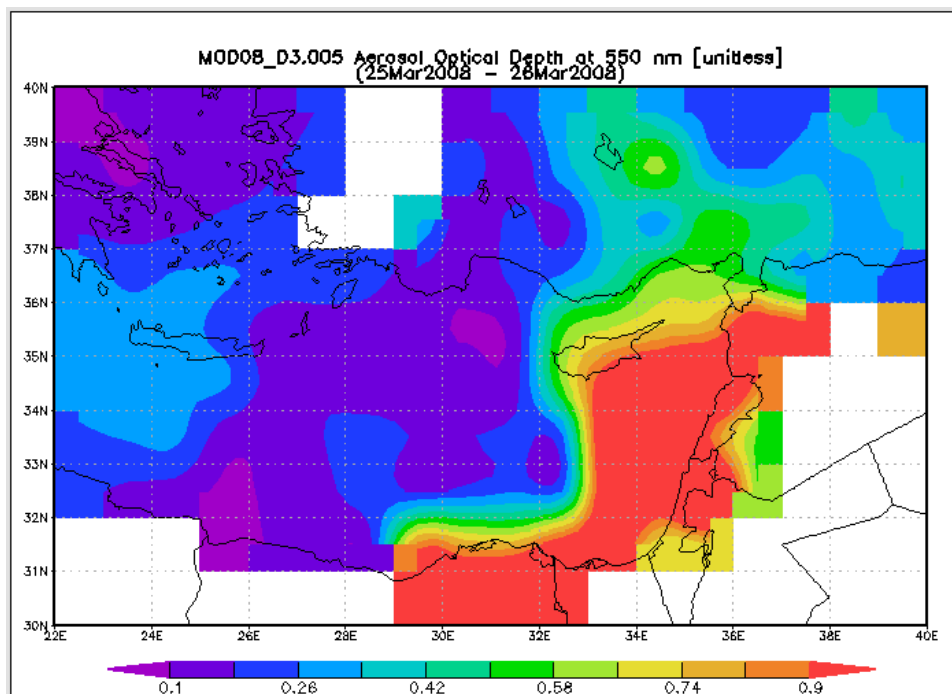Abraham H.J. (2001) Zusammensetzung der Feinstaubfraktion in Berlin (speciation of fine particulate matter in Berlin). Proceedings of the 36th Messtechnische Kolloqium, Grainau, May 2001. Ed.: Environment Agency of North-Rhine Westphalia, Essen, Germany.

Balis, D.S., Amiridis, V., Zerefos, C., Gerasopoulos, E., Andreae, M.O., Zanis, P., Kazantzidis, A., Kazadzis, S. and Papayannis, A. (2003) Raman lidar and sunphotometric measurements of aerosol optical properties during a biomass burning episode over Thessaloniki, Greece. *Atmos. Environ., 37*, 4529-4538.

Ban-Weiss, G.A., Lunden, M.M., Kirchstetter, T.W. and Harley, R.A. (2009) Measurement of black carbon and particle number emission factors from individual heavy duty trucks. *Environ. Sci. Technol., 43*, 1419-1424.

Bell, M.L., Ebisu, K., Pen, R.D., Samet, J.M. and Dominici, F. (2009) Hospital admissions and chemical composition of fine particle air pollution. *Am. J. Respir. Crit. Care Med., 179*, 1115-1120.

Birch, M.E. and Cary, R.A. (1996) Elemental carbon-based method for monitoring occupational exposures to particulate diesel exhaust. *Aerosol Sci. Tech., 25,* 221-241.

Bond, T., Streets, D.G., Yarber, K.F., Nelson, S.M., Woo, J.-H. and Klimont, Z. (2004) A technology-based global inventory of black and organic carbon emissions from combustion. *J. Geophys. Res., 109*, D14203, doi: 10.1029/2003JD003697.

Bond, T.C., Anderson, T.L. and Campbell, D. (1999) Calibration and intercomparison of filter-based measurements of visible light absorption by aerosols. *Aerosol Sci. Technol., 30,* 582-600.

Bond, T.C., Habib, G. and Bergstrom, R.W. (2006) Limitations in the enhancement of visible light absorption due to mixing state. *J. Geophys. Res., 111*, D20211, doi:10.1029/2006JD007315.

Cavalli, F., Viana, M., Yttri, K.E., Genberg, J. and Putaud, J.-P. (2010) Toward a standardised thermal-optical protocol for measuring atmospheric organic and elemental carbon: the EUSAAR protocol. *Atmos. Meas. Technol., 3,* 79-89.

Cavalli, F., Viana, M., Yttri, K.E., Kiss, G., Genberg, J. and Putaud, J.-P. (2010) Towards a standardized thermal-optical protocol for measuring atmospheric organic and elemental carbon: The EUSAAR protocol. *Atmos. Meas. Tech., 3*, 79-89.

Denier van der Gon, H., Visschedijk, A., Dröge, R., Johansson, C. and Klimont, Z. (2010) A high resolution emission inventory of particulate elemental carbon and organic carbon for Europe in 2005. *Atmos. Environ.* (submitted).

Donahue, N.M., Robinson, A.L. and Pandis, S.N. (2009) Atmospheric organic particulate matter: From smoke to secondary organic aerosol. *Atmos. Environ., 43*, 94-106.

Donahue, N.M., Robinson, A.L., Stanier, C.O. and Pandis, S.N. (2006) Coupled partitioning, dilution, and chemical aging of semivolatile organics. *Environ. Sci. Technol.*, *40*, 2635-2643.

Durbin, T.D., Norbeck, J.M., Smith, M.R. and Truex, T.J. (1999) Particulate emission rates from light duty vehicles in the south coast air quality management district. *Environ. Sci. Technol., 33*, 4401-4406.

EC (2004) Second Position Paper on Particulate Matter – CAFE Working Group on Particulate Matter, D.G. Environment December 20th, 2004. European Commission. **URL:** http://ec.europa.eu/environment/archives/cafe/pdf/working_groups/2nd_position_paper_pm.pdf [2010-08-06].

ECE (2007) Methods and procedures for the technical review of air pollutant emission inventories reported under the Convention and its protocols. Geneva (EB.AIR/GE.1/2007/16).

ECE (2009) Guidelines for reporting emission data under the Convention on Long-Range Transboundary Air Pollution. Geneva (ECE/EB.AIR/97). **URL:** http://www.ceip.at/fileadmin/inhalte/emep/reporting_2009/Rep_Guidelines_ECE_EB_AIR_97_e.pdf [2010-08-09].

EEA (2009b) Proposed gap-filling procedure for the European Community LRTAP Convention emission inventory. Technical paper for the meeting of the Air and Fuels Committee under Directive 96/62/EC, concerning 'Information on the Member States' reporting under the National Emission Ceilings Directive 2001/81/EC'. 28 September 2009, Brussels. European Environment Agency. Available upon request.

EEA/CEIP (2008) KCA results 2008 (PM10 and PM2.5) . In: *Inventory review 2008. Emission data reported under the LRTAP Convention and NEC Directive. Stage 1 and 2 review. Status of gridded data.* By Mareckova K. et al. Vienna, Umweltbundesamt (CEIP technical report, 1/2008) Appendix 7.

EEA/CEIP (2010) Inventory review 2010 stage 1 and 2 and review of gridded data. Mareckova K., Wankmueller, R., Poupa, S., Anderl, M. and Joebstl. R. Vienna, EEA/CEIP (in preparation).

Elvidge, C.D., Baugh, K.E., Tuttle, B.T., Ziskin, D., Ghosh, T., Zhizhin, M. and Pack, D. (2009) Improving satellite data estimation of gas flaring volumes: year two final report to the GGFR. Boulder, US, NOAA National Geophysical Data Center. **URL:** http://www.ngdc.noaa.gov/dmsp/interest/flare_docs/NGDC_flaring_report_20090817.pdf [2010-08-23]

EMEP (2008) Transboundary acidification, eutrophication and ground level ozone in Europe in 2006. Oslo, Norwegian Meteorological Institute (EMEP MSC-W & CCC & CEIP Status Report 1/2008).

EMEP (2009) Transboundary particulate matter in Europe. Oslo, Norwegian Meteorological Institute (EMEP Status Report 4/2009).

EMEP (2009a) Transboundary acidification, eutrophication and ground level ozone in Europe in 2007. Oslo, Norwegian Meteorological Institute (EMEP MSC-W & CCC & CEIP Status Report 1/2009).

EMEP (2009b) Transboundary particulate matter in Europe. Kjeller, Norwegian Institute for Air Reseach (EMEP CCC & MSC-W & CEIP & CIAM Status Report 4/2009).

EMEP (2010) Transboundary acidification, eutrophication and ground level ozone in Europe in 2008. Oslo, Norwegian Meteorological Institute (EMEP MSC-W & CCC & CEIP Status Report 1/2010).

EMEP (2010S) Supplementary material to EMEP Status Report 1/2010. **URL:** http://www.emep.int/publ/common_publications.html [2010-08-23]

EMEP/EEA (2009) EMEP/EEA Air pollutant emission inventory guidebook. Copenhagen, European Environment Agency (EEA technical report No. 9/2009). **URL:** http://www.eea.europa.eu/publications/emep-eea-emission-inventory-guidebook-2009.

Escudero, M., Castillo, S., Querol, X., Avila, A., Alarcón, M., Viana, M.M., Alastuey, A., Cuevas, E. and Rodríguez, S. (2005) Wet and dry African dust episodes over Eastern Spain. *J. Geophys. Res., 110,* D18S08, 10.1029/2004JD004731.

Escudero, M., Querol, X., Pey, J., Alastuey, A., Pérez, N., Ferreira, F., Alonso, S., Rodríguez, S. and Cuevas, E. (2007) A methodology for the quantification of the net African dust load in air quality monitoring networks. *Atmos. Environ., 41,* 5516-5524.

Fagerli, H., Simpson, D. and Tsyro, S. (2004) Unified EMEP model: Updates. In: *Transboundary acidification, eutrophication and ground level ozone in Europe.* Oslo, Norwegian Meteorological Institute (EMEP Status Report 1/2004), pp. 11-18.

Forster, P., Ramaswamy, V., Artaxo, P., Berntsen, T., Betts, R., Fahey, D.W., Haywood, J., Lean, J., Lowe, D.C., Myhre, G., Nganga, J., Prinn, R., Raga, G., Schulz, M. and Dorland, R. Van (2007) Changes in atmospheric constituents and in radiative forcing. In: *Climate Change 2007: The physical science basis.* Contribution of Working Group I to the fourth assessment report of the Intergovernmental Panel on Climate Change. Ed. by S. Solomon, D. Qin, M. Manning, Z. Chen, M. Marquis, K.B. Averyt, M. Tignor and H.L. Miller (Eds.)]. Cambridge, Cambridge University Press.

Gangoiti, G., Millán, M.M., Salvador, R. and Mantilla, E. (2001) Long range transport and re-circulation of pollutants in the Western Mediterranean during the RECAPMA Project. *Atmos. Environ., 35*, 6267–6276.

Gelencsér, A. (2004) Carbonaceous aerosol. Springer, Dordrecht (Atmospheric and oceanographic sciences library, 30).

Gelencsér, A., May, B., Simpson, D., Sánchez-Ochoa, A., Kasper-Giebl, A., Puxbaum, H., Caseiro, A., Pio, C. and Legrand, M. (2007) Source apportionment of $PM_{2.5}$ organic aerosol over Europe: primary/secondary, natural/anthropogenic, fossil/biogenic origin. *J. Geophys. Res., 112*, D23S04, doi:10.1029/2006JD008094.

Gerasopoulos, E., Koulouri, E., Kalivitis, N., Kouvarakis, G., Saarikoski, S., Mäkelä, T., Hillamo, R. and Mihalopoulos, N. (2007) Size-segregated mass distributions of aerosols over Eastern Mediterranean: seasonal variability and comparison with AERONET columnar size-distributions. *Atmos. Chem. Phys., 7,* 2551–2561.

Gerasopoulos, E., Kouvarakis, G., Babasakalis, P., Vrekoussis, M., Putaud, J.-P. and Mihalopoulos, N. (2006) Origin and variability of particulate matter (PM10) mass concentrations over the Eastern Mediterranean. *Atmos. Environ., 40,* 4679-4690.

Giglio, L., Descloitres, J., Justice, C.O. and Kaufman, Y.J. (2003) An enhanced contextual fire detection algorithm for MODIS. *Rem. Sens. Environ.*, *87*, 273-282.

Hallquist, M., Wenger, J.C., Baltensperger, U., Rudich, Y., Simpson, D., Claeys, M., Dommen, J., Donahue, N.M., George, C., Goldstein, A.H., Hamilton, J.F., Herrmann, H., Hoffmann, T., Iinuma, Y., Jang, M., Jenkin, M.E, Jimenez, J.L., Kiendler-Scharr, A., Maenhaut, W., McFiggans, G., Mentel, T.F., Monod, A., Prévôt, A.S.H., Seinfeld, J.H., Surratt, J.D., Szmigielski, R. and Wildt, J. (2009) The formation, properties and impact of secondary organic aerosol: current and emerging issues. *Atmos. Chem. Phys.*, *9*, 5155-5236.

Harrison, R.M. and Pio, C. (1983) Size differentiated composition of inorganic aerosol of both marine and continental polluted origin. *Atmos. Environ. 17*, 1733-1738.

Hirdman, D., Burkhart, J.F., Sodemann, H., Eckhardt, S., Jefferson, A., Quinn, P.K., Sharma, S., Ström, J. and Stohl, A. (2010b) Long-term trends of black carbon and sulphate aerosol in the Arctic: Changes in atmospheric transport and source region emissions. *Atmos. Chem. Phys. Disc., 10*, 12133-12184.

Hirdman, D., Sodemann, H., Eckhardt, S., Burkhart, J.F., Jefferson, A., Mefford, T., Sharma, S., Ström, J. and Stohl, A. (2010a) Source identification of short-lived air pollutants in the Arctic using statistical analysis of measurement data and particle dispersion model output. *Atmos. Chem. Phys., 10*, 669-693.

Hitzenberger, R., Petzold, A., Bauer, H., Ctyroky, P., Pouresmaeil, P., Laskus, L. and Puxbaum, H. (2008) Intercomparison of thermal and optical measurement methods for elemental carbon and black carbon at an urban location. *Environ. Sci. Technol., 40,* 6377-6383.

Hsu, Y. and Mullen, M. (2007) Compilation of diesel emissions speciation data. Final report. Springfield, VA, E.H. Pechan & Associates, Inc. (CRC contract No. E-75) (Pechan Report No: 07.10.001/9452.000) **URL:** http://www.crcao.com/reports/recentstudies2008/E-75/CRC_E75_Final%20Report_v3.pdf [2010-08-23].

Hueglin, C., Gehrig, R., Baltensperger, U., Gysel, M., Monn, C. and Vonmont, H. (2005) Chemical characterisation of PM$_{2.5}$, PM$_{10}$ and coarse particles at urban, near-city and rural sites in Switzerland. *Atmos. Environ., 39,* 637–651.

IEA (2009) World energy outlook 2009. Paris, International Energy Agency (IEA).

Koçak, M., Mihalopoulos, N. and Kubilay, N. (2007a) Contributions of natural sources to high PM10 and PM2.5 events in the eastern Mediterranean. *Atmos. Environ., 41,* 3806–3818.

Koçak, M., Mihalopoulos, N. and Kubilay, N. (2007b) Chemical composition of the fine and coarse fraction of aerosols in the northeastern Mediterranean. *Atmos. Environ., 41,* 7351–7368.

Koulouri, E., Saarikoski, S., Theodosi, C., Markaki, Z., Gerasopoulos, E., Kouvarakis, G., Mäkelä, T., Hillamo, R. and Mihalopoulos, N. (2008) Chemical composition and sources of fine and coarse aerosol particles in the Eastern Mediterranean. *Atmos. Environ., 42,* 6542-6550.

Kulmala, M., Asmi, A., Lappalainen, H.K., Carslaw, K.S., Pöschl, U., Baltensperger, U., Hov, Ø., Brenquier, J.-L., Pandis, S.N., Facchini, M.C., Hansson, H.-C., Wiedensohler, A., and O'Dowd, C.D. (2009) Introduction: European integrated project on aerosol cloud climate and air quality interactions (EUCAARI) - integrating aerosol research from nano to global scales. *Atmos. Chem. Phys.*, *9*, 2825-2841.

Kupiainen, K. and Klimont, Z. (2004) Primary emissions of submicron and carbonaceous particles in Europe and the potential for their control. Laxenburg, International Institute for Applied Systems Analysis. (IIASA Interim Report IR-04-079) **URL:** http://www.iiasa.ac.at/Admin/PUB/Documents/IR-04-079.pdf [2010-08-23]

Kupiainen, K. and Klimont, Z. (2007) Primary Emissions of Fine Carbonaceous Particles in Europe. *Atmos. Environ., 41*, 2156-2170.

Lane, T.E., Donahue, N.M. and Pandis, S.N. (2008a) Effect of NO_x on secondary organic aerosol concentrations. *Environ. Sci. Technol.*, *42*, 6022-6027.

Lane, T.E., Donahue, N.M. and Pandis, S.N. (2008b) Simulating secondary organic aerosol formation using the volatility basis-set approach in a chemical transport model. *Atmos. Environ.*, *42*, 7439-7451.

Lawson, D.R. (2010) (On-Road) Mobile source emissions and mitigation potential. Presentation at the Workshop on Addressing Black Carbon and Ozone as Short-Lived Climate Forcers, March 4 2010, Chapel Hill, NC.

Legrand, M. and Puxbaum, H. (2007) Summary of the CARBOSOL project: Present and retrospective state of organic versus inorganic aerosol over Europe. *J. Geophys. Res., 112*, D23S01, doi:10.1029/2006JD008271.

Lin, C.-I., Baker, M. and Charlson, R.J. (1973) Absorption coefficient of atmospheric aerosol: a method for measurement. *Appl. Optic, 12,* 1356-1363.

Liousse, C., Cachier, H. and Jennings, S. (1993) Optical and thermal measurements of black carbon aerosol content in different environments: Variation of the specific attenuation cross-section, sigma (σ). *Atmos. Environ., 27A,* 1203-1211.

Mamane, Y. and Gottlieb, J. (1992) Nitrate formation on sea salt and mineral particles – a single particle approach. *Atmos. Environ., 26A*, 1763–1769.

Marelli, L., Lagler, F., Borowiak, A., Drossinos, Y., Gerboles, M., Buzica, D., Szafraniec, K, Niedzialek, J., Jimenez, J. and De Santi, G. (2006) PM measurements in Krakow during a winter campaign. In: *Outcome of the Krakow Integrated Project, PM: From Emissions to Health Effects.* Ed. by Jimenez, J. and Niedzialek, J. Brussels, European Communities (EUR 22293 EN) pp. 18-21.

McClain, C.R., Cleave, M.L., Feldman, G.C., Gregg, W.W., Hooker, S.B. and Kuring, N. (1998) Science quality SeaWiFS data for global biosphere research. *Sea Technol., 39,* 10-16.

Metzger, S., Mihalopoulos, N. and Lelieveld, J. (2006) Importance of mineral cations and organics in gas–aerosol partitioning of reactive nitrogen compounds: case study based on MINOS results. *Atmos. Chem. Phys., 6,* 2549–2567.

Mihalopoulos, N., Kerminen, V.M., Kanakidou, M., Berresheim, H. and Sciare, J. (2007) Formation of particulate sulfur species (sulphate and methanesulfonate) during summer over the Eastern Mediterranean: A modelling approach. *Atmos. Environ., 41,* 6860-6871.

Millán, M., Salvador, R., Mantilla, E. and Kallos, G. (1997) Photo-oxidant dynamics in the Mediterranean basin in summer: results from European research projects. *J. Geophys. Res., 102D*, 8811–8823.

Moulin, C., Lambert, E., Dayan, U., Masson, V., Ramonet, M., Bousquet, P., Legrand, M., Balkanski, Y. J., Guelle, W., Marticorena, B., Bergametti, G. and Dulac, F. (1998) Satellite climatology of African dust transport in the Mediterranean atmosphere. *J. Geophys. Res., 103D*, 13137-13144.

Müller, T., Henzing, J.S., de Leeuw, G.,Wiedensohler, A., Alastuey, A., Angelov, H., Bizjak, M., Collaud Coen, M., Engström, J.E., Gruening, C., Hillamo, R., Hoffer, A., Imre, K., Ivanow, P., Jennings, G., Sun, J.Y., Kalivitis, N., Karlsson, H., Komppula, M., Laj, P., Li, S.-M., Lunder, C., Marinoni, A., Martins dos Santos, S., Moerman, M., Nowak, A., Ogren, J.A., Petzold, A., Pichon, J.M., Rodriquez, S., Sharma, S., Sheridan, P.J., Teinil, K., Tuch, T., Viana, M., Virkkula, A., Weingartner, E., Wilhelm, R. and Wang, Y.Q. (2010) Characterization and intercomparison of aerosol absorption photometers: result of two intercomparison workshops. *Atmos. Meas. Technol. Discuss., 3*, 1511-1582.

Murphy, B.N. and Pandis, S.N. (2009) Simulating the formation of semivolatile primary and secondary organic aerosol in a regional chemical transport model. *Environ. Sci. Technol.*, *43*, 4722-4728.

Pakkanen, T.A., Hillamo, R.E., Aurela, M., Andersen, H.V., Grundahl, L., Ferm, M., Persson, K., Karlsson, V., Reissell, A., Royset, O., Floisand, I., Oyola, P. and Ganko, T. (1999) Nordic intercomparison for measurement of major atmospheric nitrogen species. *J. Aerosol Sci., 30*, 247–263.

Pakkanen, T.A., Loukkola, K., Korhonen, C.H., Aurela, M., Mäkelä, T., Hillamo, R.E., Aarnio, P., Koskentalo, T., Kousa, A. and Maenhaut, W. (2001) Sources and chemical composition of atmospheric fine and coarse particles in the Helsinki area. *Atmos. Environ., 35*, 5381-5391.

Papadimas, C.D., Hatzianastassiou, N., Mihalopoulos, N. Querol, X. and Vardavas, I. (2008) Spatial and temporal variability in aerosol properties over the Mediterranean basin based on 6-year (2000-2006) MODIS data. *J. Geophys. Res., 113*, D11205, doi:10.1029/2007JD009189.

Peng, R.D., Bell, M.L., Geyh, A.S., McDermott, A., Zeger, S.L., Samet, J.M. and Dominici, F. (2009) Emergency admissions for cardiovascular and respiratory diseases and the chemical composition of fine particle air pollution. *Environ. Health Perspect., 117,* 957-863.

Pérez, N., Castillo, S., Pey, J., Alastuey, A., Viana, M. and Querol, X. (2008) Interpretation of the variability of regional background aerosols in the Western Mediterranean. *Sci. Total Environ., 407*, 527-540.

Perrino, C. and Allegrini, I. (2006) Natural sources contribution of natural sources to airborne particulate matter to airborne particulate matter in central Italy. Presented at: Workshop on Contribution of Natural Sources to PM Levels in Europe. JRC ISPRA, 12th -13th October 2006. **URL:** http://ies.jrc.ec.europa.eu/uploads/h04/natsources/PERRINO_ALLEGRINI.pdf [2010-08-09].

Petzold, A., Schloesser, H., Sheridan, P.J., Arnott, W.P., Ogren, J.A. and Virkkula, A. (2005) Evaluation of multiangle absorption photometry for measuring aerosol light absorption. *Aerosol Sci. Tech., 39*, 40-51.

Pey, J., Pérez, N., Querol, X., Alastuey, A., Cusack, M. and Reche, C. (2010a) Intense winter atmospheric pollution episodes affecting the Western Mediterranean. *Sci. Total Environ., 408*, 1951-1959.

Pey, J., Querol, X. and Alastuey, A. (2010b) Discriminating the regional and urban contributions in the North-Western Mediterranean: PM levels and composition. *Atmos. Environ., 44,* 1587-1596.

Pio, C.A., Legrand, M., Oliveira, T., Afonso, J., Santos, C., Fialho, P., Barata, F., Puxbaum, H., Sanchez-Ochoa, A., Kasper-Gieb, A., Gelencsér, A., Preunkert, S. and Schock, M. (2007) Climatology of aerosol composition (organic versus inorganic) at non-urban sites on a west‐east transect across Europe. *J. Geophys. Res.*, *112*, D23S02, doi:10.1029/2006JD008038.

Putaud, J.P. (2006) PM evolution and on-line characterization. JRC Enlargement and Integration Workshop "Outcome of the Krakow Integrated Project": Particulate Matter: From Emissions to Health Effects, 15-16 May 2006, Krakow Municipal Office.

Puxbaum, H., Gomiscek, B., Kalina, M., Bauer, H., Salam, A., Stopper, S., Preining, O. and Hauck, H. (2004) A dual site study of $PM_{2.5}$ and PM_{10} aerosol chemistry in the larger region of Vienna, Austria. *Atmos. Environ., 38*, 3949-3958.

Querol, X., Alastuey, A., Pey, J., Cusack, M., Pérez, N., Mihalopoulos, N., Theodosi, C., Gerasopoulos, E., Kubilay, N. and Koçak, M. (2009a) Variability in regional background aerosols within the Mediterranean. *Atmos. Chem. Phys., 9,* 4575-4591.

Querol, X., Alastuey, A., Puicercus, J.A., Mantilla, E., Miro, J.V., Lopez-Soler, A., Plana, F. and Artíñano, B. (1998) Seasonal evolution of suspended particles around a large coal-fired power station: particulate levels and sources. *Atmos. Environ., 32*, 1963-1978.

Querol, X., Alastuey, A., Rodríguez, S., Plana, F., Mantilla, E. and Ruiz, C.R. (2001) Monitoring of PM_{10} and $PM_{2.5}$ around primary particulate anthropogenic emission sources. *Atmos. Environ., 35*, 845-858.

Querol, X., Alastuey, A., Viana, M.M., Rodríguez, S., Artiñano, B., Salvador, P., Garcia Do Santos, S., Fernández Patier, R., Ruiz, C., de la Rosa, J., Sánchez de la Campa, A., Menéndez, M. and Gil, J.I. (2004) Speciation and origin of PM_{10} and $PM_{2.5}$ in Spain. *J. Aerosol Sci., 35*, 1151–1172.

Querol, X., Pey, J., Pandolfi, M., Alastuey, A., Cusack, M., Pérez, N., Moreno, T., Viana, M., Mihalopoulos, N., Kallos, G. and Kleanthous, S. (2009b) African dust contributions to mean ambient PM_{10} mass-levels across the Mediterranean Basin. *Atmos. Environ., 43*, 4266-4277.

Ramanathan, V. and Carmichael, G. (2008) Global and regional change due to black carbon. *Nature Geosci., 1*, 221-227.

Riemer, N., Vogel, H. and Vogel, B. (2004) Soot ageing time scales in polluted regions during day and night. *Atmos. Chem. Phys., 4*, 1885-1893.

Robinson, A.L., Donahue, N.M., Shrivastava, M.K., Weitkamp, E.A., Sage, A.M., Grieshop, A.P., Lane, T.E., Pierce, J.R. and Pandis, S.N. (2007) Rethinking organic aerosols: Semivolatile emissions and photochemical aging. *Science, 315*, 1259-1262.

Rodríguez, S. Querol, X., Alastuey, A., Viana, M.M. and Mantilla, E. (2003) Events affecting levels and seasonal evolution of airborne particulate matter concentrations in the Western Mediterranean. *Environ. Sci. Technol., 37*, 216-222.

Rodríguez, S., Querol, X., Alastuey, A. and Mantilla, E. (2002) Origin of high PM_{10} and TSP concentrations in summer in Eastern Spain. *Atmos. Environ., 36*, 3101-3112.

Rodríguez, S., Querol, X., Alastuey, A., Viana, M.M., Alarcón, M., Mantilla, E. and Ruiz, C.R. (2004) Comparative PM_{10}–$PM_{2.5}$ source contribution study at rural, urban and industrial sites during PM episodes in Eastern Spain. *Sci. Total Environ., 328*, 95–113.

Rodríguez, S., Van Dingenen, R., Putaud, J.-P., Dell'Acqua, A., Pey, J., Querol, X., Alastuey, A., Chenery, S., Ho, K.-F., Harrison, R.M., Tardivo, R., Scarnato, B. and Gemelli, V. (2007) A study on the relationship between mass concentrations, chemistry and number size distribution of urban fine aerosols in Milan, Barcelona and London. *Atmos. Chem. Phys., 7*, 2217–2232.

Rodwell, M.J. and Hoskins, B.J. (2001) Subtropical anticyclones and summer monsoons. *J. Climate, 14*, 3192-3211.

Röösli, M., Theis, G., Künzli, N., Staehelin, J., Mathys, P., Oglesby, L., Camenzind, M. and Braun-Fahrländer, Ch. (2001) Temporal and spatial variation of the chemical composition of PM_{10} at urban and rural sites in the Basel area, Switzerland. *Atmos. Environ., 35*, 21, 3701-3713.

Salmi, T., Määttä, A., Anttila, P., Ruoho-Airola, T. and Amnell, T. (2002) Detecting trends of annual values of atmospheric pollutants by the Mann-Kendall test and Sen's slope estimates-the Excel template application MAKESENS. Helsinki, Finnish Meteorological Institute (Publications on air quality, 31*).*

Salvador, P., Artíñano, B., Querol, X., Alastuey, A. and Costoya, M. (2007) Characterisation of local and external contributions of atmospheric particulate matter at a background coastal site. *Atmos. Environ., 41*, 1-17.

Sciare, J., Oikonomou, K., Favez, O., Liakakou, E., Markaki, Z., Cachier, H. and Mihalopoulos, N. (2008) Long-term measurements of carbonaceous aerosols in the Eastern Mediterranean: evidence of long-range transport of biomass burning. *Atmos. Chem. Phys., 8,* 5551-5563.

Shrivastava, M.K., Lane, T.E., Donahue, N.M. et al. (2008) Effects of gas particle partitioning and aging of primary emissions on urban and regional organic aerosol concentrations. *J. Geophys. Res.*, *113*, D18301, doi:10.1029/2007JD009735.

Simpson, D., Fagerli, H., Jonson, J.E., Tsyro, S., Wind, P. and Tuovinen, J.-P. (2003) Transboundary acidification, eutrophication and ground level ozone in Europe. Part I. Unified EMEP model description. Oslo, Norwegian Meteorological Institute (EMEP/MSC-W Status report 1/2003 Part I). **URL:** http://emep.int/publ/reports/2003/emep_report_1_part1_2003.pdf [2010-08-23]

Simpson, D., Winiwarter, W., Börjesson, G., Cinderby, S., Ferreiro, A., Guenther, A., Hewitt, C.N., Janson, R., Khalil, M.A.K., Owen, S., Pierce, T.E., Puxbaum, H., Shearer, M., Skiba, U., Steinbrecher, R., Tarrasón, L. and Öquist, M.G. (1999) Inventorying emissions from Nature in Europe. *J. Geophys. Res., 104D*, 8113-8152.

Simpson, D., Yttri, K.E., Bergström, R., Denier van der Gon, H. and Tørseth, K. *(ed.)* (2009) Modelling SOA in EMEP: Experiments with the VBS Approach. In: *Transboundary Particulate Matter in Europe.* Kjeller, Norwegian Institute for Air Research (EMEP Status Report 4/2009) pp. 58-63.

Simpson, D., Yttri, K.E., Klimont, Z., Kupiainen, K., Caseiro, A., Gelencsér, A., Pio, C., Puxbaum, H. and Legrand, M. (2007) Modeling carbonaceous aerosol over Europe: Analysis of the CARBOSOL and EMEP EC/OC campaigns. *J. Geophys. Res., 112*, D23S14, doi:10.1029/2006JD008158.

Spindler, G., Brüggemann, E., Gnauk, T., Grüner, A., Müller, K., Tuch, Th.M., Wallasch, M.B., Wehner, A. and Herrmann, H. (2007) Size-segregated physical and chemical long-time characterization of particles depending from air mass origin at German lowlands (Saxony, Melpitz site). In: *EMEP Particulate Matter Assessment Report, Part B, Annex A*. Kjeller, Norwegian Institute for Air Research (EMEP/CCC-Report 8/2007) pp.178-221.

Subramanian, R., Winijkul, E., Bond, T.C., Thiansathit, W., Oanh, N.T.K., Paw-Armart, I. and Duleep, K.G. (2009) Climate-relevant properties of diesel particulate emissions: Results from a Piggyback Study in Bangkok, Thailand. *Environ. Sci. Technol., 43*, 4213-4218.

Szidat, S., Jenk, T.M., Gäggeler, H.W., Synal, H.-A., Fisseha, R., Baltensperger, U., Kalberer, M., Samburova, V., Wacker, L., Saurer, M., Schwikowski, M. and Hajdas, I. (2004a) Source apportionment of aerosols by 14C measurements in different carbonaceous particle fractions. *Radiocarbon, 46*, 475–484.

Szidat, S., Jenk, T.M., Gäggeler, H.W., Synal, H.-A., Fisseha, R., Baltensperger, U., Kalberer, M., Samburova, V., Reimann, S., Kasper-Giebl., A. and Hajdas, I. (2004b) Radiocarbon (14C)-deduced biogenic and anthropogenic contributions to organic carbon (OC) of urban aerosols from Zürich, Switzerland. *Atmos. Environ., 38*, 4035-4044.

Szidat, S., Ruff, M., Perron, N., Wacker, L., Synal, H.-A., Hallquist, M., Shannigrahi, A.S., Yttri, K.E., Dye, C. and Simpson, D. (2009) Fossil and non-fossil sources of organic carbon (OC) and elemental carbon (EC) in Göteborg, Sweden. *Atmos. Chem. Phys., 9*, 1521–1535.

ten Brink, H., Maenhaut, W., Hitzenberger, R., Gnauk, T., Spindler, G., Even, A., Chi, X., Bauer, H., Puxbaum, H., Putaud, J.-P., Tursic, J. and Berner, A. (2004) INTERCOMP2000: the comparability of methods in use in europe for measuring the carbon content of aerosol. *Atmos. Environ., 38*, 6507-6519.

Tsyro, S. (2008) Regional model for formation, dynamics, and long-range transport of atmospheric aerosol. *Russ. Meteorol. Hydrol., 33,* 82-90.

Tsyro, S., Simpson, D., Tarrasón, L., Klimont, Z., Kupiainen, K., Pio, C. and Yttri, K.E. (2007) Modelling of elemental carbon over Europe. *J. Geophys. Res., 112*, D23S19, doi:10.1029/2006JD008164.

UNECE (2009) EMEP monitoring strategy, 2010-2019. Draft revised monitoring strategy. Geneva (ECE/EB.AIR/GE.1/2009/15). URL: http://www.unece.org/env/documents/2009/EB/ge1/ece.eb.air.ge.1.2009.15.e.pdf [2010-09-01].

van der Werf, G.R., Randerson, J.T., Giglio, L., Collatz, G.J., Kasibhatla, P.S. and Arellano Jr., A.F. (2006) Interannual variability in global biomass burning emissions from 1997 to 2004. *Atmos. Chem. Phys.*, *6*, 3423-3441.

Viana, M., Maenhaut, W., Brink, H.M.T., Chi, X., Weijers, E., Querol, X., Alastuey, A., Mikuška, P. and Vecera, Z. (2007) Comparative analysis of organic and elemental carbon concentrations in carbonaceous aerosols in three European cities. *Atmos. Environ., 41* 5972–5983.

Viana, M., Querol, X., Alastuey, A., Cuevas, E. and Rodríguez S. (2002) Influence of African dust on the levels of atmospheric particulates in the Canary Islands air quality network. *Atmos. Environ., 36*, 5861-5875.

Viana, M., Querol, X., Ballester, F., Llop, S., Esplugues, A., Fernández Patier, R., García Dos Santos, S. and Herce, M.D. (2008) Characterising exposure to PM aerosols for an epidemiological study. *Atmos. Environ., 42*, 1552–1568.

Virkkula, A., Ahlquist, N.C., Covert, D.S., Arnott, W.P., Sheridan, P.J., Quinn, P.K. and Coffman, D.J. (2005) Modification, calibration and a field test of an instrument for measuring light absorption by particles. *Aerosol Sci. Technol., 39,* 68-83.

Visschedijk, A., Denier van der Gon, H., Droge, R. and van der Brugh, A. (2009) European high resolution and size-differentiated emission inventory for elemental and organic carbon for the year 2005. Utrecht, TNO (TNO-034-UT-2009-00688_RPT-ML).

Visser, H., Buringh, E. and van Breugel, P.B. (2001) Composition and origin of airborne particulate matter in the Netherlands. Bilthoven, National Institute for Public Health and the Environment (RIVM Report 650010029).

Wilson, J., Cuvelier, C. and Raes, F. (2001) A modeling study of global mixed aerosol fields. *J. Geophys. Res., 106D,* 34081-34108, 10.1029/2000JD000198.

Yanowitz, J., McCormick, R.L. and Graboski, M.S. (1999) In-Use emissions from heavy-duty diesel vehicles. *Environ. Sci. Technol., 34*, 729-740.

Yin, J. and Harrison, R.M. (2008) Pragmatic mass closure study for $PM_{1.0}$, $PM_{2.5}$ and PM_{10} at roadside, urban background and rural sites. *Atmos. Environ., 42*, 980–988.

Yttri, K.E. (2007) Concentrations of particulate matter (PM_{10}, $PM_{2.5}$) in Norway. Annual and seasonal trends and spatial variability. In: *EMEP Particulate Matter Assessment Report, Part B, Annex A.* Kjeller, Norwegian Institute for Air Research (EMEP/CCC-Report 8/2007) pp. 292-307.

Yttri, K.E., Aas, W., Bjerke, A., Cape, J.N., Cavalli, F., Ceburnis, D., Dye, C., Emblico, L., Facchini, M.C., Forster, C., Hanssen, J.E., Hansson, H.C., Jennings, S.G., Maenhaut, W., Putaud, J.P. and Tørseth, K. (2007a) Elemental and organic carbon in PM_{10}: A one year measurement campaign within the European monitoring and Evaluation Programme EMEP. *Atmos. Chem. Phys., 7,* 5711–5725.
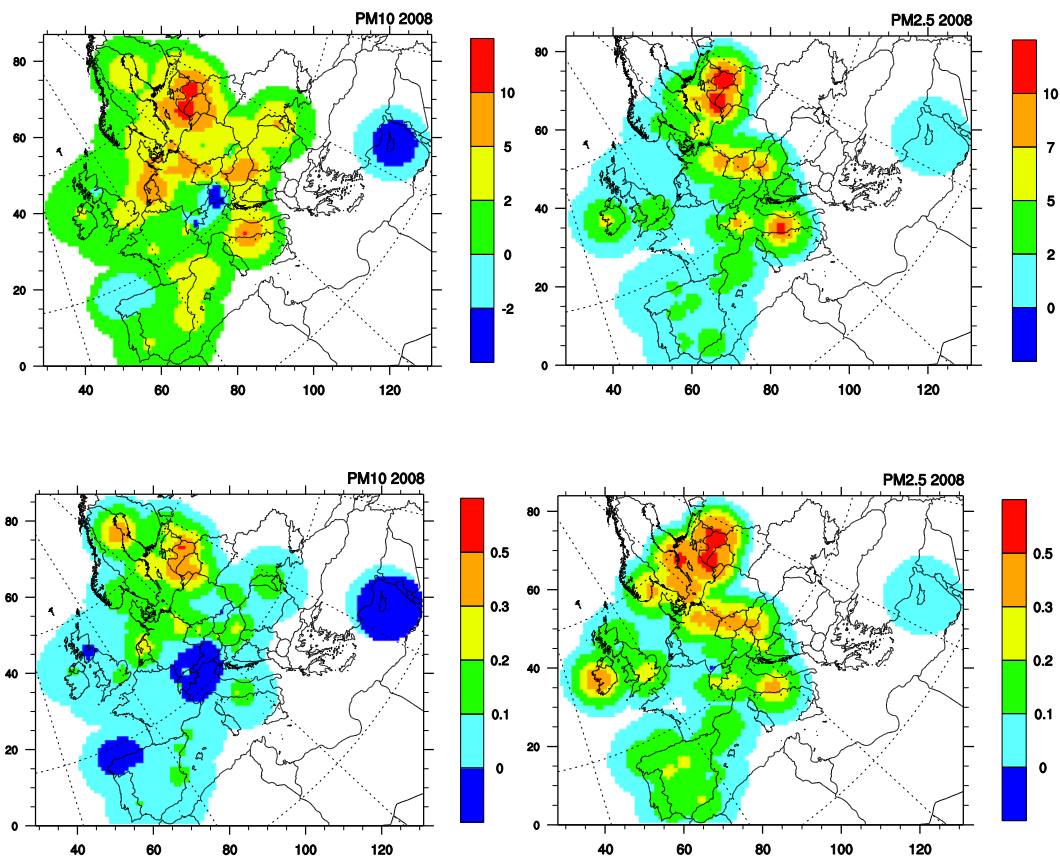
APPENDIX A

136

Figure A.1: *Interpolated annual mean differences (upper panels) and normalized differences (lower panels) between model calculated and measured PM$_{10}$ and PM$_{2.5}$ for 2008. Here, normalized differences are calculated as 2x(model – observation)/(model + observation)*

Table A.1: Statistic analysis of model calculated PM$_{2.5}$ versus observational PM$_{2.5}$ in 2008.

Here, Obs – the measured mean, Mod – the calculated mean, Bias is calculated as Σ(Mod-Obs)/Obs x 100%, R– the temporal correlation coefficient and NRMSE – the Root mean Square Error= [1/NsΣ(Mod-Obs)^2]$^{1/2}$/Obs.

Code	Station name	Obs	Mod	Rel. bias	R	NRMSE
AT02	Illmitz	16.3	7.8	-52.3	0.66	0.74
CH02	Payerne	11.8	6.0	-49	0.75	0.76
CH05	Rigi	6.9	4.9	-29	0.52	0.92
CY02	Ayia Marina	16.0	14.3	-10	0.57	0.88
CZ03[*)]	Kosetice	14.6	6.6	-55	0.67	0.66
DE02	Langenbruegge/Waldhof	10.9	6.7	-38	0.59	0.73
DE03	Schauinsland	5.3	5.0	-5	0.32	0.98
DE44	Melpitz	16.8	7.6	-55	0.49	0.82
ES07	Viznar	9.8	5.4	-45	0.42	0.88
ES08	Niembro	8.9	5.3	-41	0.61	0.66
ES09[*)]	Campisabalos	6.0	2.7	-55	0.45	0.99
ES10	Cabo de Creus	8.0	5.8	-28	0.63	0.54
ES11	Barcarrota	6.2	3.7	-40	0.63	0.59
ES12	Zarra	5.8	4.7	-19	0.68	0.51
ES13	Penausende	6.6	3.3	-51	0.42	0.81
ES14	Els Torms	8.3	5.8	-30	0.63	0.62
ES16	O Savinao	6.1	4.6	-26	0.64	0.61
ES17	Montseny	8.9	9.0	1	0.56	0.74
FI50	Hyytiälä	4.3	2.0	-53	0.60	0.84
FR09[*)]	Revin	9.8	7.8	-21	0.71	0.53
FR13[*)]	Peyrusse Vieille	7.6	9.5	25	0.53	0.90
GB36	*Harwell*	9.9	6.1	-38	0.74	0.68
GB48	Auchencorth Moss	3.2	2.8	-12	0.65	0.98
IE31	*Mace Head*	10.0	3.6	-64	0.64	0.81
IT04	Ispra	20.2	12.9	-36	0.67	0.85
LV10	Rucava	18.0	3.7	-80	0.47	0.98
LV16	Zoseni	16.2	3.1	-81	0.31	0.95
SE11[*)]	*Vavihill*	8.6	4.0	-53	0.55	0.68
SE12	*Aspvreten*	7.0	2.5	-64	0.72	0.86
SE14	*Raaoe*	6.4	4.5	-31	0.56	0.63
SI08	Iskrba	10.6	7.2	-32	0.36	0.80
NO01	Birkenes	2.9	1.2	-60	0.40	0.80

Note: Shaded cells present statistics for weekly data; [*)] Less than 180 days with measurement data; *Italic font* – hourly measurements with TEOM

Table A.2: *Statistic analysis of model calculated daily PM_{10} versus observational PM_{10} in 2008.*

Code	Station name	Obs	Mod	Rel. bias	R	NRMSE
AT02	Illmitz	20.7	10.8	-48	0.64	0.71
AT05	Vorhegg	7.9	13.3	68	0.36	2.43
AT48	Zoebelboden	8.6	11.3	32	0.56	1.69
CH01	Jungfraujoch	2.9	5.4	84	0.28	3.06
CH02	Payerne	18.7	8.4	-55	0.64	0.78
CH03	Taenikon	16.6	8.6	-49	0.48	0.85
CH04	Chaumont	9.6	8.3	-13	0.52	0.96
CH05	Rigi	9.8	6.8	-30	0.46	0.99
CY02	Ayia Marina	35.7	36.9	4	0.49	1.58
CZ01	Svratouch	19.9	9.5	-52	0.28	0.80
CZ03[*]	Kosetice	17.1	9.4	-45	0.57	0.70
DE01	Westerland/Wenningsted	18.3	12.5	-32	0.56	0.56
DE02	Langenbruegge/Waldhof	15.1	10.0	-34	0.52	0.66
DE03	Schauinsland	7.2	7.5	4	0.32	1.47
DE07	Neuglobsow	12.2	9.4	-23	0.56	0.61
DE08	Schmuecke	9.4	10.0	6	0.38	1.01
DE09	Zingst	14.2	10.6	-26	0.66	0.53
DE44	Melpitz	20.9	10.5	-50	0.48	0.75
ES07	Viznar	18.4	15.1	-18	0.43	1.16
ES08	Niembro	17.2	13.0	-24	0.46	0.74
ES09[*]	Campisabalos	7.7	6.1	-20	0.18	1.45
ES10	Cabo de Creus	17.9	11.9	-33	0.38	0.56
ES11	Barcarrota	14.0	9.1	-35	0.45	0.84
ES12	Zarra	16.7	8.9	-47	0.48	0.86
ES13	Penausende	9.8	6.3	-35	0.31	0.91
ES14	Els Torms	13.9	9.6	-31	0.49	0.77
ES16	O Savinao	10.0	8.6	-14	0.43	0.85
ES17	Montseny	14.5	12.5	-14	0.58	0.60
FI50	Hyytiälä	5.0	3.8	-25	0.46	0.90
FR09[*]	Revin	15.5	10.5	-32	0.67	0.50
FR13[*]	Peyrusse Vieille	12.2	9.9	-19	0.36	0.72
FR15	La Tardiere	13.2	9.6	-27	0.47	0.55
GB06	Lough Navar	12.7	7.4	-42	0.64	0.64
GB36	*Harwell*	18.8	10.3	-46	0.56	0.62
GB43	Narberth	17.6	11.2	-36	0.54	0.58
GB48	Auchencorth Moss	6.5	6.8	3	0.58	0.83
GR02[*]	Finokalia	17.0	33.9	100	0.65	1.45
HU02	K-puszta	26.3	13.1	-50	0.73	0.63
LV10	Rucava	25.9	8.3	-68	0.28	0.88
LV16	Zoseni	21.5	5.5	-74	0.01	1.06
MD13	Leova II	19.3	11.1	-43	0.08	1.81
NL07	Eibergen	23.6	13.0	-45	0.76	0.55
NL09	Kollumerwaard	23.7	12.1	-49	0.67	0.58
NL10	Vreedepeel	20.9	14.0	-33	0.68	0.53
NL91	De Zilk	24.3	14.9	-39	0.64	0.50
PL05	Diabla Gora	15.7	8.6	-45	0.65	0.67
SE11[*]	*Vavihill*	11.2	7.3	-35	0.75	0.50
SE12	*Aspvreten*	8.7	5.8	-33	0.60	0.68
SE14	*Raaoe*	16.0	10.8	-33	0.52	0.58
SE35	*Vindeln*	6.4	2.3	-65	0.39	0.81
SI08	Iskrba	16.1	10.8	-33	0.26	0.84
EE09	Lahemaa	7.2	5.6	-22	0.48	0.54
SK04[*]	Stara Lesna	11.3	12.9	10	0.46	0.84
SK06	Starina	14.3	14.1	2	0.45	0.59
SK07	Topolniki	18.3	9.8	-46	0.46	0.58
NO01	Birkenes	5.8	2.8	-56	0.22	0.81

Note: Shaded cells present statistics for weekly data; [*] Less than 180 days with measurement data; *Italic font* – hourly measurements with TEOM

emep

PM10 in 2008 (ug/m3)   PM25 in 2008 (ug/m3)
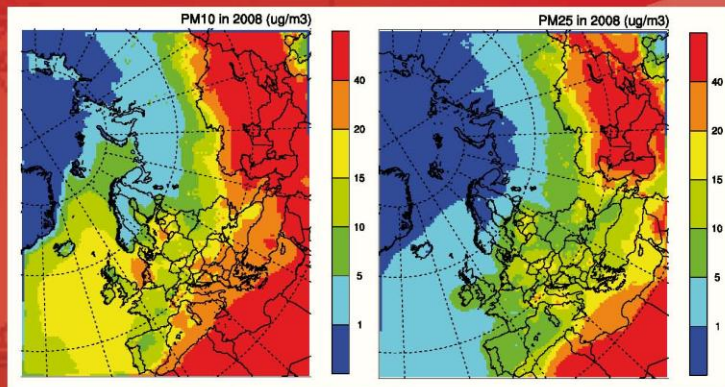
NILU

ccc
NILU
Norwegian Institute for Air Research
P.O. Box 100
NO-2027 Kjeller
Norway
Phone: +47 63 89 80 00
Fax: +47 63 89 80 50
E-mail: kjetil.torseth@nilu.no
Internet: www.nilu.no

IIASA

ciam
International Institute for
Applied Systems Analysis
(IIASA)
A-2361 Laxenburg
Austria
Phone: +43 2236 80 70
Fax: +43 2236 71 31
E-mail: amann@iiasa.ac.at
Internet: www.iiasa.ac.at

umweltbundesamt

ceip
Umweltbundesamt GmbH
Spittelauer Lände 5
1090 Vienna
Austria
Phone: +43-(0)1-313 04
Fax: +43-(0)1-313 04/5400
E-mail:
  emep.emissions@umweltbundesamt.at
Internet:
  http://www.umweltbundesamt.at/

msc-e
Meteorological Synthesizing
Centre-East
Krasina pereulok, 16/1
123056 Moscow
Russia
Phone +7 495 981 15 66
Fax: +7 495 981 15 67
E-mail: msce@msceast.org
Internet: www.msceast.org

msc-w
Norwegian Meteorological
Institute (met.no)
P.O. Box 43 Blindern
NO-0313 OSLO
Norway
Phone: +47 22 96 30 00
Fax: +47 22 96 30 50
E-mail: emep.mscw@met.no
Internet: www.emep.int